UNIVERSITY OF CALIFORNIA
RIVERSIDE

The Role of the Cross Pathway Control (*cpc*)-2 Gene in the Filamentous Fungus *Neurospora Crassa*

A Thesis submitted in partial satisfaction
of the requirements for the degree of

Master of Science

in

Genetics, Genomics and Bioinformatics

by

Amruta Vikas Garud

June 2013

Thesis Committee:
Dr. Katherine Borkovich, Chairperson
Dr. Linda Walling
Dr. Wenbo Ma

The Thesis of Amruta Vikas Garud is approved:

_____

_____

_____

Committee Chairperson

University of California, Riverside

ABSTRACT OF THE THESIS

The Role of the Cross Pathway Control (*cpc*)-2 Gene in the Filamentous Fungus *Neurospora Crassa*

by

Amruta Vikas Garud

Master of Science, Graduate Program in Genetics, Genomics and Bioinformatics
University of California, Riverside, June 2013
Dr. Katherine Borkovich, Chairperson

In the filamentous fungus *Neurospora crassa*, heterotrimeric G protein pathways are major signaling cascades through which the fungus senses and adapts to its environment. The characterized Gβ subunit of *N. crassa*, GNB-1, has seven tryptophan-aspartate (WD) repeats, predicted to result in a β propeller structure. Another related *N. crassa* protein, called Cross Pathway Control-2 (CPC-2), also has a seven WD repeat structure and possesses 70% positional identity with Receptor for Activated C Kinase-1(RACK-1), a multifaceted scaffolding protein in mammals. Accumulating evidence in many organisms shows that RACK1 homologs can act as Gβ subunits.

Previous work demonstrated that CPC-2 plays an important role during general amino acid control in *N. crassa*, along with having a role in overall growth and female fertility. My research investigated a possible role for *cpc-2* in the G protein signaling pathway, and also investigated genetic epistasis between *cpc-2*, *gnb-1* and the Gα genes in *N. crassa*.

In Chapter 2, genetic analysis revealed that *gna-3* is epistatic to *gnb-1* with regard to control of submerged conidiation. *gnb-1* is epistatic to *gna-2* and *gna-3* for aerial hyphal height, while *gnb-1* appears to act upstream of *gna-1* and *gna-2* during aerial conidiation. None of the activated Gα alleles restored female fertility to Δ*gnb-1* mutants, and the *gna-3*^{Q208L} allele inhibited formation of female reproductive structures, consistent with a need for Gα proteins to cycle through the inactive GDP-bound form for these processes.

In Chapter 3, genetic epistasis genes showed that *gna-3* is epistatic to *cpc-2* during conidiation in submerged culture. *gna-1* exhibited partial epistasis to *cpc-2* during submerged culture conidiation. *gna-3*, *gnb-1* and *gng-1* operate downstream of *cpc-2* during aerial hyphae height development. Apical extension assays showed that *cpc-2* is epistatic to *gnb-1* and *gng-1*. Similar to the results for *gnb-1* in Chapter 2, none of the activated Gα alleles restored fertility to the sterile Δ*cpc-2* mutant. Analysis of apical extension rates on medium supplemented with -amino triazole (3AT) revealed a previously unknown role for *gna-1* and *gna-3* in general amino acid control. Yeast two hybrid mating assays revealed that CPC-2 interacts with GNA-1 and GNA-3.

Table of Contents

List of figures

Chapter 2

Chapter 3

List of Tables

Chapter 2

Chapter 3

Chapter 1: Introduction

Neurospora crassa, a multicellular eukaryote, belongs to the ascomycete class of fungi. It has been used as model organism to study genetics, cell biology and biochemistry due to its simple growth requirements, non-pathogenicity, genetic tractability and a short life cycle (9). The famous one-gene-one-enzyme hypothesis by Beadle and Tatum in the 1940s was the result of a study on vitamin biosynthesis in this fungus (6). More recently, *N. crassa* has emerged as a model system to study pathogenic fungi, and its evolutionary relatedness to animal and mammalian systems makes it an attractive model organism (9).

N. crassa grows by extension, branching and fusion of vegetative basal hyphae to form the thick mat called the mycelium. *N. crassa* has two asexual sporulation pathways- macroconidiation and microconidiation (64).Macroconidiation is the major pathway and involves production of aerial hyphae that develop multinucleate macroconidia at their tips. Macroconidia are disseminated in nature by wind currents and by animals, enabling the fungus to colonize new areas. The second asexual sporulation pathway, microconidiation, involves production of uninucleate conidia from structures called microconidiophores. Microconidiation can be induced under laboratory conditions, enabling researchers to purify homokaryons containing a single nucleus from heterokaryotic transformants, in a span of two-three weeks.

N. crassa is a heterothallic organism, meaning it has different 'mating types' depending on a gene present at a single locus (idiomorph; *mat A* or *mat a*). Upon nitrogen limitation, the fungus forms protoperithecia (the female reproductive structures, (55). In

the presence of a male cell (usually conidia) of the opposite mating type, pheromone detection results in chemotropic growth of specialized hyphae called trichogynes from the protoperithecium. The fruiting body, or perithecium, is then formed and contains asci, each with eight haploid spores (ascospores). Upon maturation, ascospores are ejected from the tips (beaks) of perithecia, in the direction of light. Under laboratory conditions, protoperithecial development is induced using Synthetic Crossing Medium (SCM), and progeny are obtained from sexual crosses approximately two to three weeks post-fertilization (55).

In recent years, the advancement in the available genetics and genomics tools has greatly facilitated research in *Neurospora* biology. The *N. crassa* genome was sequenced in 2003 (9). Following that, a targeted gene-disruption method using the Δ*mus-51* and Δ*mus-52* strains, that each are deleted for a gene required for non-homologous end joining (NHEJ), was developed, ensuring almost 100% homologous recombination of transforming DNA (46). Using such high-throughput strategies, gene deletion mutants have been created using the hygromycin resistance cassette to replace the target gene, generating knockout strains for a majority of the genes in the genome (15). This allows researchers to use reverse genetics for further investigations, thus conferring another advantage to work with this organism.

Heterotrimeric G protein signaling in *N. crassa.*

One of the major pathways involved in environmental sensing of nutrients, pheromones, and external stimuli in *N. crassa* is the heterotrimeric G protein signaling pathway. In this signal transduction pathway, G Protein Coupled Receptors (GPCRs) transmit extracellular signals to the intracellular heterotrimeric G proteins (α, β and γ subunits). Alternatively, a cytoplasmic protein called Resistance to *I*nhibitors of Cholinesterase (RIC)- 8 can also activate this signaling pathway (72). GPCRs and RIC8 are together classified as Guanine Nucleotide Exchange Factors (GEFs). In an inactive state, the Gαβγ subunits are associated with the GPCR at the membrane, with the Gα bound to GDP (45). The Gβγ dimer functions as a Guanine Dissociation Inhibitor (GDI), keeping the Gα-GDP bound to the Gβγ at the membrane until there is GEF activity. Stimulation by a ligand (or by cytosolic regulators of GEFs) brings about a conformational change in the GPCR, catalyzing the exchange of GDP for GTP on the Gα subunit. Subsequently, the Gβγ heterodimer dissociates from the Gα-GTP subunit. The Gα and the Gβγ subunit then bind and regulate downstream effectors, eventually leading to transcription of genes and an appropriate physiological response (45). To complete the cycle, the native GTPase activity of Gα subunits hydrolyzes GTP to GDP. This process is also accelerated by Regulators of G protein signaling (RGS) proteins. The Gα-GDP then re-associates with the Gβγ heterodimer, leading to signal termination (40).

In *N. crassa*, there are 25 putative GPCRs, three known Gα subunits (GNA-1, GNA-2 and GNA-3), one characterized Gβ subunit (GNB-1) and one known Gγ subunit (GNG-1). Major processes such as germination, conidiation, nutrient sensing and mating

are regulated by G protein signaling pathways, involving components such as GPCRs, RIC8 and G protein subunits (29, 31, 35, 39-40, 65, 72).

The Gβ subunit GNB-1 and the Gβγ heterodimer.

The GNB-1 protein from *N. crassa* is homologous to the human Gβ subunit GNB-3, sharing 65% identity, and is almost identical to the Gβ subunit from *Cryphonectria parasitica* and *Aspergillus nidulans* (74). GNB-1 regulates certain aspects of sexual and asexual growth and development in *N. crassa*. The Δ*gnb-1* gene deletion mutant conidiates inappropriately in submerged cultures, and abundantly under aerial conditions, indicating that this gene is a negative regulator of conidiation (74). The Δ*gnb-1* mutant is female-sterile, not forming perithecia during the sexual cycle (74). Levels of all three Gα proteins -GNA-1, GNA-2 and GNA-3- are low in the Δ*gnb-1* strain, but mRNA levels are normal, indicating that GNB-1 is involved in post-transcriptional regulation of Gα protein levels (74) . In contrast, GTPase- deficient Gα proteins are resistant to this effect, and are stable in the absence of the *gnb-1* gene (71) .

The GNB-1 protein consists of seven tryptophan-aspartate (WD) repeats, predicted to result in a beta propeller structure (21) . In addition, GNB-1 has a coiled-coiled region at its N-terminus that is thought to be important for interaction of other Gβ proteins with Gγ subunits. Evidence for a strong interaction between the Gβ and the Gγ subunit in *N. crassa* has been provided using co-immunoprecipitation experiments (34) .

The phenotypes of the Δ*gnb-1*, Δ*gng-1* and Δ*gnb-1* Δ*gng-1* mutants are very similar, consistent with formation of a Gβγ heterodimer (34).

RACK-1, a Gβ-related polypeptide

The Receptor for Activated C Kinase-1 (RACK-1), a WD-40 repeat protein, is a 36 kDa protein that acts as a scaffold for many signaling pathways in mammals (56). Named after its association with the active conformation of Protein Kinase C βII (PKC) it is now known that RACK1 associates with a plethora of proteins due to its WD repeat structure, and is also widely implicated in various human disorders, such as Alzheimer's disease and cancers, etc. (1).

RACK1 is known to form associations with several proteins, some of which are transient. For example, RACK1 stabilizes the active form of protein phosphatase 2A (PP2A), and binds to the tyrosine kinases Src and Fyn to maintain them in an inactive state until appropriate stimulation (11). Additionally, RACK1 is known to associate with ribosomal fractions, particularly with the 40S subunit, near the mRNA exit channel (61). Due to its conformation when bound to the ribosome, RACK1 is also thought to serve as an adaptor protein, bringing together proteins at the ribosome during translation [reviewed in (1)]. One such protein is PKCβII, and a RACK1-derived peptide that disrupts PKC binding also inhibits PKC-stimulated translation [reviewed in (1)]. Simultaneously, studies have shown that RACK1 is also involved in repression of gene expression, in that binding to the 40S ribosome is essential for nascent polypeptide dependent translation arrest (36).

It is known that RACK1 binds to the Gβγ dimer in HEK293 cells, and also regulates a subset of its functions (12). The association of RACK1 with the Gβγ dimer promotes its relocation from the cytosol to the membrane.(12). Recently, it has been shown that RACK1, along with the Gβγ dimer and another protein named WDR26, regulates chemotaxis and cell polarization in Jurkat T-cells (59) .

Fungal homologs of RACK1

Since its discovery and cloning in 1994, RACK1 homologs have been found to be conserved through the eukaryotic kingdom (68) . Fungal homologs have been studied in *Saccharomyces cerevisiae*, *Ustilago maydis*, *Crytpococcus neoformans*, *Schizosaccaromyces pombe* and *Neurospora crassa* (43, 49, 67, 75). Sharing the seven WD repeat architecture, some of the proteins have been implicated as alternative Gβ subunits during heterotrimeric G protein signaling, and to have additional regulatory roles during mating, virulence, cell cycle regulation, metabolism and translation etc.

Asc1p is the RACK1 homolog in the budding yeast *S. cerevisaie* (75) . It associates with the GDP-bound form of the Gα Gpa2, acting as a guanine dissociation inhibitor (GDI). In addition, Δasc1 mutants are defective in invasive growth, similar to Δ*gpa2* strains indicating that Asc1p not only interacts directly with Gpa2p, but also is important during Gpa2p-mediated signaling. When the roles of Asc1p and the Gβ subunit Ste4p were compared regarding phosphorylation of the Mitogen Activated Protein (MAP) kinase Kss1p, it was seen that Asc1p interacts with Ste20p, but represses basal MAP kinase activity, whereas Ste4p induces MAP kinase signaling (75). Like other Gβ

subunits, Asc1p interacts with adenylyl cyclase (Cyr1p) and inhibits cyclic AMP production through Cyr1p (75). Thus, Asc1p possess non-canonical roles as a Gβ subunit, and also has functions independently of Gα subunits (75). It is known that Asc1p associates with the 40S subunit of the ribosome, and plays a role in translation initiation, especially affecting the transcription factors Ste12p, Phd1p and Tec1p, through their 5' untranslated regions (UTRs) (54). Loss of *asc1* reduces the binding affinity for eukaryotic initiation factor-3 (eIF3) towards the 40S subunit, inhibiting translation initiation (54) Conversely, it has also been shown Asc1p and RACK1 repress gene expression, for *asc1* null strains have increased translational activity for some mRNAs (22).

Rak1, the RACK1 homolog in the filamentous basidiomycete fungus *Ustilago maydis*, exhibits 68% identity to RACK1 and 51% to Asc1p (67). An immunoprecipitation and mass spectroscopy approach to identify interactors has shown that of the proteins identified, 32 were ribosomal proteins, and the rest were involved in metabolism, energy production and rRNA processing (67). Thus a ribosomal association also seems likely in *U. maydis*. In addition, Rak1 is essential for the transcription of Rop1, which is a direct positive regulator of the pheromone response factor (*prf1*), essential for mating. However, no interaction between Rak1 and any Gα subunits has been established, and it is not known whether Rak1 functions as a Gβ subunit in this fungus (67).

The RACK1 homolog in *C. neoformans*, Gib2, acts as a multifunctional Gβ subunit (49). It interacts with the Gα Gpa1, and with the two Gγ subunits, Gpg1 and

Gpg2. Gib2 interacts with the Protein Kinase C homolog (Pkc1) *in vitro,* suggesting that Gib2 possesses a similar function to RACK1(49). Yeast two hybrid screens identified Smg1, a downstream target of Gpa1-cAMP signaling as a binding partner for Gib2 (49). Gib2 is also known to positively regulate cAMP signaling, for strains over-expressing Gib2 in *gpa1* mutant strain have wild-type levels of intracellular cyclic AMP, while the *gpa1* mutant is defective in cAMP signaling (49). Additionally, suppression of *gib2* leads to synthetically lethality, suggesting that *gib2* encodes an essential function during cellular growth, in contrast to RACK1 and CPC-2. Interaction between ribosomes and Gib2 was not shown, but higher protein content in cells depleted of GIB2 was observed (49).

Analysis of the RACK1 ortholog Cpc2 in *S. pombe* indicates a role in cell cycle regulation and stress responses through ribosomal association (43). Mutants lacking *cpc2* are increased in size, indicating a defect in the G2/M transition in the mitotic cycle. Cpc2 modulates this control by regulating protein levels and activity of the Wee1 kinase (48). In relation to oxidative stress, Cpc2 positively regulates the synthesis of a stress response transcriptional factor Atf1, and a catalase induced by hydrogen peroxide treatment (47) . Cells in which Cpc2 and its ribosomal association are disrupted exhibit down-regulation of Atf1 when subjected to osmotic saline or oxidative stress. This indicates that regulation occurs through translational control (48).

Thus, it is apparent that RACK1 homologs in the fungal kingdom are multifunctional, making this class of proteins unique, dynamic and interesting to study.

The Cross Pathway Control -2 (CPC-2) protein in *N. crassa*.

In *N. crassa*, starvation for a single amino acid leads to an up-regulation of genes involved in amino acid biosynthesis, activating the cross pathway control network (4). This mechanism helps the fungus to overcome amino acid limitation and survive in such conditions. The RACK1 homolog in *N. crassa*, *cpc-2*, is essential for derepression (increased synthesis) of amino acid biosynthetic genes under limiting conditions, thus acting as a positive, regulatory element *in trans* (33).The *cpc-2* mutant was initially isolated by mutagenezing Δ*cpc-1* using ultraviolet light. From this set, conidia that were sensitive to 3AT, p-fluoro-DL-phenylalanine (pFPA), had impaired regulation of ornithine carbamoyltransferase under starvation conditions and passed these traits to its offspring were identified, one of them being *U142* (referred to *cpc-2* from here on) (33, 50). In limiting conditions, there is no activation of target amino acid biosynthetic genes in the Δ*cpc-2* mutant. Under non-starved conditions, loss of the *cpc-2* gene decreases growth by 50% during the asexual life cycle. During the sexual cycle, Δ*cpc-2* mutants lack protoperithecia, and are therefore female-sterile (44).

In addition to CPC-2, CPC-1 and CPC-3 are also part of the cross pathway control network in *N. crassa* (50, 60). CPC-1 is a transcriptional activator, homologous to Gcn4p in yeast (4). CPC-1 and GCN4 are 70% similar in a 30-residue segment that contains basic amino acids, thought to be involved in DNA recognition (19, 50). The DNA motif recognized by CPC-1 and GCN4 is 5'-ATGACTCAT-3', thus providing additional evidence that these two proteins have similar functions (18). The Δ*cpc-1* mutant is fully fertile, indicating that the lack of protoperithecia observed in Δ*cpc-2* mutants is not due to

amino acid limitation (50). CPC-3, the other component of the cross-pathway control network, encodes a eukaryotic Initiation Factor (eIF2α), a serine/threonine kinase (60). It is the functional homolog of Gcn2p kinase in budding yeast that is required for *cpc-1* gene expression. Specifically, mutation of *cpc-3* leads to reduction in CPC-1 protein levels during amino acid starvation, but not mRNA levels, indicating that *cpc-3* acts as translational activator of *cpc-1* (60). However the Δ*cpc-3* mutant does not show any defect in vegetative growth or sexual development (similar to wild-type), indicating that this gene does not perform an essential cellular function (60). Its main defect is sensitivity to 3-aminotriazole, similar to other mutants in the cross pathway control network (60).

Genetic and protein interactions between *cpc-1*, *cpc-2* and *cpc-3* have been studied. It is observed that during amino acid-starvation conditions in the wild-type background, *cpc-1* gene is transcribed at elevated levels (44). Within an hour of amino acid starvation, the *cpc-2* mRNA levels decrease (44). Supplementation of the respective amino acid to the medium results in high expression of the *cpc-2* transcript. Data suggests that the mRNA levels of *cpc-1* and *cpc-2* are conversely related- only when the *cpc-2* transcript levels decrease do the *cpc-1* transcript levels increase. The decrease in *cpc-2* transcript level is not observed in a Δ*cpc-1* strain under amino acid limitation conditions, while *cpc-1* transcript levels are not affected in the Δ*cpc-2* mutant (33, 44). This suggests that *cpc-1* regulates expression of *cpc-2* but not vice-versa. The *cpc-3* mutation abolishes the down-regulation of the *cpc-2* mRNA during amino acid starved conditions, similar to what is seen in the Δ*cpc-1* strain, indicating that *cpc-3* also regulates the expression of

cpc-2 (60). In addition, during amino acid starved conditions, a 10-fold reduction of CPC-1 protein levels in the Δ*cpc-3* strain, but normal mRNA levels, and 1.7-fold higher *cpc-1* mRNA in the wild-type strain than in the Δ*cpc-3* strain indicate that *cpc-3* is a translational activator of *cpc-1* (60).

Double gene deletion mutants have been analyzed to understand genetic interaction between the components of this network. The Δ*cpc-1,* Δ*cpc-2* double mutants show a temperature sensitive phenotype at 42˚C, while the single mutants show only delayed growth as compared to wild-type at this temperature (33). The double mutants also demonstrated glycine sensitivity, and slow ascospore germination (33). Analysis of Δ*cpc-2,* Δ*cpc-3* and Δ*cpc-2,* Δ*cpc-1* double mutants showed that the *cpc-2* characteristic phenotypes were not masked, i.e reduced growth (50%) and female infertility. This demonstrates that *cpc-2* has broader functions outside amino acid control (60).

Objectives

In the second chapter of this thesis, I tested the genetic interactions between the Gβ subunit gene, *gnb-1*, and the three Gα genes-*gna-1*, *gna-2* and *gna-3*. Single and double gene deletion mutants, as well as Δ*gnb-1* mutants expressing constitutively activated Gα alleles were used to determine epistatic relationships between the *gnb-1* and the Gα genes during various growth and developmental stages. This chapter is a part of a published manuscript (71).

The third chapter studies the genetic relationships and physical interactions between *cpc-2* and components of the G protein signaling pathway in *N. crassa*. Genetic epistasis analysis was used to probe genetic interactions between *cpc-2*, *gnb-1*, *gng-1* and the three Gα genes. Physical interactions were determined using yeast two hybrid assays and co-immunoprecipitation methods.

Chapter 2- Genetic interaction between the Gβ subunit, *gnb-1* and the three Gα genes- *gna-1, gna-2* and *gna-3*

Introduction

The heterotrimeric G protein signaling pathway in *N. crassa* consists of three Gα subunits (GNA-1, GNA-2 and GNA-3), one Gβ (GNB-1) and one Gγ (GNG-1). It is known that GNA-1 regulates apical extension, aspects of female fertility, aerial hyphae development, and positively regulates adenylyl cyclase activity (27). GNA-3 modulates conidiation and adenylyl cyclase levels (29). GNA-2 acts as a compensatory Gα subunit, with no major defects observed in the Δ*gna-2* mutant (3) except for reduced mass accumulation when glycerol is the carbon source (39). The greatest effect of *gna-2* is that its loss amplifies the defects of strains also lacking *gna-1* or *gna-3* when double gene deletion mutants are analyzed (28) and The Δ*gna-1*Δ*gna-3* double mutant and the Δ*gna-1* Δ*gna-2* Δ*gna-3* triple mutant has major growth and developmental defects (28).

The Gβ subunit in *N. crassa,* GNB-1, shares significant identity to Gβ subunits from *Aspergillus nidulans* and humans (74), but only 38% and 45% similarity to Gβ proteins from budding yeasts and fission yeasts. The protein structure of GNB-1 is typical of almost all Gβ subunits, with seven tryptophan-aspartate (WD) repeats in its sequence, predicted to result in a β propellor structure. The GNB-1 protein associates tightly with the Gγ, GNG-1, forming a functional heterodimer essential for normal asexual and sexual development, and maintains normal protein levels of the three Gα subunits (34).

During the sexual cycle, Δ*gnb-1* and Δ*gna-1* single mutants form protoperithecia, but not perithecia, and are therefore female-sterile. It is known that GNB-1 and GNA-3

are negative regulators of conidiation; thus, Δ*gnb-1* and Δ*gna-3* single mutants conidiate abundantly and inappropriately. Single gene deletion mutants sharing similar phenotypic defects hinted towards the genes sharing an epistatic relationship. This possibility was explored in this chapter using phenotypic analysis. These studies form part of a published manuscript (71).

For this study, I constructed a Δ*gnb-1* Δ*gna-2* double mutant strain, and verified it using diagnostic PCR. I, along with another graduate student, Alexander Michkov, performed phenotypic assays, assessing submerged culture conidiation, aerial hyphae height development in standing liquid cultures, and sexual fertility on SCM medium.

Materials and Methods

Strains and media- *N. crassa* strains used in this study are listed in Table 1. Strains were cultured in Vogel's Minimal medium (VM) for vegetative growth (0.25% sodium citrate·$2H_2O$, 0.5% KH_2PO_4, 0.2% NH_4NO_3,), 2% $MgSO_4·7H_2O$, 0.01% $CaCl_2·2H_2O$, 0.5% biotin solution, and 0.5% trace elements solution (66). Trace elements contain 5% citric acid·H_2O, 5% $ZnSO_4·7H_2O$, 1% $Fe(NH_4)_2$ $(SO_4)_2$. $6H_2O$, 0.25% $CuSO_4·5$ H_2O, 0.5% $MnSO_4·H_2O$, 0.05% H_3BO_3 and 0.05% $NaMoO_4·2H_2O$.

Synthetic Crossing Medium (SCM) was used to induce sexual development. SCM contains 0.1% KNO_3, 0.07% K_2HPO_4, 0.05% KH_2PO_4, 0.05% $MgSO_4·7H_2O$, 0.01% $CaCl_2·2H_2O$, 0.01% NaCl, 0.1 ml of 50 μg/ml biotin, 0.1 ml of trace elements, 1.5% sucrose, and 1.0% agar [EMD, Darmstadt, Germany (69)]. Media was supplemented with 100 μg/ml of histidine or 200 μg/ml of hygromycin as needed. For propagating strains, 13x100 mm glass tubes filled with 2.5 ml of VM supplemented with agar (slants) were inoculated with cultures. Slants were grown in constant dark for three days at 30°C, followed by two days in constant light at 25°C. They were then stored at 4°C and used for inoculations for no longer than 2 months.

Strain Construction-The Δ*gnb-1*, Δ*gna-2* double mutant was made using genetic crosses between single mutants [(16); see Table 1]. The Δ*gna-2* strain was used as the female in this cross. The presence of the mutations in the progeny was verified by

diagnostic PCR (for Δ*gna-2*, Δ*gnb-1* double mutant), using gene-specific and hygromycin (*hph*) cassette specific primers. Primer sequences are given in Table 2.

***Neurospora* genomic DNA extraction-** Cultures for *Neurospora* genomic DNA extraction were grown in 18x150 mm glass tubes filled with 4 ml of VM liquid medium, after inoculation with a small amount of hyphae. After overnight growth at 30°C with shaking at 200 rpm, cultures were collected using a vaccum filtration system (Millipore, Billerica, MA) and filtered on grade 1 filter paper circles (Whatman, GE Healthcare, Piscataway, NJ). Cell pads were placed in 2.0 ml screw-cap tubes, frozen in liquid nitrogen and either stored at -80°C or used immediately. Using a plastic rod and liquid nitrogen, the tissue was ground and the Puregene DNA isolation kit (Qiagen, Gaithersburg, MD) was used to extract DNA according to the manufacturer's procedure. The cell lysis buffer included 20 mg/ml of Proteinase K, and the samples were incubated at 55°C for 1-2 hours.

Isolation of macroconidia- Strains were grown in 125 ml Erlenmeyer flasks containing 30 ml of VM agar plus required supplements for three days in constant dark at 30°C, followed by five days in constant light at 25°C. Conidia were harvested by adding 50 ml H_2O to the flask, agitating it using a vortex mixer and then filtering the solution through cheesecloth into another 125 ml sterilized flask. Conidia were transferred to a 50ml conical tube and centrifuged at 2500 rpm for 5 min at room temperature using the IEC CL3 centrifuge (Thermo Scientific, Waltham, MA). The pellet was then washed twice

with 30 ml of sterile H_2O and resuspended in 1 ml of H_2O. Conidia were counted using a hemacytometer.

Phenotypic Analysis. All cultures were inoculated using conidia, except for the Δ*gnb-1*, *gna-3*^{Q208L} G3-C strain that produces very little conidia; in this case, cultures were inoculated with a small amount of aerial hyphae. To determine aerial hyphae height, 13x100 mm glass tubes containing 2 ml of VM liquid medium were inoculated with the strains and then incubated for five days in dark and one day in light at room temperature. To analyze conidiation in submerged cultures, 30 ml of liquid medium was inoculated with conidia at a concentration of 1x 10^6 cells/ml (except for strain G3-C, which was inoculated using ~120 mg of packed aerial hyphae) and incubated with shaking at 200 rpm for 16 hr at 30°C. Cultures were viewed and photographed at 60X magnification, using a DIC (Differential Interference Contrast) oil immersion objective (N.A.=1.42) with an Olympus IX71 inverted microscope (Olympus America, Center Valley, PA) and a QIClickTM CCD camera (QImaging, Surrey, British Columbia, Canada). Images were analyzed using Metamorph software (Molecular Devices Corporation, Sunnyvale, CA). For fertility assays, strains were inoculated onto SCM plates and incubated for six days in constant light at 25°C. Cultures were fertilized with males (macroconidia) of opposite mating type and incubated for six more days before being photographed using an SZX9 stereomicroscope (Olympus) with a Powershot G10 camera (Canon USA, Lake Success, NY) at a magnification of 57X.

Results

Construction of a Δ*gnb-1*, Δ*gna-2* double mutant.

The Δ*gnb-1*, Δ*gna-2* double mutant was created through a sexual cross using the Δ*gna-2* mutant as the female parent, and the Δ*gnb-1* strain as the male parent. Once ascospores were collected, they were plated on FGS plates supplemented with hygromycin. The ascospores were then picked onto VM slants supplemented with hygromycin. The cultures were incubated in the dark for three days at 30˚C and then transferred to the light at 25˚C for two days. After genomic DNA extraction, PCR reactions were performed using a *gna-2* gene-specific primer and a *hph* primer to test for the presence of the Δ*gna-2* mutation (Table 2). The positive PCR product was 2.5 kb (Figure 1A). Samples that were positive for the Δ*gna-2* mutation were then tested with the *gnb-1* gene-specific and *hph* cassette primers (Table 2), to detect the *gnb-1* knock-out mutation.. A strain that had the necessary band detecting the *hph* cassette for both mutations was chosen as the Δ*gnb-1*, Δ*gna-2* double mutant.

GNA-3 and GNB-1 may operate in a linear pathway to negatively regulate submerged conidiation, while GNA-1 and GNA-2 are independent of GNB-1

Previous work has demonstrated that heterotrimeric G proteins are essential for normal asexual and sexual development of *N. crassa* (25, 30, 34, 74). The goal of this study was to identify the Gα subunits that interact with the GNB-1/GNG-1 Gβγ dimer in *N. crassa* during regulation of different cellular functions. We first utilized a genetic

approach to determine whether there was evidence for an epistatic relationship between *gnb-1* and the three Gα genes that would support a physical interaction between the encoded proteins in a heterotrimeric complex. Double mutants containing the Δ*gnb-1* and one Gα deletion mutation were produced using sexual crosses between single mutants. We also created strains expressing GTPase-deficient, constitutively activated Gα alleles in the Δ*gnb-1* background using a *N. crassa* gene targeting system that directs DNA sequences to the *his-3* locus (2). All three activated alleles were expressed using the *ccg-1* promoter (7, 42) in order to eliminate the effects of different protein expression levels.

The results of the genetic analysis were interpreted as follows (see Fig.2): The observation that the Δ*gnb-1* ΔGα double mutant has the same phenotype as the Δ*gnb-1* single mutant and that introduction of the constitutively activated Gα allele does not suppress the Δ*gnb-1* phenotype shows that *gnb-1* is epistatic to the Gα gene and supports GNB-1 acting downstream of the Gα in a linear pathway (Fig 2A). Conversely, the finding that the Δ*gnb-1* ΔGα mutant has the same phenotype as the ΔGα mutant and that the activated Gα allele at least partially bypasses the Δ*gnb-1* phenotype indicates that the Gα gene is epistatic to *gnb-1* and suggests that the Gα protein acts downstream of GNB-1 in a linear pathway (Fig. 2B). The interpretation of any other combination of results from genetic analysis was that the Gβ and Gα are at least partially independent and likely operate in different signaling pathways to regulate the cellular function being assayed.

We began by assessing several phenotypes during asexual growth and development in the strains. During the asexual phase of the lifecycle, *N. crassa* grows by

extension, branching and fusion of hyphae to form the network structure called the mycelium (64). The asexual sporulation pathway, macroconidiation/conidiation, begins with differentiation of aerial hyphae from the mycelium, followed by constriction of the aerial hyphal tips to form the mature conidia (64). Since conidiation is induced by exposure to air, wild-type liquid submerged cultures do not normally produce conidia (64). We have previously demonstrated that Δ*gna-1*, Δ*gna-3* and Δ*gnb-1* single mutants produce conidiophores in submerged culture (28, 74). Δ*gna-1* mutants do so in a cell density-dependent manner, only forming conidiophores at relatively high inoculation densities [$3x10^6$ cells/ml or greater; (26)]. In order to increase the stringency of our screen, we assessed submerged cultures for the presence of conidiophores at an inoculation density of $1x10^6$ cells/ml, a condition that leads to conidiation in Δ*gna-3* and Δ*gnb-1*, but not Δ*gna-1* mutants.

As previously shown (29, 74)the only single mutants that produce conidiophores in submerged culture are those lacking *gnb-1* or *gna-3* (Fig. 3A). Further deletion of any of the three Gα genes in the Δ*gnb-1* background leads to a phenotype identical to that of Δ*gnb-1* (Fig. 2A). Introduction of the constitutively activated *gna-1*^{Q204L} or *gna-3*^{Q208L} alleles into the Δ*gnb-1* background abolished inappropriate conidiation (Fig. 3A). In addition, hyphae in the Δ*gnb-1*, *gna-3*^{Q208L} strain were wider than in the other strains. The *gna-2* ^{Q205L} allele yielded a partial correction, with some conidiophores present among the normal hyphae. These results suggest that *gna-3* is epistatic to *gnb-1*, since single and double mutants conidiate in submerged culture and *gna-3*^{Q208L} corrects the conidiation defect in the Δ*gnb-1* background. This is consistent with GNB-1 acting

upstream of GNA-3 in a linear pathway to negatively regulate submerged conidiation. In contrast, the two genetic epistasic assays gave opposite results for *gna-1* and *gna-2*; the findings from double mutant analysis suggest that *gnb-1* is epistatic to *gna-1* and *gna-2*, while those from strains carrying the *gna-1*^{Q204L} or *gna-2* ^{Q205L} allele support *gna-1* and *gna-2* epistatic to *gnb-1*. Observation of opposite results for the two epistasis assays is most consistent with at least partial independence of GNA-1 and GNA-2 from GNB-1 during negative control of submerged conidiation.

Aerial hyphae height and production of conidia on solid medium involve different epistatic relationships

We next investigated epistatic relationships between *gnb-1* and the three Gα genes during aerial hyphae production in standing liquid cultures and conidiation on solid medium (Fig. 2B). As previously determined, Δ*gnb-1*, Δ*gna-1* and Δ*gna-3* strains have shorter aerial hyphae than wild type; (25, 29, 73-74) Fig. 3B), while Δ*gna-2* resembles wild type in its aerial hyphae height (3); Fig. 3B). Deletion of a single Gα gene in the Δ*gnb-1* background results in aerial hyphae heights similar to the Δ*gnb-1* mutant (Fig. 2B). Δ*gnb-1* strains carrying the *gna-2* or *gna-3* activated Gα alleles have aerial hyphae heights similar to Δgnb-1 (Fig. 3B). Aerial hyphae are also denser in these strains (Fig. 2C; data not shown). These results are consistent with *gnb-1* epistatic to (acting downstream of) *gna-2* and *gna-3* with respect to aerial hyphae height, as double mutants and Δ*gnb-1* strains carrying the activated *gna-2* or *gna-3* allele resemble the Δ*gnb-1* single mutant. In contrast, the relationship between *gnb-1* and *gna-1* is more consistent

with at least partial functional independence, as the Δ*gnb-1*, *gna-1*^{Q204L} strain has an aerial hyphae height greater than Δ*gnb-1*.

Δ*gnb-1* strains produced the greatest amount of conidia in plate cultures in our study, followed by Δ*gna-3* mutants (Fig. 3C). Δ*gnb-1* strains carrying any of the three activated Gα genes resulted in less conidia production than Δ*gnb-1*. For example, levels in the Δ*gnb-1*, *gna-1*^{Q204L} and Δ*gnb-1*, *gna-3*^{Q208L} strains were even lower than wild type, with Δ*gnb-1*, *gna-3*^{Q208L} near zero (Fig. 3C). This indicates that all three activated Gα genes can negatively regulate conidia production in the Δ*gnb-1* background. With regards to epistatic relationships between *gnb-1* and *gna-1* and *gna-2*, the observation that double mutants have levels of conidia much closer to Gα single mutants and that Δ*gnb-1* strains carrying *gna-1*^{Q204L} or *gna-2* ^{Q205L} have levels lower than Δ*gnb-1* mutants is most consistent with *gna-1* and *gna-2* epistatic to *gnb-1*. In contrast, the epistatic relationship between *gnb-1* and *gna-3* is less clear, as conidia levels are actually less in Δ*gnb-1* Δ*gna-3* double mutants than in either single mutant, and lower still in Δ*gnb-1*, *gna-3*^{Q208L} strains.

We also observed differences in orange pigmentation, indicative of carotenoid production, in the strains (Fig. 3D). The intensity of pigmentation roughly correlated with the extent of conidiation, with Δ*gnb-1*, *gna-1*^{Q204L} and Δ*gnb-1*, *gna-3*^{Q208L} strains much lighter than wild type. In the case of the strain Δ*gnb-1*, *gna-3*^{Q208L}, the suppression yielded a white hyphal mass (Fig. 3D).

Constitutive activation of Gα proteins does not restore sexual fertility to Δ*gnb-1* mutants

Nitrogen starvation induces the sexual cycle by leading to production of female reproductive structures (protoperithecia) (55). (55) Protoperithecia produce specialized chemotropic hyphae (trichogynes) that grow towards male cells of opposite mating type (8, 55). During the course of cell fusion, fertilization and meiosis, the protoperithecium enlarges to form the perithecium. Approximately two weeks after fertilization, sexual spores (ascospores) are ejected that can germinate to form vegetative hyphae (55).

During the sexual cycle, Δ*gnb-1* and Δ*gna-1* mutants are male-fertile, but female-sterile [(74); Fig. 4A)]. Although these strains produce protoperithecia and trichogynes, their trichogynes have a defect in chemotropism and are not attracted by male cells (25, 30, 34, 74). In contrast, Δ*gna-2* and Δ*gna-3* mutants produce protoperithecia and develop perithecia after fertilization with wild-type males (3). In this study, we observed that all Gα, Δ*gnb-1* double mutants resembled Δ*gnb-1* single mutants, forming protoperithecia but not perithecia after fertilization (Fig. 4A). The sexual cycle phenotypes of Δ*gnb-1*, *gna-1*^{Q204L} and Δ*gnb-1*, *gna-2*^{Q205L} strains were similar to Δ*gnb-1* (Fig. 3B), with the Δ*gnb-1*, *gna-1*^{Q204L} strain exhibiting a delay in protoperithecial development (data not shown). In contrast, the *gna-3*^{Q208L} allele completely inhibited protoperithecial formation in the Δ*gnb-1* background (Fig. 4B).

We have previously hypothesized that the block in fertility of Δ*gnb-1* mutants may be a consequence of low GNA-1 protein levels (74). The findings from the double mutant analysis presented here are consistent with this idea, as Δ*gnb-1* is epistatic to Δ*gna-2* and Δ*gna-3* and has the same phenotype as Δ*gna-1*. Furthermore the results with

the *gna-1*^{Q204L} allele corroborate those from a previous study showing that although GNA-1 is required for chemotropism of female trichogynes towards male cells, constitutive activation of *gna-1* cannot rescue the defect in chemotropism caused by loss of the pheromone receptor (30). The delayed perithecial development of Δ*gnb-1, gna-1*^{Q204L} strains and the complete inhibition of protoperithecial development by *gna-3*^{Q208L} suggests that GNA-1 and GNA-3 must cycle through inactive and active forms during fertilization and protoperithecial development, respectively.

Discussion

We have previously demonstrated that GNB-1 is essential for the correct functioning of Gα and Gγ protein subunits in *N. crassa* (34, 74). In the absence of GNB-1, levels of the three Gα proteins and GNG-1 are severely reduced (74), consistent with the fact that Gβ and Gγ are tightly bound to each other as a heterodimer (34). In this study, we explored the relationship between the GNB-1/GNG-1 dimer and the three Gα proteins in signal transduction using a genetic approach.

The genetic approach involved analysis of Gα Δ*gnb-1* single and double mutants and Δ*gnb-1* strains carrying activated Gα alleles. Models that summarize the different epistatic relationships are presented in Figure 4. The results indicate that *gna-3* is epistatic to *gnb-1* for negative regulation of submerged culture conidiation (Fig. 5A), while *gna-1* and *gna-2* are epistatic to *gnb-1* with regards to negative control of aerial conidiation (Fig. 5C). These observations suggest that GNB-1 is necessary for activation of the Gα proteins which then regulate conidiation. In contrast, *gnb-1* appears to act downstream of *gna-2* and *gna-3* to regulate aerial hyphae height (Fig. 5B), consistent with GNA-2 and GNA-3 as positive regulators of GNB-1 for this trait. A caveat to these conclusions is the reduced levels of Gα proteins in a mutant lacking the Gβ or Gγ subunit; this scenario complicates interpretation of the results from genetic analysis (34, 74). However, all Δ*gnb-1* mutant phenotypes cannot be explained by reduced levels of Gα proteins, as a mutant lacking all three Gα genes has much more severe defects in asexual and sexual growth and development than the Δ*gnb-1* strain (28). Finally, the observation that constitutive activation of any Gα suppresses the hyperconidiation defects

of Δ*gnb-1* mutants suggests that all three proteins are negative regulators of conidia production (Fig. 5A, C). This observation complements previous results establishing synergy between Gα gene deletion mutations during regulation of conidiation in *N. crassa* (28). However, our previous finding that *gna-2* acts in a compensatory fashion to *gna-1* and *gna-3* to regulate conidiation suggests that the role of *gna-2* is relatively minor compared to the other two Gα genes.

There was no clear epistatic relationship between *gnb-1* and *gna-3* with regards to aerial conidiation (Fig. 3B). Loss of *gna-3* leads to increased conidiation, while constitutive activation of *gna-3* in the Δ*gnb-1* background reduces conidiation to nearly zero, consistent with *gna-3* as a strong negative regulator of conidiation. However, conidia levels are lower in the Δ*gnb-1*, Δ*gna-3* double mutant than in either single mutant. This last observation may reflect the presence of low levels of constitutively active Gα proteins in the strains lacking *gnb-1*. These strains lack the Gβγ tether that prevents the Gα proteins from signaling in the absence of an activated GPCR. In this scenario, the recently discovered cytosolic guanine nucleotide exchange factor RIC8 may function to load GTP on the remaining free Gα proteins. We have shown that RIC8 binds to and regulates GDP/GTP exchange on GNA-1 and GNA-3 in *N. crassa* (72).

Our results demonstrate that the three Gα genes are epistatic to *gnb-1* for submerged (*gna-3*) or aerial (*gna-1* and *gna-2*) conidiation (Fig. 5A, C). This indicates that the Gα proteins are likely to interact directly with downstream effector proteins. Since elevated cAMP levels correlate with suppression of conidiation in *N. crassa* (57), one probable effector is adenylyl cyclase (CR-1), which converts ATP to cyclic AMP.

GTP (Gα)-dependent adenylyl cyclase activity can be assayed in submerged liquid cultures of *N. crassa* (58). We have shown that loss of *gna-1* leads to reduced GTP-dependent adenylyl cyclase (CR-1) activity (but normal CR-1 protein levels) in extracts from submerged liquid cultures, supporting adenylyl cyclase as a downstream effector of GNA-1 (27). Δ*gnb-1* mutants have normal CR-1 protein levels, but reduced GTP-stimulatable adenylyl cyclase activity, consistent with decreased GNA-1 protein amount in these strains (74). In contrast, mutation of *gna-3* leads to reduced CR-1 protein levels, but does not influence GTP-dependent activity (29), and *gna-2* has no apparent effect on adenylyl cyclase protein levels or activity (27-28). This last point implies that GNA-2 and GNA-3 interact with another/additional downstream effector(s). These observations, in combination with the known conidiation defects of *N. crassa* MAP kinase mutants (38, 51-52) suggest that additional effectors (such as MAP kinase modules) operate downstream of GNA-1,GNA-2, GNA-3 and GNB-1 to regulate conidiation.

We observed differences in pigmentation in the strains during this study. Previous work in our laboratory and others has established an inverse relationship between levels of carotenoid pigments and cAMP (10, 32, 73). For example, loss of *gna-1* leads to increased carotenoid amount and lowered cAMP, while constitutive activation results in reduced levels of carotenoids and elevated cAMP (73). Furthermore, our previous work indicates that *gna-3* has a more profound positive influence on cAMP levels than *gna-1* (27, 29). Taken together, these observations are consistent with our results showing that *gna-3*^{Q208L} strains are less pigmented than *gna-1*^{Q204L} mutants. They

also reinforce the notion that regulation of cAMP levels is an important downstream function of heterotrimeric G proteins in *N. crassa*.

Regulation of female fertility likely involves GNB-1 regulating protein levels of GNA-1, the active subunit during mating (Fig. 5D). GNA-3 plays a role in ascospore ejection and viability, as few ascospores are ejected and are viable from homozygous Δ*gna-3* crosses (29)(Fig. 5D). Female fertility was not restored by transformation of the Δ*gnb-1* mutant with any activated Gα alleles. The observation that activation of GNA-1 is not sufficient to restore full mating in Δ*gnb-1* mutants is consistent with results from a similar experiment conducted in a strain background lacking a pheromone receptor gene (30). The inability to restore female fertility by expressing a GTPase-deficient *gna-1*^{Q204L} allele may stem from a need for both GNA-1-GDP and GNA-1-GTP at different times during protoperithecial development, mating, meiosis and/or ascospore formation. Alternatively, GNB-1 may be absolutely necessary for normal sexual development and this requirement cannot be bypassed by activation of *gna-1* or the other two Gα genes. The *gna-3*^{Q208L} allele completely inhibited development of female reproductive structures, suggesting that GNA-3 needs to be in the inactive GDP-bound form during at least some critical stages of this process in *N. crassa*. This observation is consistent with the relatively normal functioning of Δ*gna-3* mutants (that completely lack GNA-3 protein) as females during crosses with wild-type males (29).

Our results can be compared to those of studies in *A. nidulans* and *C. neoformans*, where a single constitutively activated Gα allele has been tested for its ability to suppress defects of a Gα mutant. The results showed that an activated Group I Gα allele bypassed

defects resulting from mutation of the Gβ gene in *A. nidulans* but not in *C. neoformans*. In *A. nidulans*, the authors conclude that the Gα can function independently of Gβ to regulate proliferative growth. In contrast, the findings from *C. neoformans* suggest interdependence of the Gα and Gβ for downstream signaling.

Comparing and contrasting the genetic epistasis of *gnb-1* and the Gβ- like gene *cpc-2* with the Gα genes would reveal the similarities and differences in regulation of the G protein signaling pathway by these two WD-repeat proteins. This possibility is explored in the third chapter of this thesis.

Table 1- *N. crassa* strains used in this study.

Strains	Relevant genotype	Source or Reference
74 A-OR23-1A (74A)	Wild type, *mat A*	FGSC[a] 987
74 a-OR8-1a (74a)	Wild type, *mat a*	FGSC 988
a^{m1}	*a^{m1} cyh-1 ad3B*	FGSC 4564
his-3a	*his-3, mat a*	Ref. (34)
1B4	Δ*gna-1::hph*$^+$, *mat A*	Ref. (27)
1B8	Δ*gna-1::hph*$^+$, *mat a*	Ref. (27)
Δ2	Δ*gna-2::hph*$^+$, *mat a*	FGSC 12377
3lc2	Δ*gna-3::hph*$^+$, *mat A*	Ref. (29)
hβJ	Δ*gnb-1::hph*$^+$, *his-3, mat a*	"
42-5-11	Δ*gnb-1::hph*$^+$, *mat A*	Ref. (74)
42-5-18	Δ*gnb-1::hph*$^+$, *mat A*	"
5A	Δ*gng-1::hph*$^+$ FLAG-*gng-1*$^+$*::his-3*$^+$, *mat a*	Ref. (34)
G1-F	Δ*gnb-1::hph*$^+$, *his-3*$^+$*::gna-1*^{Q204L}, *mat a*	This Study
G2-C	Δ*gnb-1::hph*$^+$, *his-3*$^+$*::gna-2*^{Q205L}, *mat a*	"
G2-D	Δ*gnb-1::hph*$^+$, *his-3*$^+$*::gna-2*^{Q205L}, *mat a*	"
G3-C	Δ*gnb-1::hph*$^+$, *his-3*$^+$*::gna-3*^{Q208L}, *mat a*	"

G1-23	Δ*gna-1::hph*$^{+}$, Δ*gnb-1::hph*$^{+}$, *mat a*	”
G2-5	Δ*gna-2::hph*$^{+}$, Δ*gnb-1::hph*$^{+}$, *mat A*	”
G3-21	Δ*gna-3::hph*$^{+}$, Δ*gnb-1:: hph*$^{+}$, *mat A*	”

[a] FGSC, Fungal Genetics Stock Center, Kansas City, MO

Table 2: Primers used to make and verify Δ*gna-2* Δ*gnb-1* mutant

Primer	Sequence
gna-2ORF FW	GCATCTGGATATGCCCTCAT
gna-2ORF RV	GTTGGCCTAGGTCGAAAACA
hph FW	CGCCCCAGCACTCGTCCGAGGGC
hph RV	GGCATTCATTGTTGACCTCCA
GNB-1ORF FW	TAAAACCACTAGCGCCTTGG
GNB-1 ORF RV	GCATCTGTAACTAGGCAGG

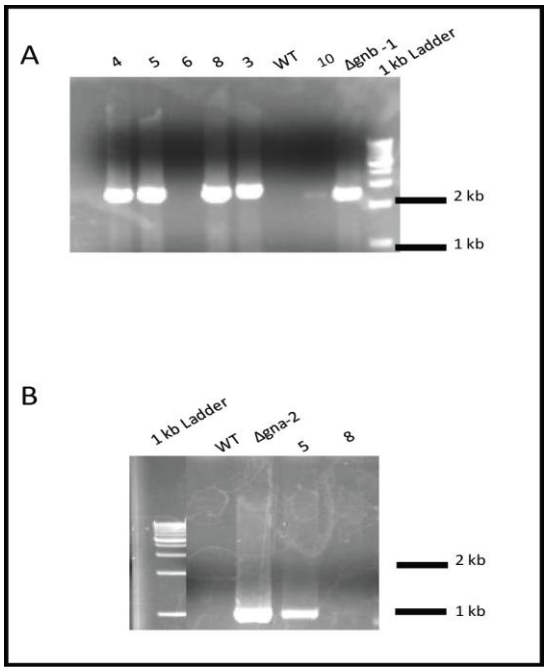

Figure 1: Analysis of progeny from a cross of Δ*gna-2* to Δ*gnb-1* using diagnostic PCR. A) PCR was performed on genomic DNA using the GNB-1 FW and *hph* FW primers (Table 2). The Δ*gnb-1* positive band is 2.5kb. B) PCR using GNA-2ORF FW and *hph* RV primers. The *gna-2* wild-type band is 1.0 kb.

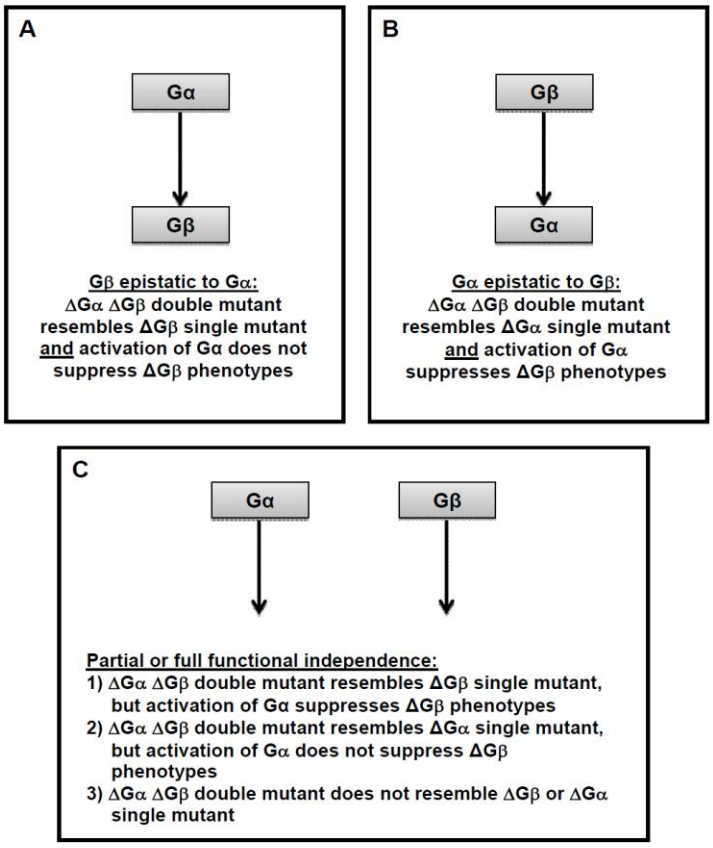

Figure 2: Scheme for determining epistasis. A) If the Δ*Gα* Δ*gnb-1* double mutant resembles the Δ*gnb-1* mutant, and introducing Gα activated alleles does not correct the phenotypic defects of Δ*gnb-1*mutant, then the Gβ is epistatic to the Gα gene. B) If the Δ*Gα* Δ*gnb-1* mutant resembles the single Δ*Gα* mutant and introducing Gα activated alleles suppresses the Δ*gnb-1*phenotype, then the Gα is epistatic to the Gβ. C) If the results from the phenotypes indicate two different relationships, then independence is assumed.

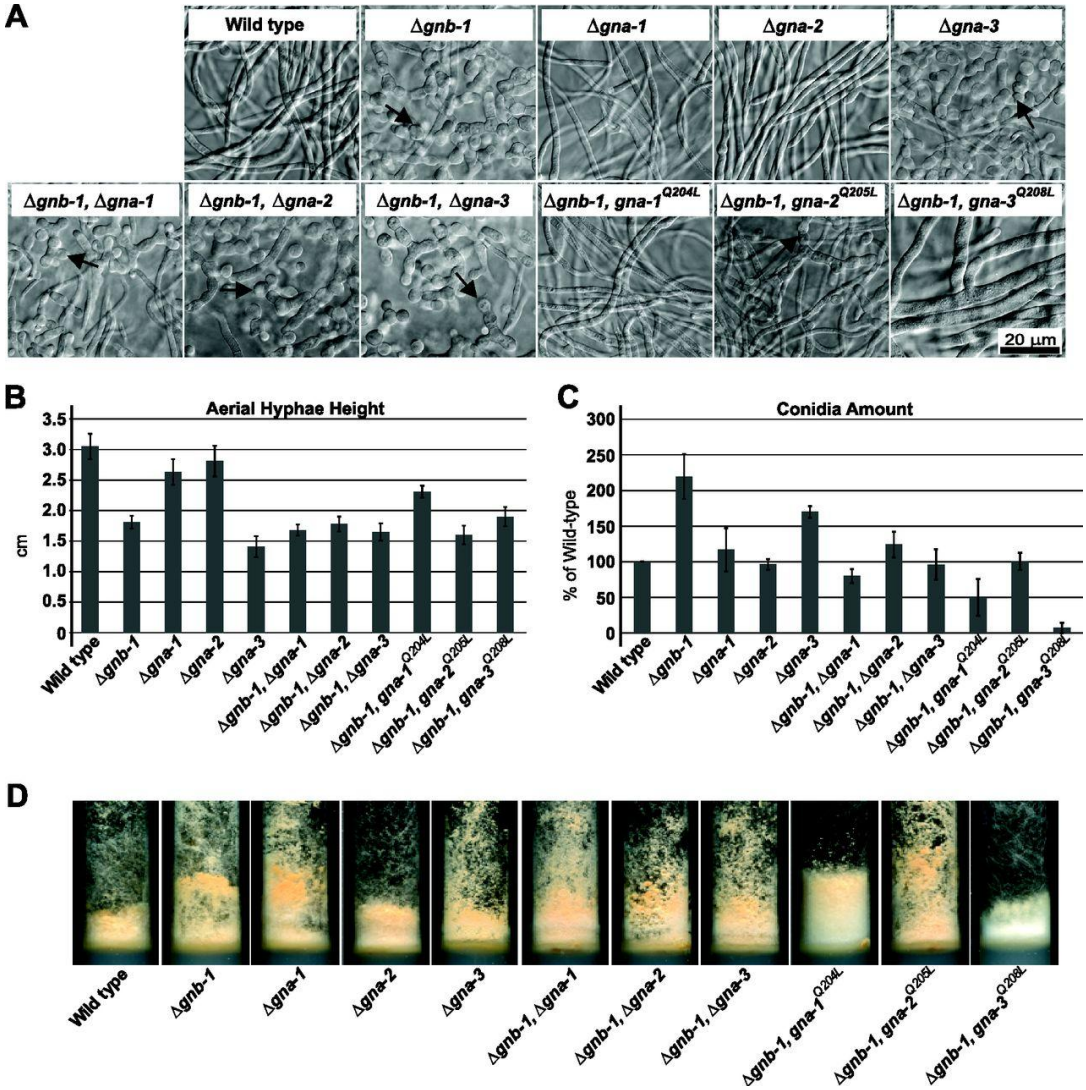

Figure 3- Phenotypes during asexual growth and development. Strains are wild type (74a) and Δ*gnb-1* (42-5-18), Δ*gna-1* (1B4), Δ*gna-2* (Δ2), Δ*gna-3* (31c2), Δ*gna-1* Δ*gnb-1* (G1-23), Δ*gna-2* Δ*gnb-1* (G2-5), Δ*gna-3* Δ*gnb-1* (G3-21), Δ*gnb-1 gna-1*^{Q204L} (G1-F), Δ*gnb-1 gna-2*^{Q205L} (G2-C), and Δ*gnb-1 gna-3*^{Q208L} (G3-C) mutants. (A) Submerged cultures. Strains were cultured in VM liquid medium for 16 h with shaking at 200 rpm in the dark at 30°C. The arrows indicate conidiophores. (B) Aerial hyphal height. To measure aerial hyphal height, liquid VM tube cultures were inoculated with the indicated strains and incubated statically for 5 days in the dark and 1 day in light at room temperature. Values are from six replicates, with error calculated as the standard error of the mean. (C) Amount of conidia. VM agar flasks were inoculated with the indicated strains and incubated for 3 days in the dark at 30°C and 5 days in light at room temperature. Conidia were harvested from flasks and quantitated using a hemacytometer. Values are expressed as percentages of the wild type from three independent experiments, with the error calculated as the standard error of the mean. (D) Strain morphology in VM agar tube cultures. Strains were cultured in tubes containing 2 ml of VM agar medium for 3 days in the dark at 30°C and 5 days in light at room temperature.

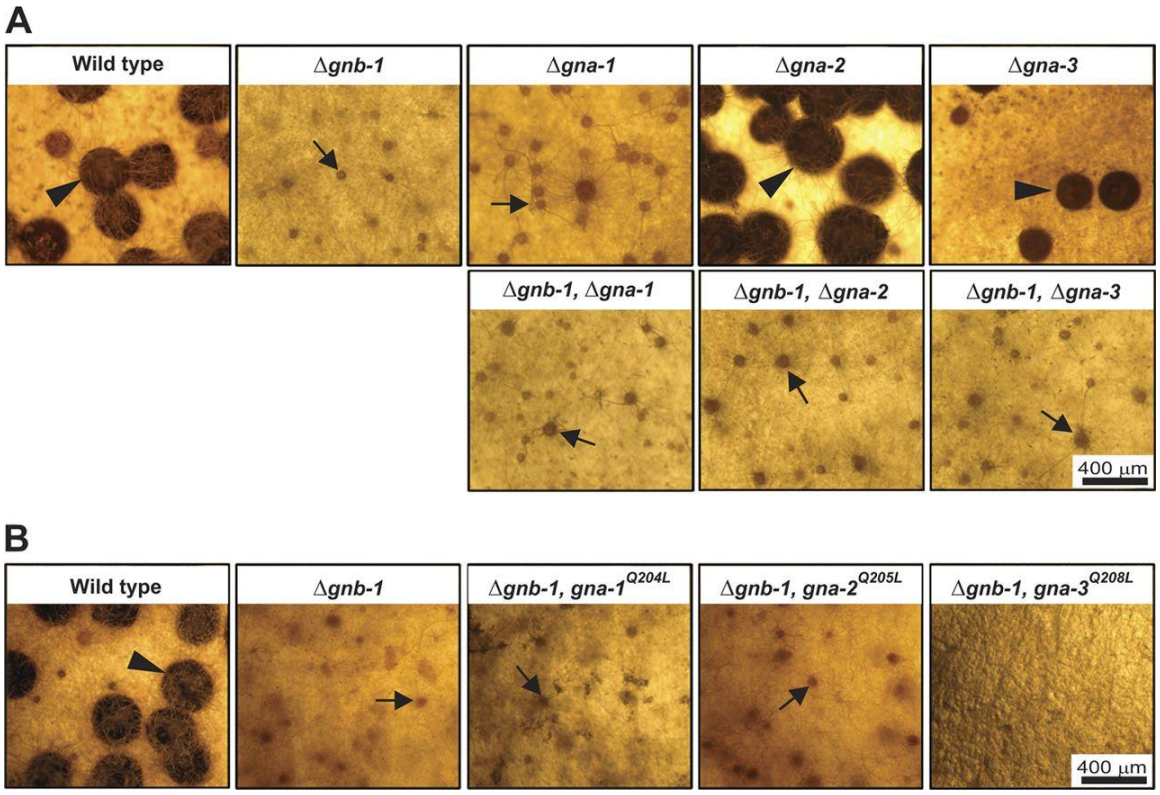

Figure 4- Sexual phase phenotypes. Strains were inoculated onto SCM plates to induce production of female reproductive structures (protoperithecia) and incubated for 6 days in constant light at 25°C. Cultures were then fertilized with males (macroconidia) of opposite mating type and incubated for six more days before being photographed. Protoperithecia are indicated by black arrows, while perithecia are marked by black arrowheads. (A) Single and double mutants. Strains are wild type (74a) and Δ*gnb-1* (42-5-11), Δ*gna-1* (1B4), Δ*gna-2* (Δ2), Δ*gna-3* (31c2), Δ*gnb-1* Δ*gna-1* (G1-23), Δ*gnb-1* Δ*gna-2* (G2-5), and Δ*gnb-1* Δ*gna-3* (G3-21) mutants. (B) Strains carrying Gα-activated alleles. Strains are wild type (74a) and Δ*gnb-1* (42-5-11), Δ*gnb-1 gna-1*^{Q204L} (G1-F), Δ*gnb-1 gna-2*^{Q205L} (G2-C), and Δ*gnb-1 gna-3*^{Q208L} (G3-C) mutants.

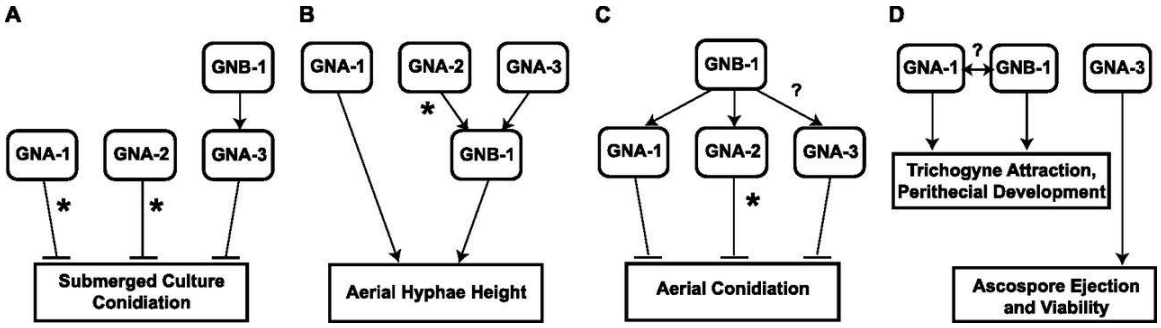

Fig 5. Models for interactions between Gα proteins and the Gβγ dimer in *Neurospora*. (A) Submerged culture conidiation. GNB-1 acts upstream of GNA-3 to suppress conidiation in submerged cultures. The independent action of GNA-1 and GNA-2 is observed only in Δ*gnb-1* strains that express constitutively activated *gna-1* or *gna-2* alleles (denoted by asterisks). (B) Aerial hyphal height. GNA-2 and GNA-3 operate upstream of GNB-1 to positively modulate aerial hyphal height. The asterisk indicates that for *gna-2*, a phenotype is seen only upon constitutive activation in the Δ*gnb-1* background. GNA-1 positively regulates aerial hyphal height independently of GNB-1. (C) Aerial conidiation. GNA-1 and GNA-2 are downstream of GNB-1 during negative regulation of conidiation on solid medium. The role for *gna-2* is revealed only by the presence of the *gna-2*^{Q205L} allele in the Δ*gnb-1* background (denoted by the asterisk). GNA-3 is a strong negative regulator of aerial conidiation, but the epistatic relationship between *gna-3* and *gnb-1* is not clear from our analysis (denoted by a question mark). (D) Female fertility. Although GNB-1 and GNA-1 regulate trichogyne attraction and perithecial development, their epistatic relationship is unclear and the role of GNB-1 may be to maintain GNA-1 protein levels (denoted by the question mark above the double-ended arrow). GNA-3 is required for ascospore ejection and viability, while GNA-2 has no obvious function in regulating female fertility.

Chapter 3- Analysis of the *Cross Pathway Control-2* (*cpc-2*) gene

In *Neurospora crassa,* the heterotrimeric G protein signaling pathway is one of the signal transduction cascades that enables the fungus to sense and respond to its environment. It consists of G Protein Coupled Receptors (GPCRs) that have a seven-helix transmembrane structure and the G protein subunits- Gα, Gβ and Gγ. In an inactive state, the Gαβγ trimer is bound to the GPCR at the membrane. Ligand stimulation causes exchange of GDP for GTP on the Gα, causing the Gα-GTP to dissociate from the Gβγ heterodimer. The Gα-GTP and the Gβγ dimer then regulate downstream effectors, leading to changes in cellular physiology. The Gα-GTP has native GTPase activity that causes release of the inorganic phosphate from the GTP. The Gα re-associates with the GDP, leading to signal termination and completion of the cycle. GPCRs are also known as the Guanine nucleotide Exchange Factors (GEFs) and recently a cytosolic non-receptor GEF, called Resistance to Inhibitors of Cholinesterase 8 (RIC8) has been identified and characterized in *N. crassa* (40, 72).

Receptor for Activated C Kinase-1 (RACK1) is a major scaffolding mammalian protein, homologous to Gβ subunit proteins. It has a seven tryptophan-aspartate (WD) repeat structure, and is one of the best studied proteins of the WD repeat in this protein family (1). Initially identified as a protein that binds to the active conformation of PKCβII, it is now known to be multifunctional (1, 56). For example, RACK1 allows cross talk between the PKC and Mitogen Activated Kinase (MAP) pathways, by acting as a scaffold for the Jun N-terminal Kinase (JNK) upon stimulation, leading to PKC-mediated phosphorylation and activation of JNK (41). Specific residues in RACK1 are

needed to stabilize the activity of Protein Phosphatase 2A (PP2A) and allow it to interact with β-1 integrin [reviewed in (1)]. With regard to the Gαβγ heterotrimer, it has been observed that RACK1 binds to the Gβγ dimer in HEK293 cells, and also regulates a subset of its functions. The association of RACK1 with the Gβγ dimer promotes its dislocation from the cytosol to the membrane.(12). Recently, it has been shown that RACK1, along with the Gβγ dimer and another protein named WDR26, regulate chemotaxis and cell polarization in Jurkat T-cells (59).

Homologs of RACK1 have been implicated as alternative Gβ subunits in the fungi kingdom, such as Asc1p in *Saccharomyces cerevisiae* and Gib2 in *Crytpococcus neoformans* (49, 75). Asc1p functions as a Guanine Dissociation Inhibitor (GDI) for the Gα Gpa2 along with being involved in regulating glucose responsiveness, through its binding with adenylyl cyclase (Cyr1) (75). *gib2*, an essential gene, in *C. neoformans*, encodes a protein that binds to the Gα Gpa1 and two Gγ subunits, Gpg1 and Gpg2. It also binds to Smg1, a downstream target of cAMP signaling, and to the protein kinase C homolog Pkc1 (49).

Additional orthologs of RACK1, such as Cpc2 in *Schizosaccaromyces pombe*, RAK1 in *Ustilago maydis* and Cross Pathway Control-2 (CPC-2) in *Neurospora crassa*, have been shown to regulate various aspects of growth and development (43-44, 67). The RACK1 ortholog Cpc2 in *S. pombe* plays a role in cell cycle regulation and stress responses through ribosomal association (47) . Mutants lacking *cpc2* are increased in size, indicating a defect in the G2/M transition in the mitotic cycle (43). Cpc2 modulates this control by regulating the protein levels and the activity of the Wee1 kinase (48). In

relation to oxidative stress, Cpc2 positively regulates the synthesis of a stress response transcriptional factor Atf1, through translation control (47). Rak1, the RACK1-related protein in *U. maydis,* is essential for the transcription of *rop*1, which is a direct positive regulator of the pheromone response factor (prf1), making it essential for mating (67). Strains lacking RAK1 also have attenuated filamentation and virulence, and abnormal cell morphology (67).

The CPC-2 protein in *N. crassa* was initially identified as a component of the general amino acid regulation network (33). Starvation for a single amino acid leads to an overall derepression of all amino acid biosynthetic genes at the level of transcription (5). Loss of the *cpc-2* gene blocks derepression of amino acid biosynthetic genes during amino acid limiting conditions (33). Under non-starved conditions, loss of the *cpc-2* gene decreases growth by 50% during the asexual cycle (44). In the sexual cycle, the Δ*cpc-2* mutant lacks protoperithecia, and is female-sterile (44). Other components of this cross pathway control network are *cpc-1*, homologous to *GCN4* (50), and *cpc-3*, the *N. crassa* equivalent of *GCN2* (60). Analysis of Δ*cpc-2* Δ*cpc-3* and Δ*cpc-2* Δ*cpc-1* double mutants showed that *cpc-2* characteristic phenotypes, such as reduced growth and female infertility, were not masked. This shows that *cpc-2* has broader functions operating outside of amino acid control (60).

Given the 70% positional identity between RACK1 and CPC-2, we have investigated the role of CPC-2 in the heterotrimeric G protein pathway. Using gene deletion mutants and strains containing constitutively activated Gα alleles, we have analyzed genetic epistasis between components of the G protein pathway and the *cpc-2*

gene. I identified binding partners for the CPC-2 protein using a yeast two hybrid approach. Furthermore, this study also revealed evidence for roles for Gα proteins in amino acid regulation.

Materials and methods

Strains and media- *N. crassa* strains used in this study are listed in Table 1. Strains were cultured in Vogel's minimal medium (VM) for vegetative growth (See Chapter 2). To induce sexual development, Synthetic Crossing Medium (SCM) was used (See Chapter 2). Media was supplemented with 100µg/ml of histidine or 200 µg/ml of hygromycin, as indicated. For media with 3- amino-triazole (3AT), a 1M stock solution of 3AT (Sigma-Aldrich, St. Louis, MO) was made by dissolving 0.84 g of 3AT in 10 ml of sterile H_2O. This solution was filter sterilized using a 0.45µm syringe filter (Fisher Scientific, Waltham, MA) and a 3 ml syringe (BD, Franklin Lakes, NJ). It was then stored in a foil-wrapped 15 ml conical tube at 4˚C for no longer than 10 days. Strains were propagated using the same methods described in Chapter 2. Conidia were isolated as described previously in Chapter 2. A concentration of $1x10^6$conidia/ml was used for inoculating liquid cultures for western blots and co-immunoprecipitation experiments.

Double mutant strain construction- Δ*cpc-2,* Δ*gna-1;* Δ*cpc-2,* Δ*gna-2*; Δ*cpc-2,* Δ*gna-3;* Δ*cpc-2,* Δ*gnb-1;* and Δ*cpc-2,* Δ*gng-1* double mutants were made using genetic crosses between single mutants [(16), see Table 1]. In cases where both single mutants in the cross are female-sterile (Δ*gnb-1,* Δ*cpc-2,* Δ*gng-1* and Δ*gna-1*), the strain used as the female was a heterokaryon with the a^{m1} helper strain (53). The presence of the mutations in the progeny was verified by diagnostic PCR using gene-specific and *hph* cassette specific primers (3, 26, 29, 74).

Construction of the Δ*cpc-2* strains containing activated Gα alleles- Vectors containing the GTPase-deficient, constitutively activating mutations *gna-1*^{Q204L} (73), *gna-2*^{Q205L} (3) and *gna-3*^{Q208L} were previously made using site-directed mutagenesis (3, 73). The final targeting plasmids were pSVK51 (*gna-1*^{Q204L}), pSVK52 (*gna-2*^{Q205L}) and pSVK53 (*gna-3*^{Q208L}). *Escherichia coli* strain DH5α was used to maintain all plasmids.

For electroporation, the washed pellet was suspended in 1 ml of cold 1M sorbitol, and a concentration of 2.5x10^9 conidia/ml was used. Electroporation of *N. crassa* with 1-2 µg of pSVK51, 52 or 53 was as previously described (25), using the Δ*cpc-2, his-3* strain as the recipient. For transformation, macroconidia were harvested as described above. A desired concentration of 2.5x10^{9}conidia per ml was obtained, and approximately 80 µl of conidia was mixed with 10 µl of plasmid DNA and kept on ice for a 5 minutes. This mix was then added to a pre-chilled 2mm plastic cuvette. Electroporation was done using a 2510 electroporator set at 2000V, with pulsing twice to achieve an efficiency of 5.2-5.4. Then 960 µl of sorbitol was added in the cuvette and placed on ice. This was incubated with shaking for 1 hr at 30°C. The transformed conidia were then mixed in regeneration agar (2 ml of 50x VM, 18.2 g sorbitol, 1 g agar, 84 ml H_2O. 10x FGS additive was added to the mix after sterilization). This was then plated on FGS plates lacking histidine. Plates were incubated for 3-5 days in the dark at 30°C. The colonies were then picked using a sterile glass pipette onto VM slants, and incubated in the dark for three days at 30°C, and then transferred to constant light at 25°C for two days. They were then stored at 4°C.

Genomic DNA was extracted from transformants as described in Chapter 2 and subjected to Southern analysis for *gna-1* and *gna-2* as described (3, 73). *gna-3*^{Q208L} was

checked by digesting genomic DNA with *Hin*dIII and *Eco*RI at 37°C overnight. The digested DNA was mixed with an appropriate volume of 6x loading dye, and, along with 2 µl of the digoxigenin (DIG) ladder (Roche Diagnostics, Mannheim, Germany), was electrophoresed on a 1% agarose gel (in buffer containing 242 g Tris base, 57.1ml Acetic acid and 100 ml of 0.5M EDTA in 1L of H_2O, TAE buffer) in 1x TAE running buffer. The gel was run at 90 volts for 3-4 hours. The gel was then stained in a 1:10 dilute solution of ethidium bromide in TAE for 10-15 minutes. The gel was photographed using a UVP imager (UVP Bioimaging Systems, Upland, CA). The gel was then treated with denaturing solution (200mM NaOH, 600mM NaCl) for 45 minutes, and then in neutralizing solution (1M Tris-Cl, pH 7.4, 1.5M NaCl) for 45 minutes and then in 2X SSC for 15 minutes. To make 20X SSC buffer, 175.3 g NaCl, and 88.2 g Sodium citrate was dissolved in 1L of H_2O. A 2X SSC solution was made by diluting the 20X stock 10-fold using water. To set up the transfer, wet filter paper (cut to the size of the gel) was placed on top of a 0.45 µm MAGNA nylon transfer membrane, (GE Water & Process Technologies, Boulder, CO) wetted with 2XSSC. Bubbles were rolled out with a plastic pipette. Parafilm was placed all around the sandwich so that no buffer would leak through. A stack of paper towels and a heavy weight was placed on the topmost filter paper. The transfer was performed at room temperature overnight. The next day, the membrane was carefully removed and then cross-linked at 1200V using CL-1000 Ultraviolet Crosslinker (UVP, Upland, CA) for 1 min on each side. The membrane was then dried and stored in the dark or probed immediately.

The *his-3* probe for Southern analysis was made using the *Hin*dIII insert from pRAUW122 [contains the *his-3* gene; (2)]. The 8.8 kb fragment was extracted from a 0.7% agarose TAE gel, using the QiaxII gel extraction kit (Qiagen, Germantown, MD). The extracted DNA fragment was boiled for 5 min. and then added to mix [4µl of 5X labeling buffer, 0.5µl of DNA, 0.8 µl BSA, 1.5 µl Klenow polymerase (Promega, Madison, WI) and 1 µl of DNTP mix]. This mixture was incubated at 37°C overnight, and then quenched by incubating at 65°C for 10 min. Subsequently, 50 µl of sterile H_2O was added to the tube and it was heated to 95°C to denature the DNA. This mixture was then added to the DIG Easy Hyb solution (Roche diagnostics, Mannheim, Germany).

The membrane was treated with 70 ml of pre-hybridization buffer for 30 min, and the probed at 42°C overnight in a hybridization oven (Fisher Scientific, Waltham, MA). The next day, the probe was removed and stored at -80°C. The membrane was washed with 70 ml of 2xSSC/1% SDS solution with shaking for 10 min at room temperature, and then with 70 ml of pre-heated (65°C) 0.1% SDS/0.1%SSC buffer at 65°C twice for 15 min. A solution containing 63ml of 1x maleic acid (0.1M maleic acid, 0.15M sodium chloride, pH 7.5) and 7 ml of 10X blocking buffer was used to block the membrane for an hour, after which the primary DIG antibody (Roche Diagnostics, Mannheim, Germany) was added to the blocking buffer at a 1:200 dilution. This solution was incubated with the blot for 30 min at room temperature. The membrane was then washed using a 1x solution of 10X DIG Set Wash Buffer Set (Roche, Mannheim Germany), 3 times for 15 min, following a wash with detection buffer. The membrane was then exposed to the CDP star detection reagent (Roche Diagnostics, Mannheim,

Germany), sandwiched between transparency sheets, and then placed in a cassette. A 8" x10" Denville film (South Plainfield, NJ) was placed over the membrane and the blot was exposed for 5min, 15 min and 2 hr to overnight. The film was then developed and analyzed. Using this probe, wild type has 3.6 and 6.0 kb hybridizing bands, while strains with *gna-3* integrated at the *his-3* locus have 3.6, 3.5 and 2.4 kb hybridizing fragments.

Purification of homokaryotic strains using microconidiation- Transformants determined to have a single integration event of the transformating DNA at the *his-3* locus were purified to homokaryons using microconidiation (20). The medium for microconidiation consisted of 0.1x SCM medium, 0.5% sucrose, 2% agar and 1 mM iodoacetic acid (IAA). The medium was made by first sterilizing a solution that contained 3.8 g agar, 0.7g sucrose in 178 ml. Then 20 ml of this sterilized SCM medium was mixed with 2 ml of filter-sterilized 0.1 M IAA. The IAA was filtered using a 5.0 micron filter unit (Millex-SV, EMD-Millipore, Billerica, MA) and a 3 ml syringe (BD) and added to the medium after cooling. An aliquot containing 5 ml of this medium was pipetted into 18 x 150 mm glass test tubes and set to cool. The slants were then inoculated with the heterokaryons, and placed in constant light at 25°C for 12-14 days. To harvest microconidia, 2 ml of sterile H_2O was added to each slant, vortexed for 30 sec. and then filtered through a 5.0 µm filter (Millex-SV, EMD-Millipore, Billerica, MA) into a sterile 1.5 ml microcentrifuge tube. The solution was then centrifuged at 2000 x g for 5 min, and all but 100 µl of the supernatant poured off. The remaining solution and pellet was plated on FGS plates, with ~50 µl/plate. The FGS plates were placed in the

dark for 2-3 days at 30°C, or until colonies were visible. The individual colonies were then picked with sterile glass pipettes and inoculated onto VM slants. These slants were then incubated in the dark for 3 days at 30 C and in the light for 2 days at 25˚C. Genomic DNA was extracted from these strains (as described above) and they were analyzed using Southern analysis (as described above) to confirm that the strains were homokaryons.

Complementation of the Δ*cpc-2* mutation *in trans*- A *cpc-2* complementation construct was generated by amplifying the *cpc-2* ORF from pKB55, using primers CPC2-XbaI FW and CPC2-BamHI RV (See Table 2), and introducing *Xba*I and *Bam*HI restriction sites, respectively. The fragment was then ligated into the pGEM-T vector (digested with *Xba*I and *Bam*HI. This resulted in plasmid pAG1 which was then sequenced to ensure that no mutations were introduced during construction. The insert was then excised using *Xba*I and *Bam*HI and ligated into pMF272 digested with the same enzymes. This resulted in generation of a *his-3* targeting vector with CPC-2 as an in-frame fusion upstream of GFP (plasmid pAG2). This plasmid was transformed into a Δ*cpc-2*, *his-3* strain (made by James Kim, unpublished data) using electroporation (as described above). Transformants were plated on FGS medium and picked on to VM slants to select for histidine prototrophs.

Transformants were checked for expression of the GFP-fusion protein by placing 50 µl of a conidial suspension in liquid VM on a glass slide with a coverslip and observing using a DIC (Differential Interference Contrast) oil immersion objective (N.A.=1.42) with the GFP filter with an Olympus IX71 inverted microscope (Olympus

America, Center Valley, PA). Images were captured using QIClickTM CCD camera (QImaging, Surrey, British Columbia, Canada). Images were analyzed using Metamorph software (Molecular Devices Corporation, Sunnyvale, CA). Wild-type and a Δ*cpc-2* strain were used as negative controls to check for auto-flourescence.

Western analysis- Submerged cultures (500 ml of liquid VM) were inoculated with conidia to a final concentration of $1x10^6$ cells/ml and grown as described for western analysis, above. Tissues were pulverized in liquid nitrogen using a mortar and pestle and then transferred into a large bead-beater chamber (Biospec) with glass beads and cold extraction buffer (10mM HEPES pH 7.5, 0.5 mM EDTA, 0.1% Fungal Protease Inhibitor Cocktail (FPIC), 200 mM PMSF and 0.1% DTT). The tissue was homogenized three times for 30 sec. and then spun at 1000 x g for 15 min at 4°C. Approximately 50 µg of supernatant protein (whole cell extract) was loaded onto a 10% SDS-PAGE gel. T

The resolving gel was made using 3.12 ml acrylamide (40% w/v), 3.06 ml H_2O, 6.25ml buffer A (2x), 60 µl of 10% ammonium persulfate (APS), and 7 µl of TEMED. 2x buffer A was made by mixing 90.75 g of Tris-Base and 2 g of SDS, adjusting the pH to 8.8 and bringing the volume of solution to 500 ml. The solution was then filter-sterilized using 0.22 µm Millipore Stericup filter (EMD-Millipore, Billerica, MA) and stored at 4°C. The stacking gel was made by mixing 500 µl of acrylamide, 2.5 mls of buffer B, 60 µl of 10% APS, 7 µl of TEMED, and 2ml of H_2O. Once the running and the stacking gels were set for about 1 hr each, the gel was loaded and run using 1x running buffer at 60mA for approximately 3 hr or until the dye front was completely run off. The 1x running

buffer was made by diluting the 10x buffer (30 g Tris base, 143.75 g glycine and 5 g SDS in 1 L H_2O). After running the gel, it was transferred to a 0.45 µm nitrocellulose membrane (GE water and process technologies, Boulder, CO), using transfer buffer (12 g Tris-base, 56.6 g glycine, 800 ml methanol and H_2O in a total volume of 1 L) in a Bio-Rad apparatus at 200 mA for 3 hr at room temperature.

Once the membrane was ready, it was dried and reacted with the specific antibody as indicated (primary and secondary). Following this reaction, chemiluminescent detection was performed using the Super Signal West Pico Chemiluminescent Substrate kit (Thermo Fisher, Rockford, IL). An aliquot containing 1 ml of the Peroxidase solution was mixed with 1 ml of the Luminol Enhancer solution, and the membrane was incubated with this solution for 5 min before imaging.

Phenotypic analysis- To determine aerial hyphae height, 13x100 mm glass tubes containing 2 ml of VM liquid medium were inoculated with conidia and then incubated for three days in dark at 25°C. The height was measured from the base of mycelium to the top of the aerial hyphae. Fertility assays and analysis of conidiation in submerged culture were performed as described in the Chapter 2. Apical extension was assessed by inoculating VM plates with 1 µl of conidial suspension followed by incubation in dark at 30°C for 24 hr, after which the diameter of the colony was measured. For assessing apical extension under amino acid-starvation conditions, the VM medium was supplemented with freshly made 3-aminotriazole (3-AT) at concentrations of 0.5, 1.0, 2.0 and 4.0 mM. For analysis of conidial germination, 10 ml of VM agar medium was poured into 100 mm

petri plates, and inoculated with 50 µl of conidia at a concentration of 8 $X10^6$ per ml and incubated at 30°C in the dark for 0, 4, 6 and 8 hr. Cells were then visualized at the time points using differential interference contrast (DIC) microscopy using an Olympus IX71 inverted microscope (Olympus America, Center Valley, PA) with a 606 oil immersion objective (NA = 1.42). Images were captured using a QIClickTM digital CCD camera (QImaging) and analyzed using Metamorph software (Molecular Devices Corporation).

Statistical Analysis- For analyzing the quantitative traits (aerial hyphae height development, apical extension on minimal medium and on medium containing 3-AT), GraphPad Prism 6.0 (GraphPad Software Inc, La Jolla, CA) was used. For detecting and eliminating outliers, the Rout's test was used (Q value = 1.0%). For detecting statistical significance, the Uncorrected Fisher's Least Significant Difference (Fisher's LSD) test was used. The P-value cutoff was set to 0.05%, confidence intervals were set at 95% and pair-wise comparisons were made. Graphs were created using Microsoft Excel (Microsoft, Redmond, WA).

Construction of a *N. crassa* strain containing an epitope-tagged version of the CPC-2 protein at the native locus for immunoprecipitation experiments- A construct containing the *cpc-2* ORF with the S epitope tag (KETAAAKFERQHMDS) at the amino terminus was targeted to the *cpc-2* locus in the Δ*mus52*::*hph* strain. Sequences for all primers are given in Table 2. To generate a S-tag fusion construct with the *bar* resistance cassette, primers CPC2ORF FW and CPC2ORF RV were used to amplify the 5'

untranslated region (UTR) and the CPC-2 ORF and the N-terminus of the S-tag. CPC2Bar FW and CPC2Bar RV amplified the C-terminus of the S-tag sequence, and the *bar* resistance cassette. Finally, CPC2UTR FW and the CPC2UTR RV amplified the 3' UTR of the *cpc2* gene. These fragments, along with pRS426 (14) linearized with *HindIII* and *XhoI*, were transformed into yeast strain FY834 (70) to facilitate yeast recombinational cloning. The final construct was pAG3 (15).

pAG3 was then transformed into the Δ*mus52*::*hph* strain using electroporation (described above). Transformants were plated on FGS plates supplemented with Ignite (20 ml 50X VM, 10 g agar 880 ml H2O, 100 ml 10X FGS solution after sterilization, 5 g L-proline). 10X FGS solution was made using 200 g sorbose, 5 g fructose in 1 L of water and filter sterilization after. Colonies were then transferred onto VM-proline slants containing Ignite. Resistant transformants were checked by PCR for the tagged *cpc-2* allele using primers S-tag FW and S-tag RV (Table 2). Strains were also checked for production of S-tagged CPC-2 using western analysis. A tube containing 5 ml of VM liquid medium was inoculated with hyphae from slants and grown for 16-18 hr with shaking at 200 rpm at 30°C. The tissue was collected using filter paper grade 1 circles (Whatman, GE Healthcare, Piscataway, NJ) by vacuum filtration. A western analysis was done (as described above) with 500-800 µl of extraction buffer (described above). The membrane was then allowed to dry, and then washed 3x in TBST [diluted from a stock of 1x TBST, which was made by mixing 24.2 g Tris base, 80 g NaCl,bringing to pH 7.6 (by adding concentrated HCl) and brought to a volume of 1L, and 0.1% Tween-20]. The membrane was blocked at room temperature with shaking for 30-60 min using 5% milk

in TBST solution. To this solution, the S-tag primary antibody (Bethyl Labs) was added at a concentration of 1:4000. The membrane was incubated with the primary antibody at 4°C overnight with shaking. The next day, the membrane was rinsed three times with TBST and then probed with the secondary antibody (Goat anti-Rabbit IgG, peroxidase conjugated, Sigma) in 5% milk in TBST solution for 1-2 hr at room temperature with shaking. The membrane was then washed three times with TBST for 15 min each.

In order to purify the heterokaryotic transformants into uninucleate homokaryons, the transformants that expressed S-tagged CPC-2 were crossed to a wild-type strain. Ascospores were collected with a wet swab and transferred into a 1.5 ml sterile tube containing 1 ml of sterile H_2O and aliquots were plated onto FGS-proline plates containing Ignite. Ascospores were picked onto VM-proline slants containing Ignite, and the slants were incubated in the dark for 3 days and in constant light for 3 days. Western analysis (described above) was performed on these samples with the S-tag antibody to identify strains with the tagged CPC-2.

Submerged cultures (500 ml of liquid VM) were inoculated with conidia to a final concentration of $1x10^6$ cells/ml and grown as described for western analysis, above. Tissues were pulverized in liquid nitrogen using a mortar and pestle and then transferred into a large bead-beater chamber (Biospec) with glass beads and cold extraction buffer [50 mM Tris-Cl pH 8.0, 1 mM EDTA, 6 mM $MgCl_2$, 0.1% Fungal Protease Inhibitor Cocktail (Sigma), 2.5 mM PMSF, and 1 mM GDP]. The tissue was homogenized three times for 30 sec. and then centrifuged using a JA-25.50 rotor (Beckman) at 1000xg for 10 min at 4ºC to remove cell debris. Protein was quantified using Bradford protein assay

(Bio-Rad), and an aliquot containing 50 mg of protein was brought to 1% lauryl maltoside and incubated on a rotating mixer at 4ºC for 2-3 hr. The sample was then centrifuged at 46,000 x g for 30 min. using a JA-25.50 rotor (Beckman). Protein was quantified using the Bradford protein assay and 15 µl S-tag agarose beads were added to 4-6 mg of extract protein in 1.5 ml tubes. The solution was incubated on a rotating mixer at 4 C overnight. The next day, tubes were centrifuged at 200 x g for 1 min at room temperature in a microcentrifuge (Beckman Coulter, Brea, CA). The supernatant was carefully pipetted out, and 200 µl extraction buffer (described above) was used to wash the beads twice, each time discarding the supernatant. The second time, 20-25 µl 5x Lammelli buffer was added to each tube, and the mixture was heated at 95°C for 5 min to release the protein from the beads. The dye and beads mixture was then centrifuged. The supernatant, along with the detergent -solubilized input was loaded onto 10% SDS-PAGE gels. Approximately 25 µl of supernatant was loaded into each lane, with 5 µl of the P7719S protein ladder (New England Biolabs, Ipswich, MA) as a molecular weight standard.

The S-tag westerns were performed as described above. For the Gα westerns (GNA-1 or GNA-3), the primary antibody was added at a concentration of 1:1000 or 1:2000 respectively, in 5% milk in TBST and incubated at a room temperature with shaking for 3 hrs. For the RIC8 western, the RIC8 antibody (Asharie Campble,, Ilva Cabrera and Katherine Borkovich, unpublished) was added at a concentration of 1:5000 in 5% milk in TBST. The membrane was incubated with the primary antibody at 4°C overnight with shaking. The next day, the membrane was rinsed three times with TBST

and then probed with the secondary antibody (Goat anti-Rabbit IgG, peroxidase conjugated, Sigma) in 5% milk in TBST solution for 1-2 hr at room temperature with shaking. The membrane was then washed three times with TBST for 15 min each, followed by imaging.

Yeast two hybrid assay- Yeast two-hybrid vector construction and yeast transformation- Using the cDNA of the *cpc-2* ORF from plasmid pKB55, the *cpc-2* ORF was amplified using primers CPC2-BamHI-FW and CPC2-PstI-RV, introducing *Bam*HI and *Pst*I restriction sites, respectively. The insert was then cloned in the pGAD424 and pGBKT7 vectors (Clonetech), using restriction digestion and ligation, and then transformed into *E. coli* competent cells (strain DH5α). DNA from transformants was then extracted, checked using colony PCR with construct-specific primers and then sequenced. This yielded plasmids pAG4 containing CPC-2 in the pGAD424 backbone, and pAG5 containing CPC-2 in the pGBKT7 backbone. These constructs were then transformed into yeast strains AH109 or Y187. For transformation, the yeast strains were grown up at 30°C for 4-5 hours with shaking at 200 rpm in baffled-bottom flasks containing 50 ml of YPDA media (6 g yeast extract, 12 g dextrose, 12 g peptone, 60 mg adenine hemisulfate, 10 g agar, bring to 600 ml, sterilized). After making sure the OD at 600 nm did not exceed 1.0, the cells were then centrifuged at 2500 rpm in 50 ml conical tubes and pellet was rinsed in 25 ml of sterile water. After centrifugation, the pellet was resuspended in 1 ml of 100 mM LiCl and then transferred to a 1.5ml microcentrifuge tube. After centrifugation at 15,000 rpm, the pelleted cells were resuspended in 400 µl of

100 mM LiCl. An aliquot containing 50 µl of these cells was combined with the transformation mix containing 240 µl of polyethylene glycol 4000, 12 µl of 3 M LiCl, 50 µl of carrier DNA (salmon sperm, boiled for 5 min prior to use), 5 µl of plasmid DNA and water, for a total volume of 360 µl. This mixture was mixed on a vortex mixer, resuspended and incubated at 30°C for 30 min, and then at 42°C for 30 min. The mixture was then spun down at 15,000 rpm and the supernatant was pipetted out. The cells were resuspended in 1 ml sterile water, and centrifuged for 15 sec. Most of the supernatant was removed, and the remainder (100-200 µl) was plated on SD selective medium (26.7 g drop out base with glucose, 2 g drop out mix, 1.5% agar, pH 5.8 with NaOH) at 30°C for three days in the dark. For plasmid pGBKT7, SD -Trp was used, and for PGAD424, SD-Leu was used.

The yeast two hybrid assay was performed as described previously (39). To generate diploids, the CPC-2 in pGAD424and CPC-2 in pGBKT7 in yeast were mated (using streaking with a sterilized metal loop) to strains containing one of the three Gα genes, GNB-1, GNG-1 or RIC8, as well as MAP Kinase pathway vectors (NRC-1, OS-4, STE7, STE50, MAK2 and MEK1) on synthetic medium lacking tryptophan and leucine and then incubated for 2-3 days at 30°C in the dark. Diploids were then streaked on medium lacking tryptophan, leucine, histidine and/or adenine and incubated in the dark at 30°C for 4-5 days to select for expression of the *ADE2* or the *HIS3* reporter gene. Appropriate positive and negative controls were used (Clonetech).

Results

***N. crassa* CPC-2 is homologous to RACK1 proteins from other organisms.-** It is known that the CPC-2 protein is 316 amino acids in length, and has 70% positional identity with RACK1 (44). Amino acid sequences of RACK1, CPC-2, its fungal homologs, and Gβ subunit proteins were first aligned by Multiple Sequence Alignment using ClustalW (37). A rooted tree with branch lengths was then made using the UPGMA method (37). It is seen that RACK1 and other Gβ like proteins cluster together, separately from the known Gβ proteins (Fig 1). The homologs of RACK1 from budding yeast (Asc1p) and *A. gossypii* (AFR199C) form an out-group as compared to the other RACK1 fungal homologs. When the Gβ subunit proteins are compared, budding yeast and *A. gossypii* proteins also cluster separately from the other proteins. Overall, CPC-2 and GNB-1 from *N. crassa* are most similar to their homologs from *S. macrospora*, *M. oryzae* and *A. clavatus* (Fig 1).

***gna-3* is epistatic to *cpc-2* during submerged culture conidiation, while *gna-1* and *gna-2* are independent**. It is known that the components of the G protein signaling pathway are crucial for asexual and sexual development of *N. crassa* (27, 29, 32, 34, 72). To understand genetic epistasis between *cpc-2*, the three Gα genes, and *gnb-1* and *gng-1*, double mutants lacking *cpc-2* and one other gene were generated using sexual crosses. In addition, strains containing a single constitutively activated, GTPase-deficient Gα allele in the Δ*cpc-2* background were generated, by targeting the Gα allele to the *his-3* locus (2).

The results were interpreted in the same manner as in Chapter 2 and in reference (71): If the phenotype of the double mutant Δ*cpc-2* Δ*Gα* resembles the phenotype of the Δ*Gα* strain, and if the activated Gα allele bypasses the phenotype of Δ*cpc-2*, then the Gα gene is downstream (epistatic) to *cpc-2.* If the opposite is true, then *cpc-2* is epistatic to the Gα gene. As indicated in Chapter 2, if contradicting results are seen, this is interpreted as the two genes being partially or completely independent in regulation of the phenotype being assessed.

We first assessed conidiation in submerged culture. During asexual growth and development, *N. crassa* grows by elongation and branching of hyphae, eventually forming a network called the mycelium (64). From this mycelium, aerial hyphae grow upward and spore-forming structures are elaborated from the tips. The spores are the multinucleate macroconidia. Since conidiation is usually induced by contact with air, wild-type *N. crassa* does not produce conidia in submerged liquid cultures (64). Using the same strategy and approach described in Chapter 2, it was seen that the Δ*cpc-2* mutant inappropriately produces chains of conidiophores in submerged cultures, similar to Δ*gna-3,* Δ*gnb-1* and Δ*gng-1* strains (Fig 2A) When activated Gα alleles are introduced into the Δ*cpc-2* background, the *gna-3*^{Q208L} allele corrected the defective phenotype of the Δ*cpc-2* strain, abolishing formation of conidiophores. Introducing *gna-1*^{Q204L} gave a partial correction of the phenotype, with some conidiophores present among hyphae in the submerged cultures. The *gna-2* ^{Q205L} yielded no correction of the conidiophore phenotype. Analyzing double mutants revealed that the Δ*cpc-2* ,Δ*gna-1* double mutant does not form conidiophores in submerged cultures, similar to wild-type and Δ*gna-1*.

Likewise, the Δ*cpc-2*, Δ*gna-2* double mutant resembles the Δ*gna-2* mutant, with only hyphae present. However, the Δ*cpc-2*, Δ*gna-3* double mutant has conidiophores, similar to those produced by Δ*gna-3.* These results suggest that *gna-3* is epistatic to *cpc-2*, since the Δ*cpc-2* Δ*gna-3* strain most resembles Δ*gna-3,* and the activated allele *gna-3*^{Q208L} corrects the conidiation defect (Fig 2A). In regards to *gna-1,* some weak epistasis is seen, because the activated allele *gna-1*^{Q204L} only partially corrects the Δ*cpc-2* defective phenotype. *gna-2* exhibits independence from *cpc-2* during submerged culture conidiation, because the Δ*cpc-2* Δ*gna-2* double mutant resembles Δ*gna2,* whereas the Δ*cpc-2, gna-2* ^{Q205L} strain resembles the Δ*cpc-2* mutant (Fig 2A)

***gnb-1* and *gng-1* operate downstream of *cpc-2* during submerged culture conidiation**- To study epistasis between *cpc-2*, *gnb-1*, and *gng-1*, Δ*cpc-2* Δ*gnb-1* and Δ*cpc-2* Δ*gng-1* double mutants were analyzed (Fig 2A). It has been previously shown that Δ*gnb-1* and Δ*gng-1* single mutants have identical phenotypes and form conidiophores in submerged culture (34). The double mutants most resembled the individual Δ*gnb-1* or the Δ*gng-1* single mutant, consistent with *gnb-1* and *gng-1* operating downstream of *cpc-2*.

***gna-3, gnb-1* and *gng-1* are epistatic to *cpc-2* with regards to aerial hyphae height.** We next investigated epistatic relationships between *cpc-2* and the other genes during aerial hyphae production in standing liquid cultures. From the data set collected, statistical outliers were identified, using the Q-test, and eliminated. Multiple pair-wise

comparisons were made. This helped us to identify statistically significant differences between strains for this quantitative trait, using the T-test. (Table 3). As seen in the graph in Fig 2B, all of the single gene deletion mutants have an aerial hyphae height defect. Δ*gnb-1* and Δ*gng-1* have similar aerial hyphae heights, with no statistically significant difference between the two mutants. Deletion of *gna-3* in the Δ*cpc-2* background results in an aerial hyphae height similar to that of the Δ*gna-3* mutant (Table 3). In addition, the *gna-3*^{Q208L} allele provides the greatest correction of the defects of the Δ*cpc-2* mutant among all the activated allele strains, consistent with *gna-3* epistatic to *cpc-2*. Analysis of the double mutant Δ*cpc-2*, Δ*gna-2* shows the opposite result: the value is significantly different than Δ*gna-2* (p=0.0148), but is statistically similar to that of Δ*cpc-2* (p=0.6619). Introducing the *gna-1*^{Q204L} allele or the *gna-2* ^{Q205L} in the Δ*cpc-2* background not only does not bypass the defects of the Δ*cpc-2* strain, but actually worsens the aerial hyphae height defect (Fig 2B). The Δ*cpc-2*, Δ*gna-1* double mutant shows a synergistic effect of the individual Δ*cpc-2* and Δ*gna-1* mutations. In agreement with this result, the Δ*cpc-2* Δ*gna-1* mutant is statistically different than the Δ*cpc-2* (p= <0.001) and Δ*gna-1* mutants (p=0.0005). These results are consistent with *gna-1* and *gna-2* regulating aerial hyphae height independently of *cpc-2*.

Analyzing the aerial hyphae height defect of Δ*cpc-2,* Δ*gnb-1* and Δ*cpc-2,* Δ*gng-1* mutants indicates that both the double mutants are statistically similar to the Δ*gnb-1* (p=0.1939) and Δ*gng-1* (p=0.1667) strains, respectively, suggesting that both *gnb-1*and Δ*gng-1* seem to be epistatic to *cpc-2* (Table 3).

***cpc-2* is epistatic to *gnb-1* and *gng-1* for apical extension of basal hyphae**. Analysis of colony growth over 24 hr in constant darkness on minimal medium revealed that Δ*cpc-2* is statistically different than wild-type during apical extension of basal hyphae (Table 4), with a growth reduction of 49% (Fig 2C). All double gene deletion mutant strains except the Δ*cpc-2* Δ*gna-2* mutant show significant differences from wild-type. With respect to epistasis between the Gα genes and *cpc-2*, analysis of the double mutants and strains carrying the activated Gα alleles in the Δ*cpc-2* background indicates functional independence. For example, the Δ*cpc-2, gna-3*^{Q208L} strain shows 80% growth as compared to wild-type, and is statistically similar to Δ*gna-3*, but different than Δ*cpc-2* (Table 4). The double mutant Δ*cpc-2* Δ*gna-3* is statistically similar to Δ*cpc-2,* but different than Δ*gna-3.*This indicates that *cpc-2* and *gna-3* independently regulate this phenotypic trait. It is noted that introduction of the *gna-1*^{Q204L} in the Δ*cpc-2* background results in minor correction of the slow growth phenotype (Fig 2C), but the Δ*cpc-2* Δ*gna-1* double mutant shows the most dramatic growth defect in the entire set of mutants, and has significantly different values than either single mutants (Table 4).

As noted previously, Δ*gnb-1* and Δ*gng-1* have a very similar apical extension defect (Fig 2c), and as indicated by statistical analysis (Table 4), are not significantly different from each other. The Δ*cpc-2* Δ*gnb-1* and Δ*cpc-2* Δ*gng-1* double mutants are statistically different (slower) than Δ*gnb-1* and Δ*gng-1* single mutants, but are not different than Δ*cpc-2.* This suggests that *cpc-2* seems to be epistatic to *gnb-1* and *gng-1* during apical extension (Table 2).

Δ*cpc-2* mutant shows no discernable defect during conidial germination- From analysis of apical extension, it is clear that Δ*cpc-2* has a growth defect. Growth defects can stem from a deficit in conidial germination or from slowed polar extension during hyphal growth. It has been previously shown that Δ*gna-3* and Δ*gna-1* Δ*gna-3* strains have significantly reduced germination rates relative to wild-type at all time points tested (18). The Δ*gna-1* mutant has a defect, but it is only statistically significant at 6 hr (18). This previous study also demonstrated that there is no significant difference in the germination rates for the Δ*gng-1* Δ*gnb-1* mutants when compared to the wild-type strain, except a slight delay in Δ*gng-1* strain at 4h post-inoculation (18). We thus assessed the conidial germination pattern of the Δ*cpc-2*, and the Δ*cpc-2* Δ*gnb-1* double mutant at 0, 4, 6 and 8 h post germination (Fig 3). It is seen that Δ*cpc-2* and the Δ*cpc-2* Δ*gnb-1* mutant has no discernible germination defect at the time points measured. Introducing the activated Gα alleles in the Δ*cpc-2* background produces results similar to the Δ*cpc-2* strain, with germination rates comparable to wild-type (Fig 3). However, it remains to be determined if deleting a single Gα gene in the Δ*cpc-2* background affects germination patterns.

Constitutive activation of the Gα alleles does not restore female fertility to the Δ*cpc-2* mutant, although the *gna-3*^{Q208L} leads to further progression in the sexual cycle. Results from the Chapter 2 show that the activated *gna-1*^{Q204L}, *gna-2* ^{Q205L} and *gna-3*^{Q208L} alleles were not able to restore fertility to the Δ*gnb-1* mutant. In fact, introduction of *gna-3*^{Q208L} resulted in complete inhibition of protoperithecial development, a phenotype that

was worse than that of the Δ*gnb-1* mutant (71). Δ*gnb-1* Δ*Gα* double mutant strains resembled the Δ*gnb-1* mutant, in that they formed protoperithecia, but no perithecia after fertilization (71).

During the sexual cycle, the Δ*cpc-2* mutant does not form protoperithecia (Fig 4). Therefore, it is blocked very early in the sexual cycle. Δ*cpc-2* Δ*Gα* double mutants do not form protoperithecia, similar to the Δ*cpc-2* strain. The sexual cycle phenotypes of the Δ*cpc-2, gna-1*^{Q204L} and the Δ*cpc-2, gna-2*^{Q205L} strains were similar to the Δ*cpc-2* mutant, with an absence of protoperithecia (Figure 4). The Δ*cpc-2, gna-3*^{Q208L} strain exhibited a unique phenotype--the strain progressed to produce protoperithecia, perithecia upon fertilization with conidia of the opposite mating type, and ascospores after perithecial maturation. These ascospores, however, do not germinate. Thus, the constitutively activated *gna-3*^{Q208L} allele allows the Δ*cpc-2* mutant to progress during the sexual cycle, but complete fertility is not restored.

As noted previously, the Δ*gnb-1* and the Δ*gng-1* strains form protoperithecia, but no perithecia, upon fertilization (34). The Δ*cpc-2* Δ*gnb-1* and the Δ*cpc-2* Δ*gng-1* mutants resemble the Δ*cpc-2* mutant with no protoperithecia produced (Fig 4). Thus, with regards to G protein subunit genes and mating, this analysis shows that *cpc-2* is the ultimate downstream regulator of the sexual cycle phenotype, as deletion of any G protein subunit gene in this background does not alter the Δ*cpc-2* sexual defect.

GNA-1 and GNA-3 interact with CPC-2 in a yeast two-hybrid assay. In related fungi, it has been shown that alternative Gβ subunits and homologs of CPC-2 interact

with Gα proteins (49, 75). No interaction has been been previously demonstrated between CPC-2 and the three Gα proteins in *N. crassa*. Using a yeast two-hybrid assay, we assayed components of the G protein signaling pathway to determine whether they interacted with CPC-2. It was observed that GNA-1 and GNA-3 interacted with CPC-2 in this assay (Fig 5). Interestingly, CPC-2 only interacts with GNA-1 and GNA-3 as a Gal4p binding domain fusion protein, but not as a Gal4p binding domain fusion protein (data not shown). This may indicate specific binding sites on CPC-2, GNA-1 and GNA-3 that produce such a result. No interaction was seen between CPC-2 and other known components of the G protein pathway, including GNA-2, GNB-1, GNG-1 and the RIC8 GEF. Several Mitogen Activated Protein (MAP) kinase pathway components were also tested for interaction with CPC-2, including NRC-1 (MAPKKK), OS-4 (MAPKKK; made by Carol Jones), MEK-1 (MAPKKK; obtained from Stephan Seiler), MAK-2 (MAPK; obtained from Stephan Seiler) STE7 (MAPKK; obtained from Stephan Seiler), STE50 (both N-terminus truncated and full-length versions; obtained from James Kim and Patrick Schacht, respectively) in the pGAD424 vector. All proteins were also tested in the pGKBT7 vector, except for STE50, to test for interaction in both orientations on medium lacking leucine, tryptophan, adenine and histidine. No interaction was seen with any of the MAP kinase pathway vectors (data not shown). Appropriate positive and negative controls (provided from Clonetech) were included in each testing of this assay.

Immunoprecipitation experiments with S-tagged CPC-2. An epitope-tagged version of the CPC-2 protein was created, with an S-tag (KETAAAKFERQHMDS) in the vector

backbone PRS426, using yeast recombinational cloning (14). The construct was targeted to the native *cpc-2* locus in the Δ*mus52*::*hph* strain (15), ensuring almost 100% homologous recombination. The transformed strain was checked for appropriate expression of the S-tag, using western analysis.

For immunoprecipitation, whole cell extracts, were prepared from a strain carrying the S-tagged CPC-2 and then immunoprecipitated using S-tag antibody coupled to agarose beads. A wild-type strain without the tagged protein was used as a negative control. The 32kDa S-tag band was detected in the whole cell extracts, input (protein solubilized with 1% lauryl maltoside) and the immunoprecipitated samples of the CPC-2-S-tag strain, but not in the negative control strain, as expected (Fig 6). This showed that the S-tag antibody was specific for the tagged CPC-2 protein.

To test for interaction between CPC-2 and components of the G protein signaling pathway, the immunoprecipitated fractions were analyzed for cross-reactivity using GNA-1, GNA-3 and RIC8 antibodies using western analysis (Fig 6B-6D). The results indicate that high background was observed. Also, it was seen that the protein was sticking to the beads, producing a band in the control samples (the wild-type strain) in the western blots. Therefore, the results were inconclusive.

In a reciprocal approach, extracts from the S-tagged CPC-2 strain and the negative control strain were immunoprecipitated using the RIC8 antibody, to test for a possible interaction between CPC-2 and RIC8. Using western analysis, the fractions from both strains exhibited a specific RIC8 band (50-53kDa), indicating that the antibody was able to immunoprecipitate RIC8 from these extracts (Fig 6E). However, due to high

background and proteins sticking to the beads, no conclusion could be drawn from this experiment.

GNA-1 and GNA-3 may play a role in cross-pathway control of amino acid synthesis- It is known that the Δ*cpc-2* mutant is sensitive to amino acid limitation conditions(33). Based on the results from genetic epistasis analysis and the interaction observed between CPC-2 and GNA-1 and GNA-3 in the yeast two-hybrid assay, I decided to explore a possible role for G proteins in cross pathway control. For these experiments, I analyzed apical extension of mutants on medium containing 3-aminotriazole (3-AT). 3-AT interferes with the activity of imidazole glycerol phosphate dehydrase, thus inhibiting histidine synthesis (63). Mutants were grown on medium containing 0.5, 1.0, 2.0 and 4.0 mM concentrations of 3-AT. Medium lacking 3-AT and medium containing 3-AT supplemented with histidine were used as negative controls. To calculate the relative growth of strains, colony diameters on different concentrations of 3-AT were divided by colony diameters on minimal medium. This accounted for the inherent growth defects of certain strains, and normalized the data set for all 15 mutants. Supplementation of 3-AT medium with 100 μg/ml of histidine restored growth of all sensitive mutants, comparable to growth on minimal medium (data not shown). This showed that any growth defects on 3-AT resulted from histidine starvation.

The results showed that the wild-type strain is sensitive to 3-AT, ranging from 49% growth on 1.0 mM, to only 17% growth on 4 mM 3-AT (Fig 7A). The Δ*cpc-2* mutant showed increased sensitivity to 3-AT, growing only 63% on 0.5 mM, and 8% on 1 mM and not surviving at concentrations of 2 mM or greater 3-AT (Fig 7A). In

agreement with this, the Δ*cpc-2* strain is significantly different than wild-type at each concentration examined (Table 5A-D).

The single Gα mutants exhibited interesting results during growth on 3-AT (Fig 7A). The Δ*gna-1* mutant growth is 80% on 0.5 mM 3AT, 45% on 1.0mM 3AT, and this strainwas inviable on 2 mM and 4 mM 3AT (Fig 7A). At all concentrations examined, the Δ*gna-1* mutant was significantly different than the wild-type strain, which indicates that the mutant had increased sensitivity to 3-AT as compared to wild-type (Table 5A-D, data not shown). Surprisingly, the Δ*gna-1* mutant was similar to (not significantly different than) the Δ*cpc-2* mutant at all concentrations except 1.0mM, demonstrating a potential novel role for *gna-1* in general amino acid control. The Δ*gna-3* mutant grew poorly on 4.0 mM 3-AT (3.1%), and is significantly different than Δ*cpc-2* at all concentrations except 4.0 mM 3-AT (Table 5A-D). At 0.5mM and 4.0mM 3AT, Δ*gna-3* also differs from wild-type. This indicates that *gna-3* plays a role in cross-pathway control, but it might be minor relative to *gna-1*. The Δ*gna-2* mutant grows 21% on 4 mM 3-AT, the highest among all Gα mutants (Fig 7A). Additionally, Δ*gna-2* is not significantly different than wild-type at all concentrations examined, indicating that *gna-2* does not have an obvious impact on cross-pathway control.

Deletion of *gna-1* or *gna-3* in the Δ*cpc-2* background results in double mutants with increased sensitivity to 3-AT at 1.0 mM, with the Δ*cpc-2* Δ*gna-1* mutant showing no growth and the Δ*cpc-2* Δ*gna-3* growing only 1.6% at this concentration (Fig 7C). In agreement with this result, it is seen that at 1.0 mM and 2.0 mM 3-AT, Δ*cpc-2*, Δ*gna-1* or the Δ*cpc-2* Δ*gna-3* mutant are not significantly different than Δ*cpc-2*, but different than

the respective single Gα mutants. At 0.5mM, the two double mutants are significantly different than either single mutant (Table 5A-D). This suggests weak epistasis between *cpc-2* and these two Gα genes;it appears that , *cpc-2* is epistatic to *gna-1* and *gna-3* at high concentrations of 3-AT. Introducing the constitutively activated forms of *gna-1* or *gna-3*, restores growth of the Δ*cpc-2* strain by 4.9% and 6.2% respectively at 4.0 mM 3-AT (Fig 7D).The Δ*cpc-2* mutant is significantly different than the Δ*cpc-2, gna-3*^{Q208L} at all concentrations examined, supporting the hypothesis that *gna-3* does provide a genetic bypass mechanism for apical growth on 3-AT (Fig 7D and Table 5D). The Δ*cpc-2, gna-1*^{Q204L} strain shows significant differences than the Δ*cpc-2* strain only at 1.0 mM and 4.0 mM 3AT, indicating that it too might provide a bypass mechanism, albeit a weaker one (TABLE 5B, D). The Δ*cpc-2, gna-2* mutant shows little sensitivity to 3-AT at all concentrations, with its growth patterns not being significantly different than wild-type at all concentrations except at 4.0 mM (Fig 7C, and Table 5A-D). Introduction of the allele *gna-2*^{Q205L} in the Δ*cpc-2* mutant shows sensitivity similar to or worse than the Δ*cpc-2* mutant at all concentrations (Fig 7D). The growth of this strain is not significantly different than that of the Δ*cpc-2*, indicating that activating *gna-2* does not provide a genetic bypass mechanism (Table 5A-D). Surprisingly, the Δ*cpc-2* Δ*gna-2* mutant has less sensitivity to 3 AT than the Δ*cpc-2* mutant (Fig 7C).

***cpc-2* is epistatic to *gnb-1* during amino acid limitation conditions**. With respect to *gnb-1* and *gng-1*, it is seen that the Δ*gnb-1* and Δ*gng-1* show decreased growth on 4 mM 3-AT medium (2.3% and 5.70% respectively, Fig 7B). The Δ*cpc-2,* Δ*gnb-1* double

mutant is similar to the Δ*cpc-2* mutant at all concentrations except 4.0 mM. This shows that *cpc-2* is largely epistatic to *gnb-1* for this phenotype. A different relationship is seen with *gng-1* and *cpc-2.* At 0.5-2 mM 3-AT, the Δ*cpc-2*, Δ*gng-1* double mutant is significantly different than either of its parental single mutant (Table 5A-D). This result suggests that these two mutations are synergistic.

Table 1: *N. crassa* strains used in this study

Strains	Relevant genotype	Source or Reference
74A-OR23-1A (74A)	Wild type, *mat A*	FGSC[a] 987
74 a-OR8-1a (74a)	Wild type, *mat a*	FGSC 988
a^{m1}	a^{m1} *cyh-1 ad3B*	FGSC 4564
his-3a	*his-3, mat a*	(71)
1B4	Δ*gna-1::hph*$^+$, *mat A*	(71)
1B8	Δ*gna-1::hph*$^+$, *mat a*	(71)
Δ2	Δ*gna-2::hph*$^+$, *mat a*	FGSC 12377
3lc2	Δ*gna-3::hph*$^+$, *mat A*	Ref. (29)
42-5-11	Δ*gnb-1::hph*$^+$, *mat A*	This Study
42-5-18	Δ*gnb-1::hph*$^+$, *mat A*	(73)
	Δ*gng-1::hph*$^+$	Ref
#1	Δ*cpc-2::hph*	This Study
	Δ*cpc-2::hph, his-3*$^-$, *mat A*	”
cpc-2 $a^{m\,1}$	Δ*cpc-2::hph, his-3,* $a^{m\,1}$ *cyh-1 ad3B, mat A*	
44	Δ*cpc-2::hph*$^+$, *his-3*$^+$*::gna-1*^{Q204L}, *mat A*	”
4	Δ*cpc-2::hph*$^+$, *his-3*$^+$*::gna-2*^{Q205L}, *mat A*	”
60	Δ*cpc-2::hph*$^+$, *his-3*$^+$*::gna-2*^{Q205L}, *mat A*	”

39	Δ*cpc-2::hph*$^{+}$, Δ*gna-1::hph*$^{+}$, *mat a*	”
48	Δ*gna-2::hph*$^{+}$, Δ*cpc-2::hph*$^{+}$, *mat A*	”
15	Δ*gna-3::hph*$^{+}$, Δ*cpc-2:: hph*$^{+}$, *mat a*	”
#58	Δ*gnb-1::hph*$^{+}$, Δ*cpc-2:: hph*$^{+}$, *mat a*	”
#30	Δ*cpc-2::hph*$^{+}$, Δ*gng-1:: hph*$^{+}$, *mat a*	”
	Δ*mus 52*::*hph*,	FGSC
#3	Δ*mus 52*::*hph*, S-CPC-2, *cpc-2* native locus	This study

Table 2- Oligonucleotides used in this study

Name	Sequence
CPC2-BamHI-FW	5’ GAATTAATTCGGATCCTATGGCTGAGCAACTC 3’
CPC2-Pst1-RV	5’ GATCTCTGCAGCTTAGCGCGGGACATGA 3’
CPC2ORF FW	5’ GTAACGCCAGGGTTTTCCCAGTCAATGGCTGAGCAACTCATC CTCAAGGGCA 3’
CPC2ORF RV	5’GCCTGGGGTGTCATGTCCCGCGCTGGCGGAGGCGGCGGAAAAGA ACCGCTGCTGCTAAATTC 3’
CPC2Bar FW	5’GCTGCTGCTAAATTCGAACGCCAGCACATGGACAGCTAATAATCGACAGAAGATGATATTGAAGGA 3’
CPC2BarRV	5’ AGTCCCGGCTCCGACGTCTCCGCGACGGATCAGATCTCGGTGACG 3’
CPC2UTR FW	5’CGTCACCGAGATCTGATCCGTCGCGGAGACGTCGGAGCCGGGACTG 3’
CPC2UTR RV	5’ GCGGATAACAATTTCACACAGGAAACAGCTGCTTGAACTCAGGC ATACCAACGCACAAA 3’
CPC2-XbaI- Fw	5’GCGCAAATTTCTAGAATGGCTGAGCAACTCATCCTCAAGGG 3’
CPC2-BamHI RV	5’ CTTGCGCAATTTGGATCCCTTAGCGCGGGACATGACAC 3’
S-tag FW	ATGGCTGAGCAACTCATCCTCAA
S-tag RV	CGTCACCGAGATCTGATCCGTC

Table 3- Statistical significance for Aerial Hyphae height Data

Uncorrected Fisher's LSD	Mean Diff.	Significant	Individual P Value
Wildtype vs. Δ*gna*-1	1.283	Yes	< 0.0001
Wildtype vs. Δ*gna*-2	0.7389	Yes	0.0037
Wildtype vs. Δ*gna*-3	1.794	Yes	< 0.0001
Wildtype vs. Δ*cpc*-2	1.306	Yes	< 0.0001
Wildtype vs. Δ*gnb-1*	2.072	Yes	< 0.0001
Wildtype vs. Δ*gng-1*	2.139	Yes	< 0.0001
Wildtype vs. Δ*cpc-2*Δ*gna*-1	2.257	Yes	< 0.0001
Wildtype vs. Δ*cpc-2*Δ*gna-2*	1.406	Yes	< 0.0001
Wildtype vs. Δ*cpc-2*Δ*gna-3*	2.247	Yes	< 0.0001
Wildtype vs. Δ*cpc-2*Δ*gnb-1*	2.266	Yes	< 0.0001
Wildtype vs. Δ*cpc-2*Δ*gng-1*	2.306	Yes	< 0.0001
Wildtype vs. Δ*cpc-2, gna-1*^{Q204L}	2.006	Yes	< 0.0001
Wildtype vs. Δ*cpc-2, gna-2*^{Q205L}	1.989	Yes	< 0.0001
Wildtype vs. Δ*cpc-2, gna3*^{Q209L}	1.156	Yes	0.0001
Δ*gna*-1 vs. Δ*gna*-2	-0.5444	No	0.0613
Δ*gna*-1 vs. Δ*gna*-3	0.5111	No	0.0788
Δ*gna*-1 vs. Δ*cpc*-2	0.02222	No	0.9293
Δ*gna*-1 vs. Δ*gnb-1*	0.7889	Yes	0.0071
Δ*gna*-1 vs. Δ*gng-1*	0.8556	Yes	0.0019
Δ*gna*-1 vs. Δ*cpc-2*Δ*gna-1*	0.9737	Yes	0.0005
Δ*gna*-1 vs. Δcpc-2Δgna-2	0.1222	No	0.6515
Δ*gna*-1 vs. Δ*cpc-2*Δ*gna-3*	0.9639	Yes	0.0005
Δ*gna*-1 vs. Δ*cpc-2*Δ*gnb-1*	0.9828	Yes	0.0005
Δ*gna*-1 vs. Δ*cpc-2*Δ*gng-1*	1.022	Yes	0.0019
Δ*gna*-1 vs. Δcpc-2, gna-1^{Q204L}	0.7222	Yes	0.0268
Δ*gna*-1 vs. Δ*cpc-2, gna-2*^{Q205L}	0.7056	Yes	0.0305
Δ*gna*-1 vs. Δcpc-2, *gna-3*^{Q209L}	-0.1278	No	0.6927
Δ*gna*-2 vs. Δ*gna*-3	1.056	Yes	0.0004
Δ*gna*-2 vs. Δ*cpc*-2	0.5667	Yes	0.0249
Δ*gna*-2 vs. Δ*gnb-1*	1.333	Yes	< 0.0001
Δ*gna*-2 vs. Δ*gng-1*	1.4	Yes	< 0.0001
Δ*gna*-2 vs. Δ*cpc-2*Δ*gna*-1	1.518	Yes	< 0.0001
Δ*gna*-2 vs. Δ*cpc-2*Δ*gna-2*	0.6667	Yes	0.0148

Δ*gna*-2 vs. Δ*cpc-2*Δ*gna-3*	1.508	Yes	< 0.0001
Δ*gna*-2 vs. Δ*cpc-2*Δ*gnb-1*	1.527	Yes	< 0.0001
Δ*gna*-2 vs. Δ*cpc-2*Δ*gng-1*	1.567	Yes	< 0.0001
Δ*gna*-2 vs. Δcpc-2, *gna-1*^{Q204L}	1.267	Yes	0.0001
Δ*gna*-2 vs. Δ*cpc-2, gna-2*^{Q205L}	1.25	Yes	0.0002
Δ*gna*-2 vs. Δ*cpc-2, gna-3*^{Q209L}	0.4167	No	0.1988
Δ*gna*-3 vs. Δ*cpc*-2	-0.4889	No	0.0525
Δ*gna*-3 vs. Δ*gnb-1*	0.2778	No	0.3375
Δ*gna*-3 vs. Δ*gng-1*	0.3444	No	0.2042
Δ*gna*-3 vs. Δ*cpc-2*Δ*gna-1*	0.4626	No	0.095
Δ*gna*-3 vs. Δcpc-2Δ*gna-2*	-0.3889	No	0.152
Δ*gna*-3 vs. Δ*cpc-2*Δ*gna-3*	0.4528	No	0.0958
Δ*gna*-3 vs. Δ*cpc-2*Δ*gnb-1*	0.4717	No	0.0887
Δ*gna*-3 vs. Δ*cpc-2*Δ*gng-1*	0.5111	No	0.1155
Δ*gna*-3 vs. Δ*cpc-2, gna-1*^{Q204L}	0.2111	No	0.5141
Δ*gna*-3 vs. Δ*cpc-2, gna-2*^{Q205L}	0.1944	No	0.5478
Δ*gna*-3 vs. Δcpc-2, *gna-3*^{Q209L}	-0.6389	Yes	0.0497
Δ*cpc*-2 vs. Δ*gnb-1*	0.7667	Yes	0.0026
Δ*cpc*-2 vs. Δ*gng-1*	0.8333	Yes	0.0004
Δ*cpc*-2 vs. Δ*cpc-2*Δ*gna-1*	0.9515	Yes	< 0.0001
Δ*cpc*-2 vs. Δcpc-2Δ*gna-2*	0.1	No	0.6619
Δ*cpc*-2 vs. Δ*cpc-2*Δ*gna-3*	0.9417	Yes	< 0.0001
Δ*cpc*-2 vs. Δ*cpc-2*Δ*gnb-1*	0.9606	Yes	< 0.0001
Δ*cpc*-2 vs. Δ*cpc-2*Δ*gng-1*	1	Yes	0.0007
Δ*cpc*-2 vs. Δ*cpc-2, gna-1*^{Q204L}	0.7	Yes	0.0166
Δ*cpc*-2 vs. Δ*cpc-2, gna-2*^{Q205L}	0.6833	Yes	0.0193
Δ*cpc*-2 vs. Δ*cpc-2, gna-3*^{Q209L}	-0.15	No	0.6041
Δ*gnb-1* vs. Δ*gng-1*	0.06667	No	0.8053
Δ*gnb-1* vs. Δ*cpc-2*Δ*gna-1*	0.1848	No	0.5029
Δ*gnb-1* vs. Δ*cpc-2*Δ*gna-2*	-0.6667	Yes	0.0148
Δ*gnb-1* vs. Δ*cpc-2*Δ*gna-3*	0.175	No	0.518
Δ*gnb-1* vs. Δ*cpc-2*Δ*gnb-1*	0.1939	No	0.4822
Δ*gnb-1* vs. Δ*cpc-2*Δ*gng-1*	0.2333	No	0.4709
Δ*gnb-1* vs. Δ*cpc-2, gna-1*^{Q204L}	-0.0667	No	0.8366
Δ*gnb-1* vs. Δcp*c-2, gna-2*^{Q205L}	-0.0833	No	0.7966

Δ*gnb-1* vs. Δ*cpc-2, gna3*^{Q209L}	-0.9167	Yes	0.0052
Δ*gng-1* vs. Δ*cpc-2*Δ*gna-1*	0.1182	No	0.6445
Δ*gng-1* vs. Δ*cpc-2*Δ*gna-2*	-0.7333	Yes	0.0039
Δ*gng-1* vs. Δ*cpc-2*Δ*gna-3*	0.1083	No	0.6654
Δ*gng-1* vs. Δ*cpc-2*Δgnb-1	0.1273	No	0.6193
Δ*gng-1* vs. Δ*cpc-2*Δg*ng-1*	0.1667	No	0.587
Δ*gng-1* vs. Δ*cpc-2, gna-1*^{Q204L}	-0.1333	No	0.6639
Δ*gng-1* vs. Δ*cpc-2, gna-2*^{Q205L}	-0.15	No	0.6249
Δgng-1 vs. Δcpc-2, gna3Q209L	-0.9833	Yes	0.0016
Δcpc-2Δgna-1 vs. Δcpc-2Δgna-2	-0.8515	Yes	0.0011
Δcpc-2Δgna-1 vs. Δcpc-2Δgna-3	-0.0098	No	0.9693
Δcpc-2Δgna-1 vs. Δcpc-2Δgnb-1	0.00909	No	0.9723
Δcpc-2Δgna-1 vs. Δcpc-2Δgng-1	0.04848	No	0.8762
Δcpc-2Δgna-1 vs. Δcpc-2, gna-1Q204L	-0.2515	No	0.4197
Δcpc-2Δgna-1 vs. Δcpc-2, gna-2Q205L	-0.2682	No	0.3896
Δcpc-2Δgna-1 vs. Δcpc-2, gna3Q209L	-1.102	Yes	0.0005
Δcpc-2Δgna-2 vs. Δcpc-2Δgna-3	0.8417	Yes	0.001
Δcpc-2Δgna-2 vs. Δcpc-2Δgnb-1	0.8606	Yes	0.001
Δcpc-2Δgna-2 vs. Δcpc-2Δgng-1	0.9	Yes	0.0038
Δcpc-2Δgna-2 vs. Δcpc-2, gna-1Q204L	0.6	No	0.052
Δcpc-2Δgna-2 vs. Δcpc-2, gna-2Q205L	0.5833	No	0.0588
Δcpc-2Δgna-2 vs. Δcpc-2, gna3Q209L	-0.25	No	0.4156
Δcpc-2Δgna-3 vs. Δcpc-2Δgnb-1	0.01894	No	0.941
Δcpc-2Δgna-3 vs. Δcpc-2Δgng-1	0.05833	No	0.8492
Δcpc-2Δgna-3 vs. Δcpc-2, gna-1Q204L	-0.2417	No	0.4312
Δcpc-2Δgna-3 vs. Δcpc-2, gna-2Q205L	-0.2583	No	0.4002
Δ*cpc-2*Δ*gna-3* vs. Δcpc-2, gna3Q2^{09L}	-1.092	Yes	0.0005
Δ*cpc-2*Δ*gnb-1* vs. Δcpc-2Δ*gng-1*	0.03939	No	0.8993
Δ*cpc-2*Δ*gnb-1* vs. Δcpc-2, gna-1Q2^{04L}	-0.2606	No	0.4031
Δ*cpc-2*Δ*gnb-1* vs. Δcpc*-2, gna-2Q2*^{05L}	-0.2773	No	0.3738
Δ*cpc-2*Δ*gnb-1* vs. Δcpc-2, gna3Q2^{09L}	-1.111	Yes	0.0005
Δ*cpc-2*Δ*gng-1* vs. Δcpc-2, gna-1Q2^{04L}	-0.3	No	0.3975
Δ*cpc-2*Δ*gng-1* vs. Δcpc*-2, gna-2Q2*^{05L}	-0.3167	No	0.3719
Δ*cpc-2*Δ*gng-1* vs. Δcpc-2, gna3Q2^{09L}	-1.15	Yes	0.0014

Δcpc-2, gna-1^{Q204L} vs. Δcp*c-2, gna-2Q2*^{05L}	-0.0167	No	0.9625
Δcpc-2, gna-1^{Q204L} vs. Δcpc-2, gna3Q2^{09L}	-0.85	Yes	0.0175
Δ*cpc-2, gna-2*^{Q205L} vs. Δcpc-2, gna3^{Q209L}	-0.8333	Yes	0.0198

Table 4- Statistical significance for Apical Extension Data

Uncorrected Fisher's LSD	Mean Diff.	Significant	Individual P Value
WT vs. Δcpc-2	3.406	Yes	< 0.0001
WT vs. Δgnb-1	1.917	Yes	< 0.0001
WT vs. Δgna-1	4.183	Yes	< 0.0001
WT vs. Δgna-2	1.339	Yes	0.0049
WT vs. Δgna-3	1.139	Yes	0.0162
WT vs. Δgng-1	1.472	Yes	0.002
WT vs. Δcpc-2Δgna-1	6.217	Yes	< 0.0001
WT vs. Δcpc-2Δgna-2	0.4389	No	0.3495
WT vs. Δcpc-2Δgna-3	4.306	Yes	< 0.0001
WT vs. Δcpc-2Δgnb-1	4.161	Yes	< 0.0001
WT vs. Δcpc-2Δgng-1	3.861	Yes	< 0.0001
WT vs. Δcpc-2, gna-1Q204L	2.861	Yes	< 0.0001
WT vs. Δcpc-2, gna-2Q205L	3.406	Yes	< 0.0001
WT vs. Δcpc-2, gna3Q209L	1.594	Yes	0.0009
Δcpc-2 vs. Δgnb-1	-1.489	Yes	0.0018
Δcpc-2 vs. Δgna-1	0.7778	No	0.0985
Δcpc-2 vs. Δgna-2	-2.067	Yes	< 0.0001
Δcpc-2 vs. Δgna-3	-2.267	Yes	< 0.0001
Δcpc-2 vs. Δgng-1	-1.933	Yes	< 0.0001
Δcpc-2 vs. Δcpc-2Δgna-1	2.811	Yes	< 0.0001
Δcpc-2 vs. Δcpc-2Δgna-2	-2.967	Yes	< 0.0001
Δcpc-2 vs. Δcpc-2Δgna-3	0.9	No	0.0564
Δcpc-2 vs. Δcpc-2Δgnb-1	0.7556	No	0.1084
Δcpc-2 vs. Δcpc-2Δgng-1	0.4556	No	0.3316
Δcpc-2 vs. Δcpc-2, gna-1Q204L	-0.5444	No	0.2463
Δcpc-2 vs. Δcpc-2, gna-2Q205L	-2.6E-08	No	> 0.9999
Δcpc-2 vs. Δcpc-2, gna3Q209L	-1.811	Yes	0.0002
Δgnb-1 vs. Δgna-1	2.267	Yes	< 0.0001
Δgnb-1 vs. Δgna-2	-0.5778	No	0.2187
Δgnb-1 vs. Δgna-3	-0.7778	No	0.0985
Δgnb-1 vs. Δgng-1	-0.4444	No	0.3435
Δgnb-1 vs. Δcpc-2Δgna-1	4.3	Yes	< 0.0001
Δgnb-1 vs. Δcpc-2Δgna-2	-1.478	Yes	0.002
Δgnb-1 vs. Δcpc-2Δgna-3	2.389	Yes	< 0.0001
Δgnb-1 vs. Δcpc-2Δgnb-1	2.244	Yes	< 0.0001

Δgnb-1 vs. Δcpc-2Δgng-1	1.944	Yes	< 0.0001
Δgnb-1 vs. Δcpc-2, gna-1Q204L	0.9444	Yes	0.0454
Δgnb-1 vs. Δcpc-2, gna-2Q205L	1.489	Yes	0.0018
Δgnb-1 vs. Δcpc-2, gna3Q209L	-0.3222	No	0.4918
Δgna-1 vs. Δgna-2	-2.844	Yes	< 0.0001
Δgna-1 vs. Δgna-3	-3.044	Yes	< 0.0001
Δgna-1 vs. Δgng-1	-2.711	Yes	< 0.0001
Δgna-1 vs. Δcpc-2Δgna-1	2.033	Yes	< 0.0001
Δgna-1 vs. Δcpc-2Δgna-2	-3.744	Yes	< 0.0001
Δgna-1 vs. Δcpc-2Δgna-3	0.1222	No	0.7941
Δgna-1 vs. Δcpc-2Δgnb-1	-0.02222	No	0.9622
Δgna-1 vs. Δcpc-2Δgng-1	-0.3222	No	0.4918
Δgna-1 vs. Δcpc-2, gna-1Q204L	-1.322	Yes	0.0054
Δgna-1 vs. Δcpc-2, gna-2Q205L	-0.7778	No	0.0985
Δgna-1 vs. Δcpc-2, gna3Q209L	-2.589	Yes	< 0.0001
Δgna-2 vs. Δgna-3	-0.2	No	0.6694
Δgna-2 vs. Δgng-1	0.1333	No	0.7759
Δgna-2 vs. Δcpc-2Δgna-1	4.878	Yes	< 0.0001
Δgna-2 vs. Δcpc-2Δgna-2	-0.9	No	0.0564
Δgna-2 vs. Δcpc-2Δgna-3	2.967	Yes	< 0.0001
Δgna-2 vs. Δcpc-2Δgnb-1	2.822	Yes	< 0.0001
Δgna-2 vs. Δcpc-2Δgng-1	2.522	Yes	< 0.0001
Δgna-2 vs. Δcpc-2, gna-1Q204L	1.522	Yes	0.0014
Δgna-2 vs. Δcpc-2, gna-2Q205L	2.067	Yes	< 0.0001
Δgna-2 vs. Δcpc-2, gna3Q209L	0.2556	No	0.5855
Δgna-3 vs. Δgng-1	0.3333	No	0.477
Δgna-3 vs. Δcpc-2Δgna-1	5.078	Yes	< 0.0001
Δgna-3 vs. Δcpc-2Δgna-2	-0.7	No	0.1367
Δgna-3 vs. Δcpc-2Δgna-3	3.167	Yes	< 0.0001
Δgna-3 vs. Δcpc-2Δgnb-1	3.022	Yes	< 0.0001
Δgna-3 vs. Δcpc-2Δgng-1	2.722	Yes	< 0.0001
Δgna-3 vs. Δcpc-2, gna-1Q204L	1.722	Yes	0.0003
Δgna-3 vs. Δcpc-2, gna-2Q205L	2.267	Yes	< 0.0001
Δgna-3 vs. Δcpc-2, gna3Q209L	0.4556	No	0.3316
Δgng-1 vs. Δcpc-2Δgna-1	4.744	Yes	< 0.0001
Δgng-1 vs. Δcpc-2Δgna-2	-1.033	Yes	0.0288
Δgng-1 vs. Δcpc-2Δgna-3	2.833	Yes	< 0.0001
Δgng-1 vs. Δcpc-2Δgnb-1	2.689	Yes	< 0.0001
Δgng-1 vs. Δcpc-2Δgng-1	2.389	Yes	< 0.0001

Δgng-1 vs. Δcpc-2, gna-1Q204L	1.389	Yes	0.0035
Δgng-1 vs. Δcpc-2, gna-2Q205L	1.933	Yes	< 0.0001
Δgng-1 vs. Δcpc-2, gna3Q209L	0.1222	No	0.7941
Δcpc-2Δgna-1 vs. Δcpc-2Δgna-2	-5.778	Yes	< 0.0001
Δcpc-2Δgna-1 vs. Δcpc-2Δgna-3	-1.911	Yes	< 0.0001
Δcpc-2Δgna-1 vs. Δcpc-2Δgnb-1	-2.056	Yes	< 0.0001
Δcpc-2Δgna-1 vs. Δcpc-2Δgng-1	-2.356	Yes	< 0.0001
Δcpc-2Δgna-1 vs. Δcpc-2, gna-1Q204L	-3.356	Yes	< 0.0001
Δcpc-2Δgna-1 vs. Δcpc-2, gna-2Q205L	-2.811	Yes	< 0.0001
Δcpc-2Δgna-1 vs. Δcpc-2, gna3Q209L	-4.622	Yes	< 0.0001
Δcpc-2Δgna-2 vs. Δcpc-2Δgna-3	3.867	Yes	< 0.0001
Δcpc-2Δgna-2 vs. Δcpc-2Δgnb-1	3.722	Yes	< 0.0001
Δcpc-2Δgna-2 vs. Δcpc-2Δgng-1	3.422	Yes	< 0.0001
Δcpc-2Δgna-2 vs. Δcpc-2, gna-1Q204L	2.422	Yes	< 0.0001
Δcpc-2Δgna-2 vs. Δcpc-2, gna-2Q205L	2.967	Yes	< 0.0001
Δcpc-2Δgna-2 vs. Δcpc-2, gna3Q209L	1.156	Yes	0.0147
Δcpc-2Δgna-3 vs. Δcpc-2Δgnb-1	-0.1444	No	0.7578
Δcpc-2Δgna-3 vs. Δcpc-2Δgng-1	-0.4444	No	0.3435
Δcpc-2Δgna-3 vs. Δcpc-2, gna-1Q204L	-1.444	Yes	0.0025
Δcpc-2Δgna-3 vs. Δcpc-2, gna-2Q205L	-0.9	No	0.0564
Δcpc-2Δgna-3 vs. Δcpc-2, gna3Q209L	-2.711	Yes	< 0.0001
Δcpc-2Δgnb-1 vs. Δcpc-2Δgng-1	-0.3	No	0.5221
Δcpc-2Δgnb-1 vs. Δcpc-2, gna-1Q204L	-1.3	Yes	0.0062
Δcpc-2Δgnb-1 vs. Δcpc-2, gna-2Q205L	-0.7556	No	0.1084
Δcpc-2Δgnb-1 vs. Δcpc-2, gna3Q209L	-2.567	Yes	< 0.0001
Δcpc-2Δgng-1 vs. Δcpc-2, gna-1Q204L	-1	Yes	0.0343
Δcpc-2Δgng-1 vs. Δcpc-2, gna-2Q205L	-0.4556	No	0.3316
Δcpc-2Δgng-1 vs. Δcpc-2, gna3Q209L	-2.267	Yes	< 0.0001
Δcpc-2, gna-1Q204L vs. Δcpc-2, gna-2Q205L	0.5444	No	0.2463
Δcpc-2, gna-1Q204L vs. Δcpc-2, gna3Q209L	-1.267	Yes	0.0077
Δcpc-2, gna-2Q205L vs. Δcpc-2, gna3Q209L	-1.811	Yes	0.0002

Table 5A-- **Statistical significance for Apical Extension Data on 0.5 mM 3AT**

Uncorrected Fisher's LSD	Mean Diff.	Significant	Individual P Value
WT vs. Δ*cpc-2*	2.844	Yes	< 0.0001
WT vs. Δ*gnb-1*	1.344	Yes	0.0002
WT vs. Δ*gna-1*	2.856	Yes	< 0.0001
WT vs. Δ*gna-3*	0.9	Yes	0.0035
WT vs. Δ*cpc-2*Δ*gna-1*	4.811	Yes	< 0.0001
WT vs. Δ*cpc-2*Δ*gna-3*	3.756	Yes	< 0.0001
WT vs. Δ*cpc-2*Δ*gnb-1*	3.467	Yes	< 0.0001
WT vs. Δ*cpc-2*Δ*gng-1*	3.456	Yes	< 0.0001
WT vs. Δcpc-2, gna-1^{Q204L}	2.767	Yes	0.0009
WT vs. Δ*cpc-2, gna-2*^{Q205L}	3.489	Yes	< 0.0001
WT vs. Δcpc-2, gna3^{Q209L}	1.067	Yes	0.003
Δ*cpc-2* vs. Δ*gnb-1*	-1.5	Yes	0.0006
Δ*cpc-2* vs. Δ*gna-2*	-2.756	Yes	< 0.0001
Δ*cpc-2* vs. Δ*gna-3*	-1.944	Yes	0.0005
Δ*cpc-2* vs. Δ*gng-1*	-2.533	Yes	< 0.0001
Δ*cpc-2* vs. Δ*cpc-2*Δ*gna-1*	1.967	Yes	< 0.0001
Δ*cpc-2* vs. Δ*cpc-2*Δ*gna-2*	-2.033	Yes	0.027
Δ*cpc-2* vs. Δ*cpc-2*Δ*gna-3*	0.9111	Yes	0.0015
Δ*cpc-2* vs. Δ*cpc-2*Δ*gng-1*	0.6111	Yes	0.0212
Δ*cpc-2* vs. Δ*cpc-2, gna-2*^{Q205L}	0.6444	Yes	0.0044
Δ*cpc-2* vs. Δcpc-2, gna3^{Q209L}	-1.778	Yes	< 0.0001
Δ*gnb-1* vs. Δ*gna-1*	1.511	Yes	0.0032
Δ*gnb-1* vs. Δ*gna-2*	-1.256	Yes	< 0.0001
Δ*gnb-1* vs. Δ*gng-1*	-1.033	Yes	0.0129
Δ*gnb-1* vs. Δ*cpc-2*Δ*gna-1*	3.467	Yes	< 0.0001
Δ*gnb-1* vs. Δ*cpc-2*Δ*gna-3*	2.411	Yes	< 0.0001
Δ*gnb-1* vs. Δ*cpc-2*Δ*gnb-1*	2.122	Yes	0.0034
Δ*gnb-1* vs. Δ*cpc-2*Δ*gng-1*	2.111	Yes	0.0016
Δ*gnb-1* vs. Δcpc-2, gna-1^{Q204L}	1.422	Yes	0.0061
Δ*gnb-1* vs. Δ*cpc-2, gna-2*^{Q205L}	2.144	Yes	0.0003
Δ*gna-1* vs. Δ*gna-2*	-2.767	Yes	< 0.0001
Δ*gna-1* vs. Δ*gna-3*	-1.956	Yes	0.0009
Δ*gna-1* vs. Δ*gng-1*	-2.544	Yes	< 0.0001
Δ*gna-1* vs. Δ*cpc-2*Δ*gna-1*	1.956	Yes	< 0.0001
Δ*gna-1* vs. Δ*cpc-2*Δ*gna-2*	-2.044	Yes	0.0342
Δ*gna-1* vs. Δ*cpc-2*Δ*gna-3*	0.9	Yes	0.012

Δ*gna-1* vs. Δ*cpc-2*Δ*gnb-1*	0.6111	Yes	0.0184
Δ*gna-1* vs. Δ*cpc-2*Δ*gng-1*	0.6	Yes	0.0013
Δ*gna-1* vs. Δ*cpc-2, gna-2*^{Q205L}	0.6333	Yes	0.0111
Δ*gna-1* vs. Δcpc-2, gna3^{Q209L}	-1.789	Yes	< 0.0001
Δ*gna-2* vs. Δ*gna-3*	0.8111	Yes	0.0145
Δ*gna-2* vs. Δ*cpc-2*Δ*gna-1*	4.722	Yes	< 0.0001
Δ*gna-2* vs. Δ*cpc-2*Δ*gna-3*	3.667	Yes	< 0.0001
Δ*gna-2* vs. Δ*cpc-2*Δ*gnb-1*	3.378	Yes	< 0.0001
Δ*gna-2* vs. Δ*cpc-2*Δ*gng-1*	3.367	Yes	< 0.0001
Δ*gna-2* vs. Δcpc-2, gna-1^{Q204L}	2.678	Yes	0.0002
Δ*gna-2* vs. Δ*cpc-2, gna-2*^{Q205L}	3.4	Yes	< 0.0001
Δ*gna-2* vs. Δcpc-2, gna3^{Q209L}	0.9778	Yes	0.0022
Δ*gna-3* vs. Δ*gng-1*	-0.5889	Yes	0.0245
Δ*gna-3* vs. Δ*cpc-2*Δ*gna-1*	3.911	Yes	< 0.0001
Δ*gna-3* vs. Δ*cpc-2*Δ*gna-3*	2.856	Yes	< 0.0001
Δ*gna-3* vs. Δ*cpc-2*Δ*gnb-1*	2.567	Yes	0.0019
Δ*gna-3* vs. Δ*cpc-2*Δ*gng-1*	2.556	Yes	0.0005
Δ*gna-3* vs. Δcpc-2, gna-1^{Q204L}	1.867	Yes	0.014
Δ*gna-3* vs. Δ*cpc-2, gna-2*^{Q205L}	2.589	Yes	0.0007
Δ*gng-1* vs. Δ*cpc-2*Δ*gna-1*	4.5	Yes	< 0.0001
Δ*gng-1* vs. Δ*cpc-2*Δ*gna-3*	3.444	Yes	< 0.0001
Δ*gng-1* vs. Δ*cpc-2*Δ*gnb-1*	3.156	Yes	< 0.0001
Δ*gng-1* vs. Δ*cpc-2*Δ*gng-1*	3.144	Yes	< 0.0001
Δ*gng-1* vs. Δcpc-2, gna-1^{Q204L}	2.456	Yes	0.0053
Δ*gng-1* vs. Δ*cpc-2, gna-2*^{Q205L}	3.178	Yes	< 0.0001
Δ*cpc-2*Δ*gna-1* vs. Δ*cpc-2*Δ*gna-2*	-4	Yes	0.0014
Δ*cpc-2*Δ*gna-1* vs. Δ*cpc-2*Δ*gna-3*	-1.056	Yes	0.0021
Δ*cpc-2*Δ*gna-1* vs. Δ*cpc-2*Δ*gnb-1*	-1.344	Yes	0.0001
Δ*cpc-2*Δ*gna-1* vs. Δ*cpc-2*Δ*gng-1*	-1.356	Yes	< 0.0001
Δ*cpc-2*Δ*gna-1* vs. Δcpc-2, gna-1^{Q204L}	-2.044	Yes	0.0114
Δ*cpc-2*Δ*gna-1* vs. Δ*cpc-2, gna-2*^{Q205L}	-1.322	Yes	< 0.0001
Δ*cpc-2*Δ*gna-1* vs. Δcpc-2, gna3^{Q209L}	-3.744	Yes	< 0.0001
Δ*cpc-2*Δ*gna-2* vs. Δ*cpc-2*Δ*gna-3*	2.944	Yes	0.0029
Δ*cpc-2*Δ*gna-2* vs. Δ*cpc-2*Δ*gnb-1*	2.656	Yes	0.0283
Δ*cpc-2*Δ*gna-2* vs. Δ*cpc-2*Δ*gng-1*	2.644	Yes	0.016
Δ*cpc-2*Δ*gna-2* vs. Δcpc-2, gna-1^{Q204L}	1.956	Yes	0.0206

Δ*cpc-2*Δ*gna-2* vs. Δ*cpc-2, gna-2*^{Q205L}	2.678	Yes	0.0158
Δ*cpc-2*Δ*gna-3* vs. Δcpc-2, gna-1^{Q204L}	-0.9889	Yes	0.0412
Δ*cpc-2*Δ*gna-3* vs. Δcpc-2, gna3^{Q209L}	-2.689	Yes	< 0.0001
Δ*cpc-2*Δ*gnb-1* vs. Δcpc-2, gna3^{Q209L}	-2.4	Yes	< 0.0001
Δ*cpc-2*Δ*gng-1* vs. Δcpc-2, gna3^{Q209L}	-2.389	Yes	< 0.0001
Δcpc-2, gna-1^{Q204L} vs. Δcpc-2, gna3^{Q209L}	-1.7	Yes	0.0086
Δ*cpc-2, gna-2*^{Q205L} vs. Δcpc-2, gna3^{Q209L}	-2.422	Yes	< 0.0001

Table 5B-- **Statistical significance for Apical Extension Data on 1.0 mM 3AT**

Uncorrected Fisher's LSD	Mean Diff.	Significant		Individual P Value
WT vs. Δ*cpc-2*	3.167	Yes		< 0.0001
WT vs. Δ*gnb-1*	1.067	Yes		< 0.0001
WT vs. Δ*gna-1*	2.144	Yes		< 0.0001
WT vs. Δ*cpc-2*Δ*gna-1*	3.456	Yes		< 0.0001
WT vs. Δ*cpc-2*Δ*gna-3*	3.456	Yes		< 0.0001
WT vs. Δ*cpc-2*Δ*gnb-1*	2.922	Yes		< 0.0001
WT vs. Δ*cpc-2*Δ*gng-1*	3.222	Yes		< 0.0001
WT vs. Δcpc-2, gna-1^{Q204L}	2.311	Yes		< 0.0001
WT vs. Δ*cpc-2, gna-2*^{Q205L}	3.2	Yes		< 0.0001
WT vs. Δcpc-2, gna3^{Q209L}	0.9667	Yes		0.0002
Δ*cpc-2* vs. Δ*gnb-1*	-2.1	Yes		< 0.0001
Δ*cpc-2* vs. Δ*gna-1*	-1.022	Yes		< 0.0001
Δ*cpc-2* vs. Δ*gna-2*	-3.122	Yes		< 0.0001
Δ*cpc-2* vs. Δ*gna-3*	-2.789	Yes		< 0.0001
Δ*cpc-2* vs. Δ*gng-1*	-2.967	Yes		< 0.0001
Δ*cpc-2* vs. Δ*cpc-2*Δ*gna-2*	-3.422	Yes		< 0.0001
Δ*cpc-2* vs. Δcpc-2, gna-1^{Q204L}	-0.8556	Yes		0.001
Δ*cpc-2* vs. Δcpc-2, gna3^{Q209L}	-2.2	Yes		< 0.0001
Δ*gnb-1* vs. Δ*gna-1*	1.078	Yes		< 0.0001
Δ*gnb-1* vs. Δ*gna-2*	-1.022	Yes		< 0.0001
Δ*gnb-1* vs. Δ*gna-3*	-0.6889	Yes		0.0076
Δ*gnb-1* vs. Δ*gng-1*	-0.8667	Yes		0.0009
Δ*gnb-1* vs. Δ*cpc-2*Δ*gna-1*	2.389	Yes		< 0.0001
Δ*gnb-1* vs. Δ*cpc-2*Δ*gna-2*	-1.322	Yes		< 0.0001

Δ*gnb-1* vs. Δ*cpc-2*Δ*gna-3*	2.389	Yes		< 0.0001
Δ*gnb-1* vs. Δ*cpc-2*Δ*gnb-1*	1.856	Yes		< 0.0001
Δ*gnb-1* vs. Δ*cpc-2*Δ*gng-1*	2.156	Yes		< 0.0001
Δ*gnb-1* vs. Δcpc-2, gna-1^{Q204L}	1.244	Yes		< 0.0001
Δ*gnb-1* vs. Δ*cpc-2, gna-2*^{Q205L}	2.133	Yes		< 0.0001
Δ*gna-1* vs. Δ*gna-2*	-2.1	Yes		< 0.0001
Δ*gna-1* vs. Δ*gna-3*	-1.767	Yes		< 0.0001
Δ*gna-1* vs. Δ*gng-1*	-1.944	Yes		< 0.0001
Δ*gna-1* vs. Δ*cpc-2*Δ*gna-1*	1.311	Yes		< 0.0001
Δ*gna-1* vs. Δ*cpc-2*Δ*gna-2*	-2.4	Yes		< 0.0001
Δ*gna-1* vs. Δ*cpc-2*Δ*gna-3*	1.311	Yes		< 0.0001
Δ*gna-1* vs. Δ*cpc-2*Δ*gnb-1*	0.7778	Yes		0.0027
Δ*gna-1* vs. Δ*cpc-2*Δ*gng-1*	1.078	Yes		< 0.0001
Δ*gna-1* vs. Δ*cpc-2, gna-2*^{Q205L}	1.056	Yes		< 0.0001
Δ*gna-1* vs. Δcpc-2, gna3^{Q209L}	-1.178	Yes		< 0.0001
Δ*gna-2* vs. Δ*cpc-2*Δ*gna-1*	3.411	Yes		< 0.0001
Δ*gna-2* vs. Δ*cpc-2*Δ*gna-3*	3.411	Yes		< 0.0001
Δ*gna-2* vs. Δ*cpc-2*Δ*gnb-1*	2.878	Yes		< 0.0001
Δ*gna-2* vs. Δ*cpc-2*Δ*gng-1*	3.178	Yes		< 0.0001
Δ*gna-2* vs. Δcpc-2, gna-1^{Q204L}	2.267	Yes		< 0.0001
Δ*gna-2* vs. Δ*cpc-2, gna-2*^{Q205L}	3.156	Yes		< 0.0001
Δ*gna-2* vs. Δcpc-2, gna3^{Q209L}	0.9222	Yes		0.0004
Δ*gna-3* vs. Δ*cpc-2*Δ*gna-1*	3.078	Yes		< 0.0001
Δ*gna-3* vs. Δ*cpc-2*Δ*gna-2*	-0.6333	Yes		0.0138
Δ*gna-3* vs. Δ*cpc-2*Δ*gna-3*	3.078	Yes		< 0.0001
Δ*gna-3* vs. Δ*cpc-2*Δ*gnb-1*	2.544	Yes		< 0.0001
Δ*gna-3* vs. Δ*cpc-2*Δ*gng-1*	2.844	Yes		< 0.0001
Δ*gna-3* vs. Δcpc-2, gna-1^{Q204L}	1.933	Yes		< 0.0001
Δ*gna-3* vs. Δ*cpc-2, gna-2*^{Q205L}	2.822	Yes		< 0.0001
Δ*gna-3* vs. Δcpc-2, gna3^{Q209L}	0.5889	Yes		0.0219
Δ*gng-1* vs. Δ*cpc-2*Δ*gna-1*	3.256	Yes		< 0.0001
Δ*gng-1* vs. Δ*cpc-2*Δ*gna-3*	3.256	Yes		< 0.0001
Δ*gng-1* vs. Δ*cpc-2*Δ*gnb-1*	2.722	Yes		< 0.0001
Δ*gng-1* vs. Δ*cpc-2*Δ*gng-1*	3.022	Yes		< 0.0001
Δ*gng-1* vs. Δcpc-2, gna-1^{Q204L}	2.111	Yes		< 0.0001
Δ*gng-1* vs. Δ*cpc-2, gna-2*^{Q205L}	3	Yes		< 0.0001
Δ*gng-1* vs. Δcpc-2, gna3^{Q209L}	0.7667	Yes		0.0031
Δ*cpc-2*Δ*gna-1* vs. Δ*cpc-2*Δ*gna-2*	-3.711	Yes		< 0.0001

Δ*cpc-2*Δ*gna-1* vs. Δ*cpc-2*Δ*gnb-1*	-0.5333	Yes		0.0375
Δ*cpc-2*Δ*gna-1* vs. Δcpc-2, gna-1^{Q204L}	-1.144	Yes		< 0.0001
Δ*cpc-2*Δ*gna-1* vs. Δcpc-2, gna3^{Q209L}	-2.489	Yes		< 0.0001
Δ*cpc-2*Δ*gna-2* vs. Δ*cpc-2*Δ*gna-3*	3.711	Yes		< 0.0001
Δ*cpc-2*Δ*gna-2* vs. Δ*cpc-2*Δ*gnb-1*	3.178	Yes		< 0.0001
Δ*cpc-2*Δ*gna-2* vs. Δ*cpc-2*Δ*gng-1*	3.478	Yes		< 0.0001
Δ*cpc-2*Δ*gna-2* vs. Δcpc-2, gna-1^{Q204L}	2.567	Yes		< 0.0001
Δ*cpc-2*Δ*gna-2* vs. Δ*cpc-2, gna-2*^{Q205L}	3.456	Yes		< 0.0001
Δ*cpc-2*Δ*gna-2* vs. Δcpc-2, gna3^{Q209L}	1.222	Yes		< 0.0001
Δ*cpc-2*Δ*gna-3* vs. Δcpc-2, gna-1^{Q204L}	-1.144	Yes		< 0.0001
Δ*cpc-2*Δ*gna-3* vs. Δcpc-2, gna3^{Q209L}	-2.489	Yes		< 0.0001
Δ*cpc-2*Δ*gnb-1* vs. Δcpc-2, gna-1^{Q204L}	-0.6111	Yes		0.0175
Δ*cpc-2*Δ*gnb-1* vs. Δcpc-2, gna3^{Q209L}	-1.956	Yes		< 0.0001
Δ*cpc-2*Δ*gng-1* vs. Δcpc-2, gna-1^{Q204L}	-0.9111	Yes		0.0005
Δ*cpc-2*Δ*gng-1* vs. Δcpc-2, gna3^{Q209L}	-2.256	Yes		< 0.0001
Δcpc-2, gna-1^{Q204L} vs. Δ*cpc-2, gna-2*^{Q205L}	0.8889	Yes		0.0006
Δcpc-2, gna-1^{Q204L} vs. Δcpc-2, gna3^{Q209L}	-1.344	Yes		< 0.0001
Δ*cpc-2, gna-2*^{Q205L} vs. Δcpc-2, gna3^{Q209L}	-2.233	Yes		< 0.0001

Table 5C-- **Statistical significance for Apical Extension Data on 2.0mM 3AT**

Uncorrected Fisher's LSD	Mean Diff.	Significant	Individual P Value
WT vs. Δcpc-2	1.986	Yes	< 0.0001
WT vs. Δgnb-1	1.175	Yes	< 0.0001
WT vs. Δgna-1	1.986	Yes	< 0.0001
WT vs. Δgng-1	0.6857	Yes	0.0048
WT vs. Δcpc-2Δgna-1	1.986	Yes	< 0.0001
WT vs. Δcpc-2Δgna-3	1.986	Yes	< 0.0001
WT vs. Δcpc-2Δgnb-1	1.986	Yes	< 0.0001
WT vs. Δcpc-2Δgng-1	1.986	Yes	< 0.0001
WT vs. Δcpc-2, gna-1Q204L	1.986	Yes	< 0.0001
WT vs. Δcpc-2, gna-2Q205L	1.986	Yes	< 0.0001
WT vs. Δcpc-2, gna3Q209L	0.819	Yes	0.0008
Δcpc-2 vs. Δgnb-1	-0.8111	Yes	0.0004
Δcpc-2 vs. Δgna-2	-1.867	Yes	< 0.0001
Δcpc-2 vs. Δgna-3	-1.622	Yes	< 0.0001
Δcpc-2 vs. Δgng-1	-1.3	Yes	< 0.0001
Δcpc-2 vs. Δcpc-2Δgna-2	-1.6	Yes	< 0.0001

Δcpc-2 vs. Δcpc-2, gna3Q209L	-1.167	Yes	< 0.0001
Δgnb-1 vs. Δgna-1	0.8111	Yes	0.0004
Δgnb-1 vs. Δgna-2	-1.056	Yes	< 0.0001
Δgnb-1 vs. Δgna-3	-0.8111	Yes	0.0004
Δgnb-1 vs. Δgng-1	-0.4889	Yes	0.0303
Δgnb-1 vs. Δcpc-2Δgna-1	0.8111	Yes	0.0004
Δgnb-1 vs. Δcpc-2Δgna-2	-0.7889	Yes	0.0006
Δgnb-1 vs. Δcpc-2Δgna-3	0.8111	Yes	0.0004
Δgnb-1 vs. Δcpc-2Δgnb-1	0.8111	Yes	0.0004
Δgnb-1 vs. Δcpc-2Δgng-1	0.8111	Yes	0.0004
Δgnb-1 vs. Δcpc-2, gna-1Q204L	0.8111	Yes	0.0009
Δgnb-1 vs. Δcpc-2, gna-2Q205L	0.8111	Yes	0.0004
Δgna-1 vs. Δgna-2	-1.867	Yes	< 0.0001
Δgna-1 vs. Δgna-3	-1.622	Yes	< 0.0001
Δgna-1 vs. Δgng-1	-1.3	Yes	< 0.0001
Δgna-1 vs. Δcpc-2Δgna-1	0	No	> 0.9999
Δgna-1 vs. Δcpc-2Δgna-2	-1.6	Yes	< 0.0001
Δgna-1 vs. Δcpc-2, gna3Q209L	-1.167	Yes	< 0.0001
Δgna-2 vs. Δgng-1	0.5667	Yes	0.0124
Δgna-2 vs. Δcpc-2Δgna-1	1.867	Yes	< 0.0001
Δgna-2 vs. Δcpc-2Δgna-3	1.867	Yes	< 0.0001
Δgna-2 vs. Δcpc-2Δgnb-1	1.867	Yes	< 0.0001
Δgna-2 vs. Δcpc-2Δgng-1	1.867	Yes	< 0.0001
Δgna-2 vs. Δcpc-2, gna-1Q204L	1.867	Yes	< 0.0001
Δgna-2 vs. Δcpc-2, gna-2Q205L	1.867	Yes	< 0.0001
Δgna-2 vs. Δcpc-2, gna3Q209L	0.7	Yes	0.0021
Δgna-3 vs. Δcpc-2Δgna-1	1.622	Yes	< 0.0001
Δgna-3 vs. Δcpc-2Δgna-3	1.622	Yes	< 0.0001
Δgna-3 vs. Δcpc-2Δgnb-1	1.622	Yes	< 0.0001
Δgna-3 vs. Δcpc-2Δgng-1	1.622	Yes	< 0.0001
Δgna-3 vs. Δcpc-2, gna-1Q204L	1.622	Yes	< 0.0001
Δgna-3 vs. Δcpc-2, gna-2Q205L	1.622	Yes	< 0.0001
Δgna-3 vs. Δcpc-2, gna3Q209L	0.4556	Yes	0.0433
Δgng-1 vs. Δcpc-2Δgna-1	1.3	Yes	< 0.0001
Δgng-1 vs. Δcpc-2Δgna-3	1.3	Yes	< 0.0001
Δgng-1 vs. Δcpc-2Δgnb-1	1.3	Yes	< 0.0001
Δgng-1 vs. Δcpc-2Δgng-1	1.3	Yes	< 0.0001
Δgng-1 vs. Δcpc-2, gna-1Q204L	1.3	Yes	< 0.0001
Δgng-1 vs. Δcpc-2, gna-2Q205L	1.3	Yes	< 0.0001

Δcpc-2Δgna-1 vs. Δcpc-2Δgna-2	-1.6	Yes	< 0.0001
Δcpc-2Δgna-1 vs. Δcpc-2, gna3Q209L	-1.167	Yes	< 0.0001
Δcpc-2Δgna-2 vs. Δcpc-2Δgna-3	1.6	Yes	< 0.0001
Δcpc-2Δgna-2 vs. Δcpc-2Δgnb-1	1.6	Yes	< 0.0001
Δcpc-2Δgna-2 vs. Δcpc-2Δgng-1	1.6	Yes	< 0.0001
Δcpc-2Δgna-2 vs. Δcpc-2, gna-1Q204L	1.6	Yes	< 0.0001
Δcpc-2Δgna-2 vs. Δcpc-2, gna-2Q205L	1.6	Yes	< 0.0001
Δcpc-2Δgna-3 vs. Δcpc-2, gna3Q209L	-1.167	Yes	< 0.0001
Δcpc-2Δgnb-1 vs. Δcpc-2, gna3Q209L	-1.167	Yes	< 0.0001
Δcpc-2Δgng-1 vs. Δcpc-2, gna3Q209L	-1.167	Yes	< 0.0001
Δcpc-2, gna-1Q204L vs. Δcpc-2, gna3Q209L	-1.167	Yes	< 0.0001
Δcpc-2, gna-2Q205L vs. Δcpc-2, gna3Q209L	-1.167	Yes	< 0.0001

Table 5D-- **Statistical significance for Apical Extension Data on 4.0 mM 3AT**

Uncorrected Fisher's LSD	Mean Diff.	Significant	Individual P Value
WT vs. Δcpc-2	1.2	Yes	< 0.0001
WT vs. Δgnb-1	1.2	Yes	< 0.0001
WT vs. Δgna-1	1.2	Yes	< 0.0001
WT vs. Δgna-3	1	Yes	< 0.0001
WT vs. Δgng-1	0.9	Yes	< 0.0001
WT vs. Δcpc-2Δgna-1	1.2	Yes	< 0.0001
WT vs. Δcpc-2Δgna-2	0.4889	Yes	0.001
WT vs. Δcpc-2Δgna-3	1.2	Yes	< 0.0001
WT vs. Δcpc-2Δgnb-1	1.2	Yes	< 0.0001
WT vs. Δcpc-2Δgng-1	1.2	Yes	< 0.0001
WT vs. Δcpc-2, gna-1Q204L	0.8667	Yes	< 0.0001
WT vs. Δcpc-2, gna-2Q205L	1.2	Yes	< 0.0001
WT vs. Δcpc-2, gna3Q209L	0.8667	Yes	< 0.0001
Δcpc-2 vs. Δgna-2	-1.2	Yes	< 0.0001
Δcpc-2 vs. Δgng-1	-0.3	Yes	0.0404
Δcpc-2 vs. Δcpc-2Δgna-2	-0.7111	Yes	< 0.0001
Δcpc-2 vs. Δcpc-2, gna-1Q204L	-0.3333	Yes	0.0231
Δcpc-2 vs. Δcpc-2, gna3Q209L	-0.3333	Yes	0.0231
Δgnb-1 vs. Δgna-2	-1.2	Yes	< 0.0001
Δgnb-1 vs. Δcpc-2Δgna-2	-0.7111	Yes	< 0.0001
Δgnb-1 vs. Δcpc-2, gna-1Q204L	-0.3333	Yes	0.0333

Δgnb-1 vs. Δcpc-2, gna3Q209L	-0.3333	Yes	0.0333
Δgna-1 vs. Δgna-2	-1.2	Yes	< 0.0001
Δgna-1 vs. Δgng-1	-0.3	Yes	0.0404
Δgna-1 vs. Δcpc-2Δgna-2	-0.7111	Yes	< 0.0001
Δgna-1 vs. Δcpc-2, gna-1Q204L	-0.3333	Yes	0.0231
Δgna-1 vs. Δcpc-2, gna3Q209L	-0.3333	Yes	0.0231
Δgna-2 vs. Δgna-3	1	Yes	< 0.0001
Δgna-2 vs. Δgng-1	0.9	Yes	< 0.0001
Δgna-2 vs. Δcpc-2Δgna-1	1.2	Yes	< 0.0001
Δgna-2 vs. Δcpc-2Δgna-2	0.4889	Yes	0.001
Δgna-2 vs. Δcpc-2Δgna-3	1.2	Yes	< 0.0001
Δgna-2 vs. Δcpc-2Δgnb-1	1.2	Yes	< 0.0001
Δgna-2 vs. Δcpc-2Δgng-1	1.2	Yes	< 0.0001
Δgna-2 vs. Δcpc-2, gna-1Q204L	0.8667	Yes	< 0.0001
Δgna-2 vs. Δcpc-2, gna-2Q205L	1.2	Yes	< 0.0001
Δgna-2 vs. Δcpc-2, gna3Q209L	0.8667	Yes	< 0.0001
Δgna-3 vs. Δcpc-2Δgna-2	-0.5111	Yes	0.0006
Δgng-1 vs. Δcpc-2Δgna-1	0.3	Yes	0.0404
Δgng-1 vs. Δcpc-2Δgna-2	-0.4111	Yes	0.0053
Δgng-1 vs. Δcpc-2Δgna-3	0.3	Yes	0.0404
Δgng-1 vs. Δcpc-2Δgnb-1	0.3	Yes	0.0404
Δgng-1 vs. Δcpc-2Δgng-1	0.3	Yes	0.0404
Δgng-1 vs. Δcpc-2, gna-2Q205L	0.3	Yes	0.0404
Δcpc-2Δgna-1 vs. Δcpc-2Δgna-2	-0.7111	Yes	< 0.0001
Δcpc-2Δgna-1 vs. Δcpc-2, gna-1Q204L	-0.3333	Yes	0.0231
Δcpc-2Δgna-1 vs. Δcpc-2, gna3Q209L	-0.3333	Yes	0.0231
Δcpc-2Δgna-2 vs. Δcpc-2Δgna-3	0.7111	Yes	< 0.0001
Δcpc-2Δgna-2 vs. Δcpc-2Δgnb-1	0.7111	Yes	< 0.0001
Δcpc-2Δgna-2 vs. Δcpc-2Δgng-1	0.7111	Yes	< 0.0001
Δcpc-2Δgna-2 vs. Δcpc-2, gna-1Q204L	0.3778	Yes	0.0102
Δcpc-2Δgna-2 vs. Δcpc-2, gna-2Q205L	0.7111	Yes	< 0.0001
Δcpc-2Δgna-2 vs. Δcpc-2, gna3Q209L	0.3778	Yes	0.0102
Δcpc-2Δgna-3 vs. Δcpc-2, gna-1Q204L	-0.3333	Yes	0.0231
Δcpc-2Δgna-3 vs. Δcpc-2, gna3Q209L	-0.3333	Yes	0.0231
Δcpc-2Δgnb-1 vs. Δcpc-2, gna-1Q204L	-0.3333	Yes	0.0231
Δcpc-2Δgnb-1 vs. Δcpc-2, gna3Q209L	-0.3333	Yes	0.0231
Δcpc-2Δgng-1 vs. Δcpc-2, gna-1Q204L	-0.3333	Yes	0.0231
Δcpc-2Δgng-1 vs. Δcpc-2, gna3Q209L	-0.3333	Yes	0.0231

Δcpc-2, gna-1Q204L vs. Δcpc-2, gna-2Q205L	0.3333	Yes	0.0231
Δcpc-2, gna-2Q205L vs. Δcpc-2, gna3Q209L	-0.3333	Yes	0.0231

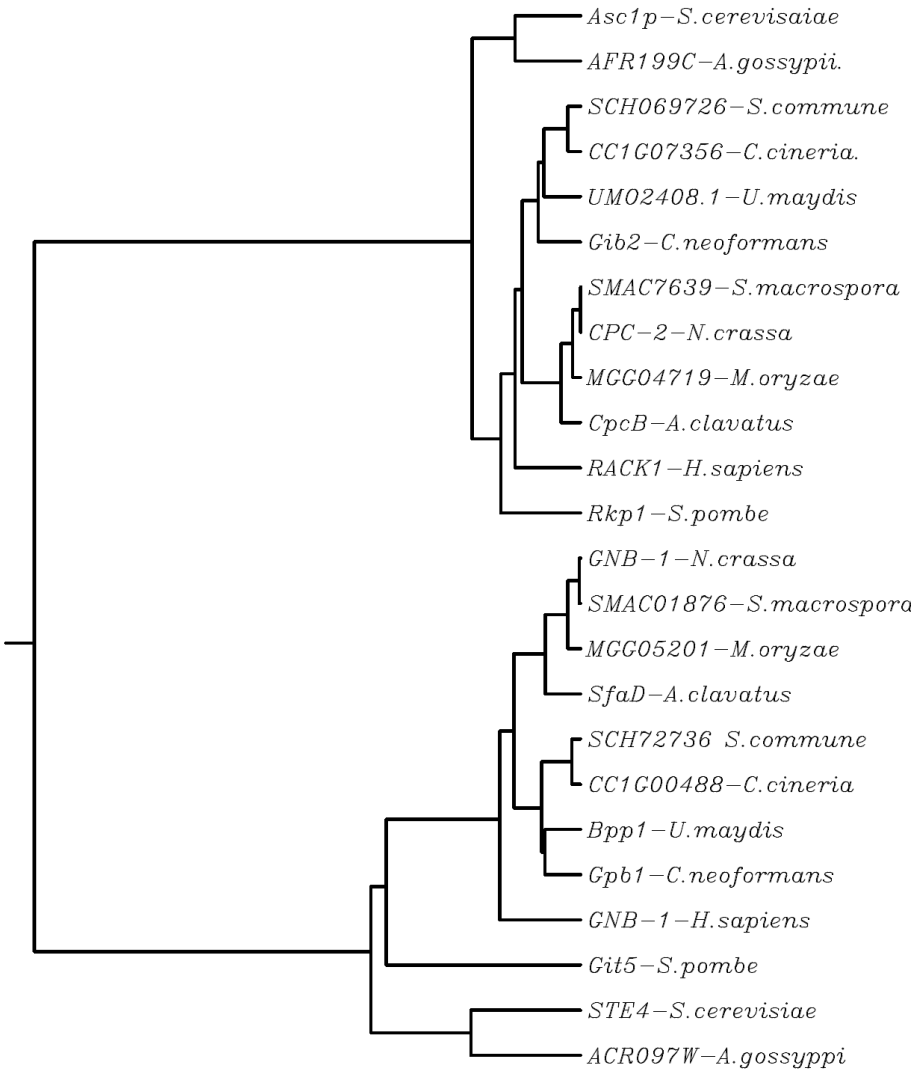

Figure 1: Phylogenetic analysis of Gβ and RACK1-like proteins. Amino acid sequences were aligned using ClustalW multiple sequence alignment program, with a gap open penalty of 10 and a gap extension of 0.1. Organism and accession numbers are- *Saccharomyces cerevisiae* (*S. cerevisiae*) Asc1p (NP_013834), *Ashbya gossypii* (*A. gossypii*) AFR199c (NP_985746.1), *Schizophyllum commune* (*S. commune*) SCH069726 (XP_003029882.1), *Coprinopsis cineria* (*C. cineria*) CCG107356 (XP_001830441.1), *Ustilago maydis* (*U. maydis*) UMO2408.1 (XP_758555.1), *Cryptococcus neoformans* (*C. neoformans*) Gib2 (XP _0031970031), *Sordaria macrospora* (*S. macrospora*) SMAC07639 (XP_003351440.1), *Neurospora crassa* (*N. crassa*) CPC-2 (CAA57460), *Magnaportha oryzae (M. oryzae)* MGG04719 (XP_003710816.1), *Aspergillus clavatus* (*A. clavatus*) CpcB (XP_001272169.1), *Homo sapiens* (*H. sapiens*) RACK1 (NP_006089.1), *Schizosaccharomyces pombe* (*S. pombe*) RKP1 (AAA56865), *N. crassa* GNB-1 (XP_956704.2), M. orzyae (XP_003712746.1), *A. clavatus* SfaD (XP_001274512.1), *S. commune* XP_003037057.1), *C. cineria* (XP_001829309.2), *U. maydis* Bpp1 (AF536325.1), *C. neoformans* Gpb1 (AAD03596.1) *H. sapiens* GNB-1 (NP_006089.1), *S. pombe* (AAD09020), S. *cerevisiae* Ste4 (AAA35114), *A. gossypii* (NP_983499.1).

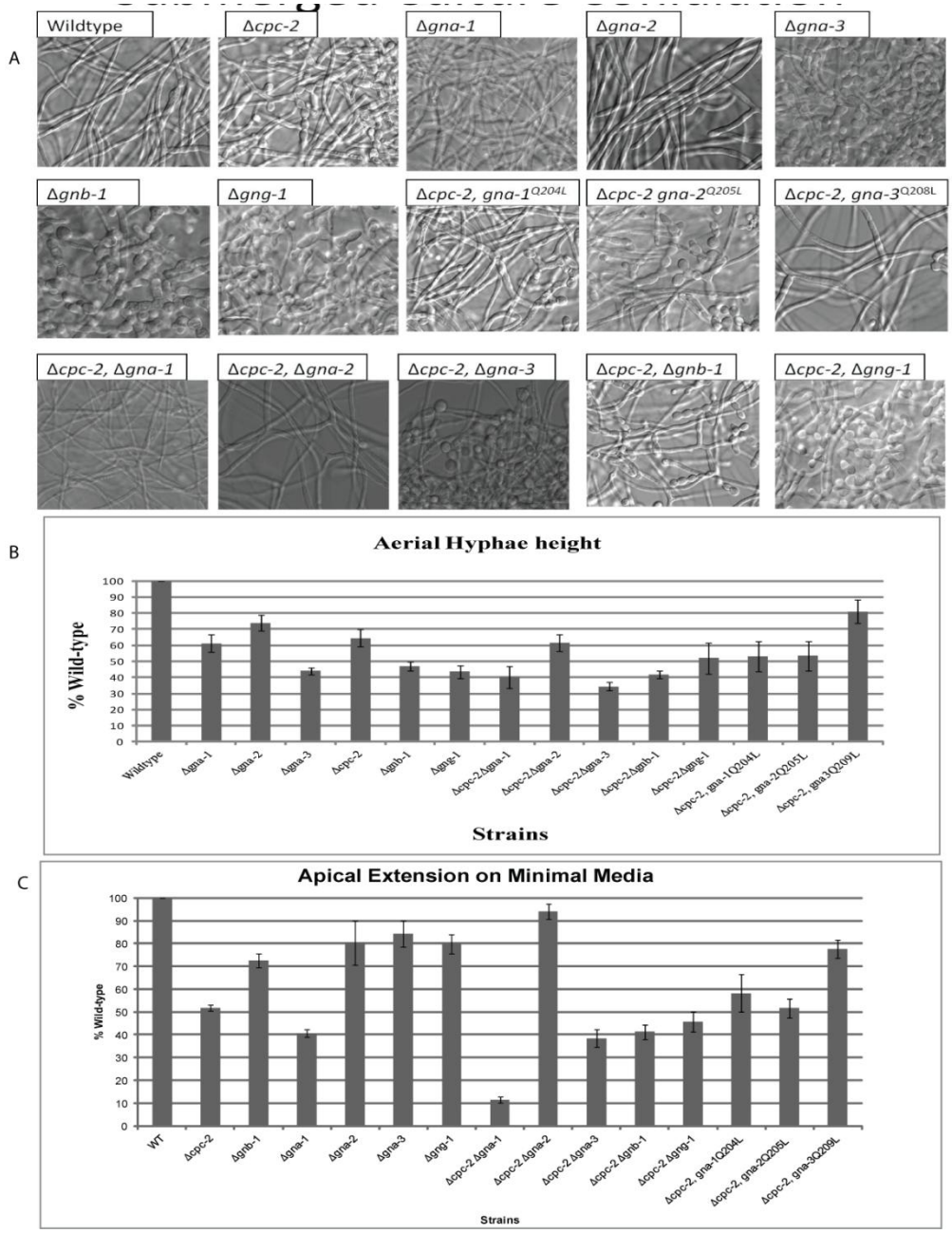

Figure 2. Phenotypes during asexual growth and development. (A) Submerged cultures. Strains were cultured in VM liquid medium for 16 h with shaking at 200 rpm in the dark at 30°C. (B) Aerial hyphal height. To measure aerial hyphal height, liquid VM tube cultures were inoculated with the indicated strains and incubated statically for 3 days at room temperature. Values are expressed as % of wild-type. The standard error is the error calculated based on average percent values. (C). Apical extension on minimal media. Strains were grown on VM medium for 24 h in the dark at 30°C. Colony growth was measured for nine replicates of each strain. The values are expressed as % of wild-type. The standard error is the error calculated based on average percent values.

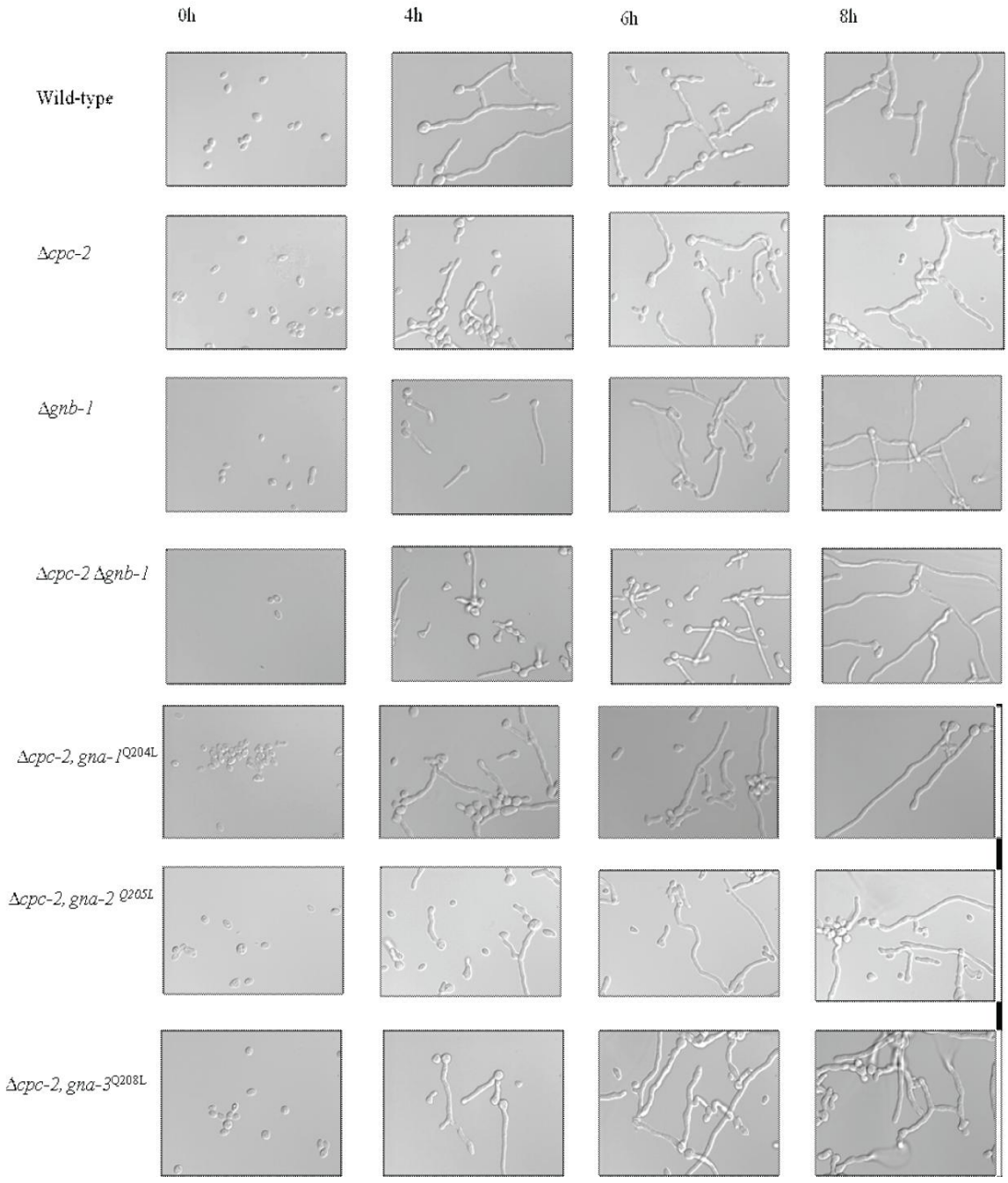

Figure 3. Conidial germination assays. Conidia were harvested as described in the Materials and Methods. An aliquot containing 8×10^6 conidia was spread on a 100 mm 10 ml VM solid medium plate and spore germination monitored at 30°C over time. DIC (differential interference contrast) micrograph images were obtained using an Olympus IX71 microscope with a QIClick digital CCD camera and analyzed using Metamorph software. Strains used were wild-type, Δ*cpc-2*, Δ*gna-1*, Δ*gna-2*, Δ*gna-3*, Δ*cpc-2*, Δ*gna-1*; Δ*cpc-2* Δ*gna-2;* and Δ*cpc-2* Δ*gna-3*, Δ*cpc-2 gna-1*^{Q204L}, Δ*cpc-2 gna-2*^{Q205L}, and Δ*cpc-2 gna-3*^{Q208L}.

A.

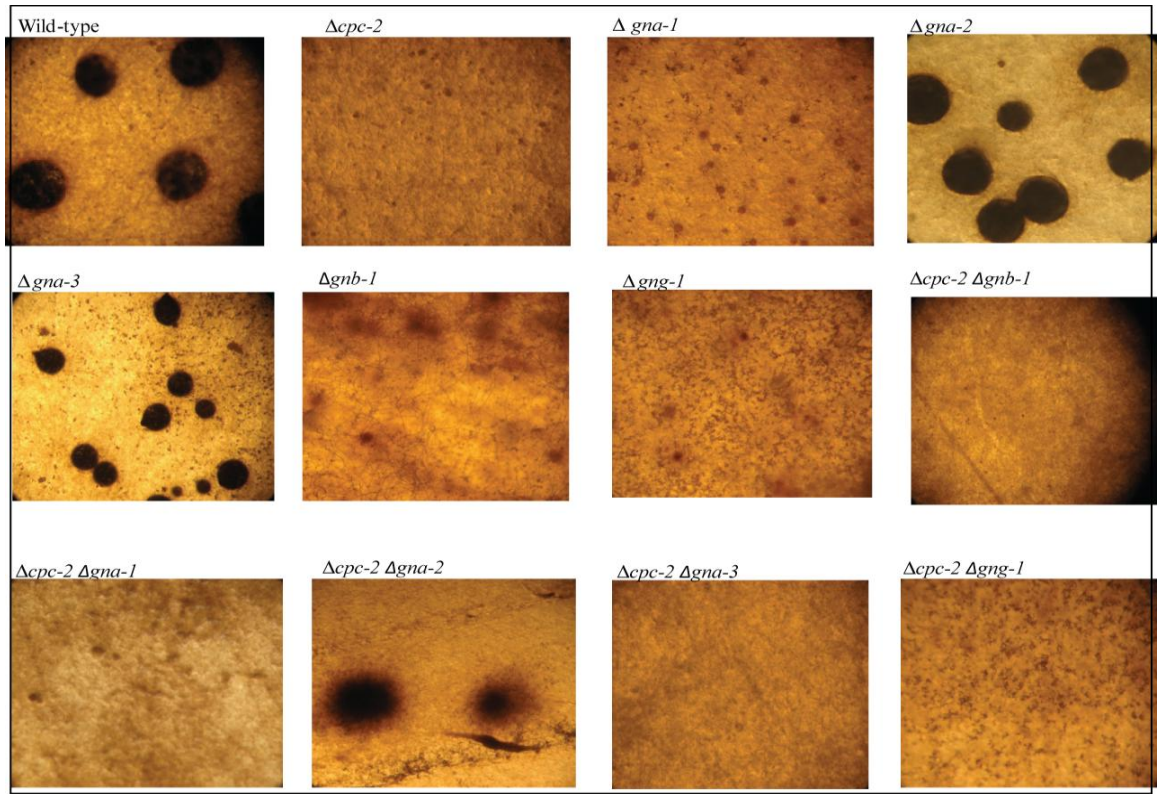

B.

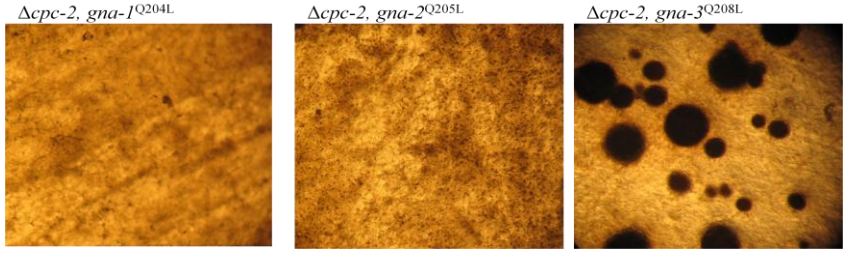

Figure 4- Sexual phase phenotypes. Strains were inoculated onto SCM plates to induce production of female reproductive structures (protoperithecia) and incubated for 6 days in constant light at 25°C. Cultures were then fertilized with males (macroconidia) of opposite mating type and incubated for six more days before being photographed. A. Strains used are wild-type, Δ*cpc-2*, Δ*gna-1*, Δ*gna-2*, Δ*gna-3,* Δ*gnb-1*, Δ*gng-1*, Δ*cpc-2* Δ*gnb-1*, Δ*cpc-2* Δ*gng-1*, Δ*cpc-2*, Δ*gna-1*; Δ*cpc-2* Δ*gna-2;* and Δ*cpc-2* Δ*gna-3*. B. Δ*cpc-2 gna-1*^{Q204L}, Δ*cpc-2 gna-2*^{Q205L}, and Δ*cpc-2 gna-3*^{Q208L}.

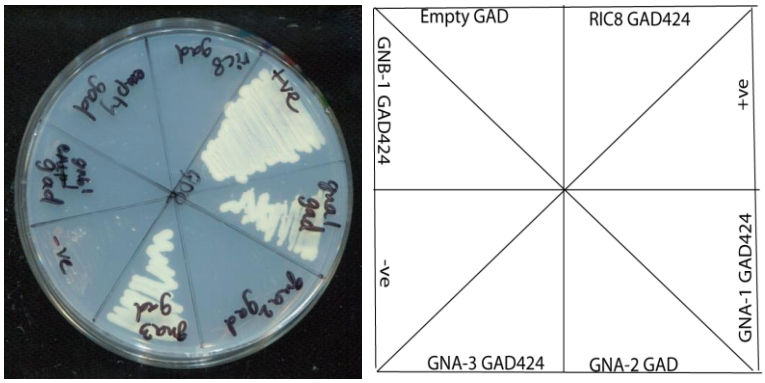

Figure 5- CPC-2 interacts with GNA-1 and GNA-3 in a yeast two hybrid assay. Yeast two-hybrid analysis was employed using diploid strains containing the GAL4 activation domain (pGAD424) and the DNA-binding domain (pGBKT7) vectors. CPC-2pGBKT7 was mated with GNA-1, GNA-2, GNA-3, GNB-1 and RIC8 in pGAD424 vectors. Positive and negative controls are denoted with +ve and -ve respectively. As another control, the CPC-2pGBKT7 strain was mated with a strain carrying an empty pGAD424 vector.

.

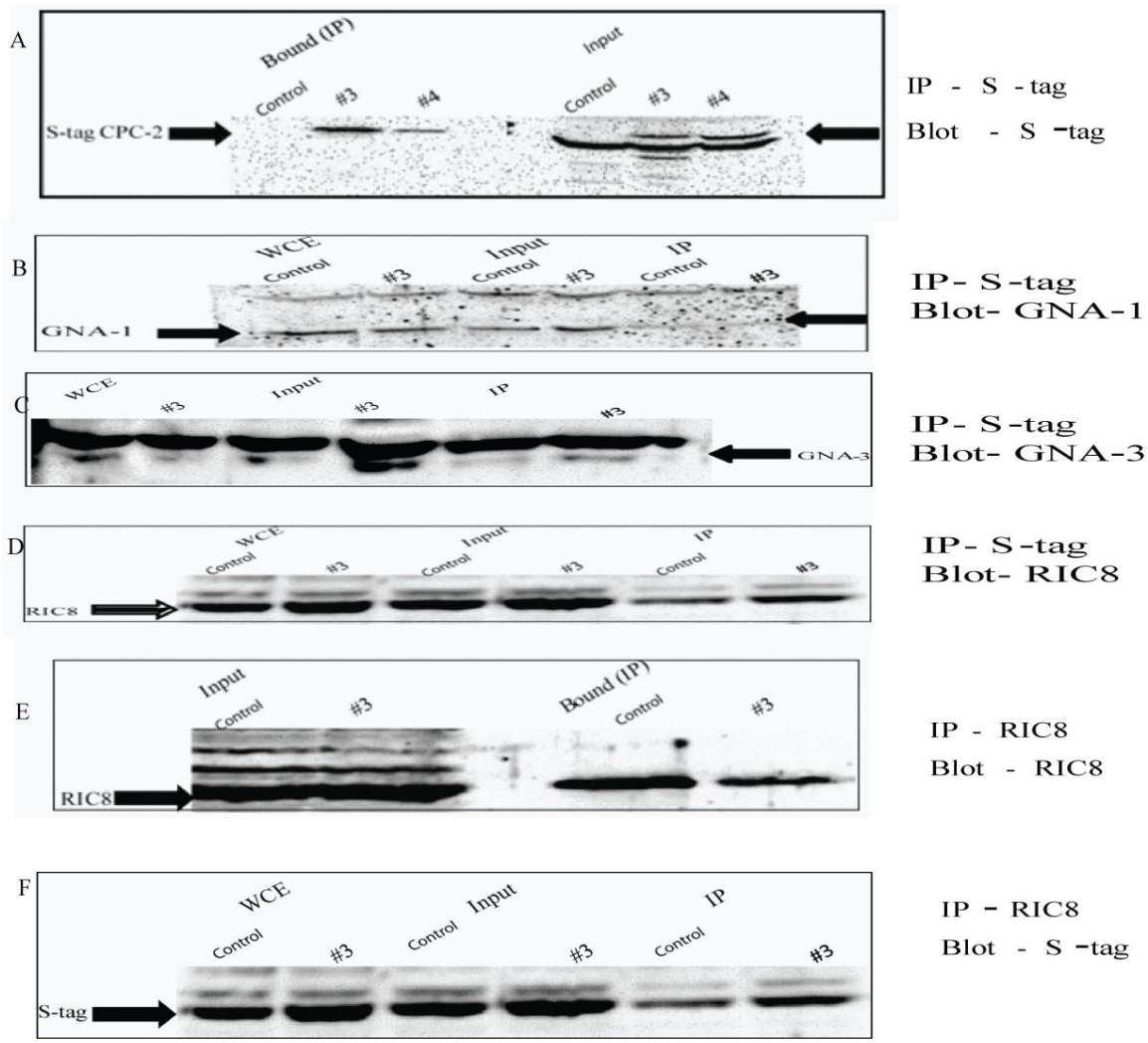

Fig 6- Immunoprecipitation experiments. Control (WT) and the CPC-2-S tag strain (#3 and #4) were grown for 16 hr in submerged VM cultures. A-D:The whole cell extract was solubilized using 1% lauryl maltoside and immunoprecipitated using anti S-tag antibody coupled to agarose beads. Samples of the Whole Cell Extract (WCE), original input (Input), and the immunoprecipitated (IP) fractions were subjected to Western analysis using S-tag, GNA-1, GNA-3 and RIC8 antibodies. The results indicate that the CPC-2 protein is immunoprecipitated but high background is observed. E-F- Wildtype (WT) and the CPC-2 S tag strain (#3) were grown (as described above) and whole cell fractions were solubilized using 1% lauryl maltoside. They were immunoprecipitated using the RIC8 antibody, coupled to Protein A beads. Samples of the Input and Bound (IP) were subjected to western analysis using RIC8 and S-tag antibodies. The results indicates that there is high background observed in these experiments.

A.

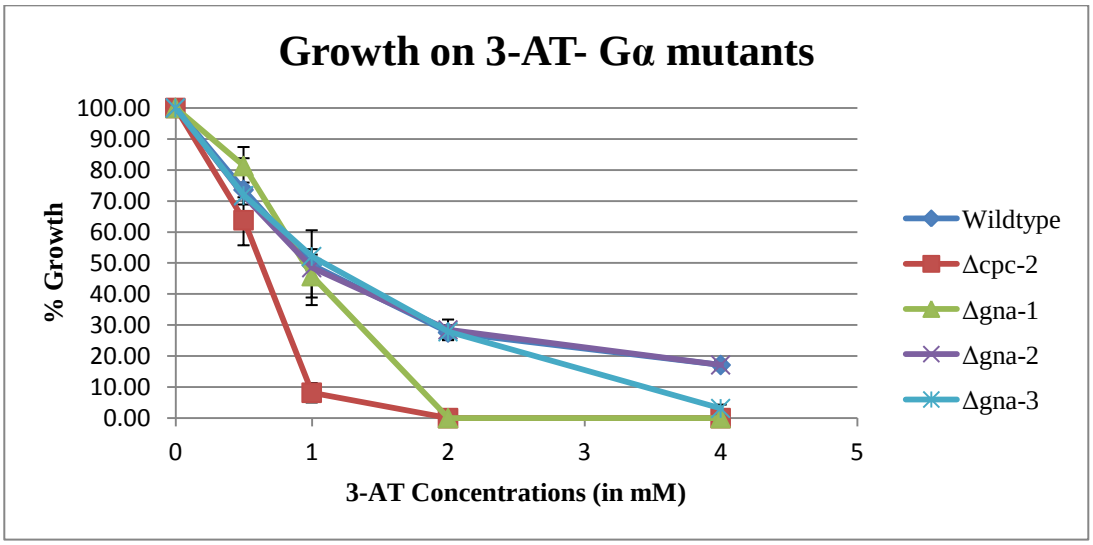
Growth on 3-AT- Gα mutants
% Growth
100.00
90.00
80.00
70.00
60.00
50.00
40.00
30.00
20.00
10.00
0.00
0
1
2
3
4
5
3-AT Concentrations (in mM)
Wildtype
Δcpc-2
Δgna-1
Δgna-2
Δgna-3

.

B.

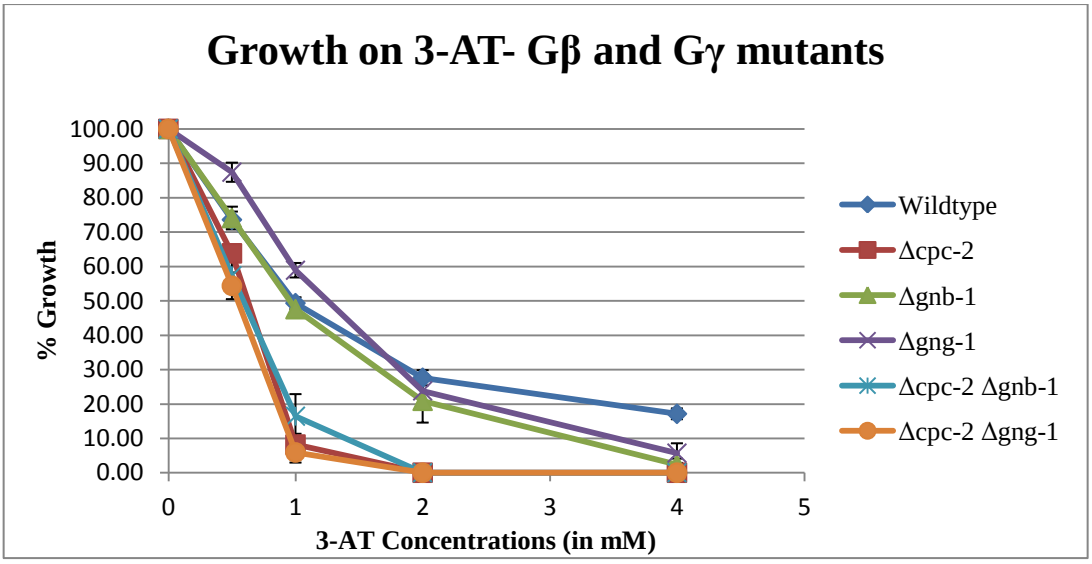
Growth on 3-AT- Gβ and Gγ mutants
% Growth
100.00
90.00
80.00
70.00
60.00
50.00
40.00
30.00
20.00
10.00
0.00
0
1
2
3
4
5
3-AT Concentrations (in mM)
Wildtype
Δcpc-2
Δgnb-1
Δgng-1
Δcpc-2 Δgnb-1
Δcpc-2 Δgng-1

C.

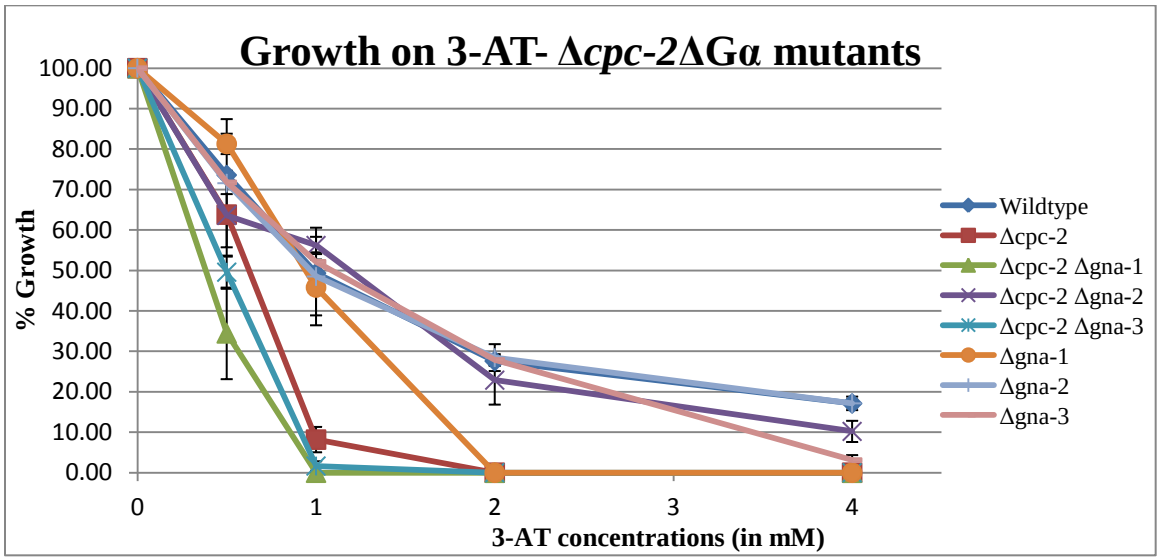

D.

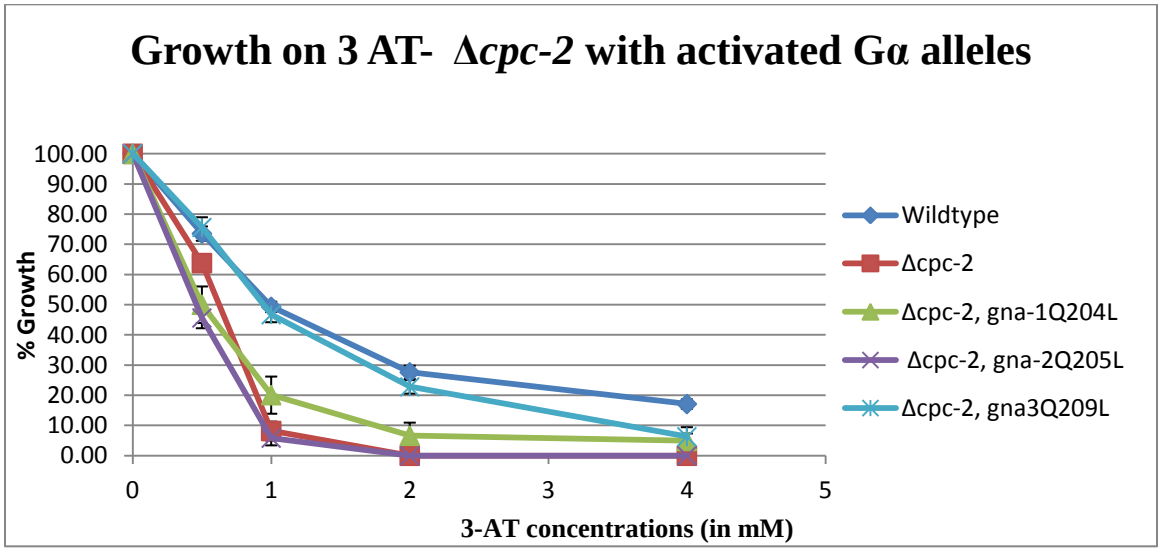

Figure 7- Apical extension on medium containing 3-aminotriazole (3-AT). Strains were incubated at 30˚C for 24 h and colony growth was measured. Values are expressed as % growth on minimal medium from three different experiments, resulting in nine replicates for each strain. Error is calculated as the standard error of the mean. A) Strains used are wild-type, Δ*cpc-2*, Δ*gna-1*, Δ*gna-2* and Δ*gna-3*. B) Strains used are wild-type, Δ*cpc-2*, Δ*gnb-1*, Δ*gng-1*, Δ*cpc-2* Δ*gnb-1* and Δ*cpc-2* Δ*gng-1*. C) Strains used are wild-type, Δ*cpc-2*, Δ*gna-1*, Δ*gna-2*, Δ*gna-3*, Δ*cpc-2*, Δ*gna-1*; Δ*cpc-2* Δ*gna-2;* and Δ*cpc-2* Δ*gna-3*. D) Strains used are wild-type, Δ*cpc-2*, Δ*cpc-2 gna-1*^{Q204L}, Δ*cpc-2 gna-2*^{Q205L}, and Δ*cpc-2 gna-3*^{Q208L}.

Discussion

The *N. crassa* CPC-2 protein clusters together with other fungal homologs of RACK1 during phylogenetic analysis (Fig 1). The two separate clusters of the RACK1-like proteins and the canonical Gβ proteins in the phylogenetic tree indicate that these two proteins might have diverged evolutionarily or might be paralogous to each other. This similar clustering of these two groups of proteins has been previously demonstrated (49). As a comparision, the RACK1 and the Gβ proteins from humans were added to the tree and it is clear that these two proteins are more closely related to their *N. crassa* counterparts than to budding yeast.

Genetic epistasis between *cpc-2* and components of the G protein pathway was performed using double deletion mutants, and strains containing Gα activated alleles. The model used to interpret epistatic relationships was the same as was shown in Chapter 2 and in (71). If introduction of the activated Gα allele bypass the defects of the Δ*cpc-2*, and the Δ*cpc-2* ΔGα double mutant resembles the single ΔGα mutant, then it is assumed that the Gα gene is downstream (epistatic) of *cpc-2*. If the activated alleles do not correct the defects of the Δ*cpc-2*, and the Δ*cpc-2* ΔGα double mutant resembles the Δ*cpc-2* mutant, then *cpc-2* is thought to be downstream (epistatic) of Gα. If conflicting results are seen, then partial or full independence of genetic regulation is assumed.

In the case of sporulation in submerged culture, it is seen that *gna-3* and *cpc-2* work in a linear pathway to regulate sporulation in this medium. This is similar to the relationship seen with *gnb-1* and *gna-3* in regulation of this phenotype, where *gna-3* is

epistatic to *gnb-1*, as shown in Chapter 2 and in (71). *gna-1* demonstrates partial epistasis with *cpc-2*, and *gna-2* seems independent of *cpc-2* during the regulation of this trait. The data presented in Chapter 2 is consistent with *gna-1* and *gna-2* also beingindependent of *gnb-1* during submerged growth (71). This indicates that *cpc-2*, like *gnb-1*, is a negative regulator of conidiation, and activation of *gna-3* offers a genetic bypass mechanism to restore hyphal growth.

An interaction between RACK1 and other WD-40 repeat proteins has been shown previously in mammalian systems (13). Using yeast two hybrid and pull-down assays, RACK1 has shown to interact with the Gβ subunit, Gβ1 (13). Specifically, the WD repeats 1-5, as well as the N-terminal and C-terminal regions are thought to interact with the Gβγ dimer (13, 17). Another WD repeat protein, Dynein Intermediate Chain (DIC)1A, containing six WD repeats, was also found to interact with RACK1 in co-immunoprecipitation assays (17). The significance of this interaction is speculated to play a role in apical transport through the involvement of G proteins, or other intracellular processes (13). Competitive binding was seen between the Gβγ dimer, RACK1 and another protein, dynamin (17).

Aerial hyphae height development assays show that *gna-3* is epistatic to *cpc-2*, whereas *gna-1* and *gna-2* appear to be independent. Results from Chapter 2 showed that *gnb-1* operates downstream of *gna-2* and *gna-3* (71). Thus in both cases, *gna-1* demonstrates independence from *gnb-1* and *cpc-2* for aerial hyphae elongation, even

though Δ*gna-1* has an aerial hyphae height that is significantly different, and defective as compared to wild-type (26, 71, 73).

Apical extension on minimal medium is regulated independently by the Gα genes and *cpc-2*. The drastically defective phenotype of the Δ*cpc-2* Δ*gna-1* strain indicates that *cpc-2* and *gna-1* regulate major aspects of growth through different pathways, producing synergistic effects in the double mutant. Defects in apical growth on minimal medium can be attributed to defects in conidial germination patterns or defects during apical extension, or all three. It is known that the Δ*gna-1* mutant has a defect in conidial germination only at 6 hours post germination (18), and has a growth rate approximately 40% of wildtype. This defect can be attributed to a conidial germination defect (25). Δ*gna-3* has a significant defect in conidial germination (18). As the results here indicate, Δ*cpc-2* does not have a conidial germination defect, similar to the Δ*gnb-1* and the Δ*gng-1* mutants. This indicates that the colony growth defect in the Δ*cpc-2* mutant is likely due to a defect in apical extension of hyphae. The Δ*cpc-2* Δ*gnb-1* mutant also does not exhibit any drastic germination defects. This suggests that conidial germination is not influenced by Gβ or Gγ proteins. It remains to be determined whether loss of *cpc-2* in a Gα mutant background further affects conidial germination.

Analysis of the sexual cycle demonstrated that the Δ*cpc-2* forms no protoperithecia, and upon fertilization is female sterile (Figure 4). Deleting a Gα gene, *gnb-1* or *gng-1* in the Δ*cpc-2* background results in strains that resemble the Δ*cpc-2* mutant. Activation of the GTPase-deficient *gna-3* allele provides a partial bypass to this

defect; the mutant strain makes perithecia and ejects ascospores, but the ascospores are inviable (Fig 4). Thus, fertility is not completely restored. Interestingly enough, other components of the cross pathway control network (*cpc-1* and *cpc-3*) have normal sexual cycles (50, 60), indicating that the halt in the sexual cycle of *cpc-2* is not solely due to amino acid limitation conditions. But there is a possibility that the two processes might be linked. It has been seen in *Aspergillus nidulans* that the RACK1 homolog CpcB and c-Jun regulates sexual differentiation by blocking the sexual fruit body formation (24). Extraneous addition of amino acids removes this block in the sexual cycle, whereas deletion of CpcB or over-expression of c-Jun induces the block. This shows that the sexual cycle program is linked to the network that regulates amino acid biosynthesis (24).

It is important to note the different relationships between RACK1 and the Gβ proteins seen in other species. While RACK1 in mammalian cells shows interaction with the Gβγ heterodimer, and regulation of its functions (12), RACK1 in plants reveals a different relationship. RACK1A, the most abundant RACK1 in *Arabidopsis thaliana* does not seem to interact with the sole heterotrimeric Gα protein Gpa1, or the sole Gβ protein Agb1(23), while Gpa1 and Agb1 do interact with each other . Genetic studies show that morphological and developmental defects of *rack1A* mutants are different from *gpa1* or *agb* mutants(23).

Apical extension on 3-AT suggested that while activating the *gna-1* and the *gna-3* allele in the *cpc-2* background can partially rescue the sensitive phenotype of *cpc-2* mutant, *gna-1* and *gna-3* have a role in amino acid regulation in *N. crassa*. The sensitivity

observed on different concentrations of 3-AT, and significant difference from wild-type, suggests that these two Ga subunits might be acting together with *cpc-2* to regulate some aspect of amino acid control. Since the Δ*cpc-2* Δ*gna-1* double mutant has the most drastic phenotype on 3-AT, it could be that *gna-1* plays a major role in this process, independent of cpc-2. Introducing the *gna-3*^{Q208L} allele into the Δ*cpc-2* mutant background shows maximum correction of the sensitivity defect, suggesting that *gna-3* is the major Gα player in this network. The involvement of a Gα protein in cross pathway control has not been previously shown. Possible mechanisms are ribosomal association of the Ga proteins, along with CPC-2. It is already known that RACK1 and its homologs associate with the ribosomal machinery and regulate translation of certain transcripts or have a global effect on translation. In budding yeast, Asc1p forms a part of the ribosomal machinery and represses gene expression (22). In *S. pombe*, Cpc2p promotes efficient translation (62). In *U. maydis*, several interactors of RAK1 were known to be ribosomal proteins, consistent with the trend (67).

An interesting result is seen with the Δ*cpc-2* Δ*gna-2* mutant, where deletion of *gna-2* improves the sensitivity of Δ*cpc-2* in amino acid starvation conditions. The Δ*cpc-2* Δ*gna-2* mutant resembles wild-type, which is unexpected. This suggests that loss of *gna-2* might compensate for mutation of *cpc-2*. However, constitutive activation of *gna-2* does not rescue the cpc-2 defect. This result currently cannot be explained and future work is needed to probe the mechanism.

All the phenotypic assays performed also included the Δ*cpc-2,* Δ*gnb-1* and the Δ*cpc-2,* Δ*gng-1*double mutants along with the Δ*gnb-1* and the Δ*gng-1* single mutant. Statistical significance in more than one instance showed that the double mutant is statistically similar to the Δ*gnb-1* or the Δ*gng-1* single mutant, and different than the Δ*cpc-2* mutant. However, no conclusion about genetic epistasis can be made between these genes because over-expression of *gnb-1* and *gng-1* respectively in the Δ*cpc-2* mutant background is needed to confirm that *gnb-1* is truly epistatic to *cpc-2*. But preliminary evidence suggests that the *gnb-1* and *gng-1* genes seem to be downstream of *cpc-2*.

A physical interaction between CPC-2 and two Gα proteins-GNA-1 and GNA-3-was demonstrated using the yeast two hybrid assay. No conclusion could be drawn regarding interactions between CPC-2 and any Gα proteins using co-immunoprecipitation experiments, due to the high background and protein sticking to the beads. The finding that genetic epistasis is clearly observed between *gna-3* and *cpc-2*, presents compelling evidence for a physical association of these two proteins. Utilizing methods such as co-localization of GFP-tagged CPC-2 with RFP-tagged Gα proteins (18) would shed light on localization of CPC-2, as well as indicate interaction patterns with the Gα proteins. However, the possibility of no interaction cannot be completely ruled out, since some RACK1 homologs such as RAK1 in *U. maydis* do not show any physical interaction with the Gα Gpa3 or the Gγ UM11209 (67).

In conclusion, this study successfully demonstrates genetic relationships between *cpc-2* and components of the G protein signaling pathway, with evidence for a physical association with GNA-1 and GNA-3. Several areas of study, such as interaction with the ribosomal machinery, the role of Gα genes in amino acid regulation or translational control need to be addressed, which will provide additional insights into the varied roles of *cpc-2.*

Chapter 4- Future Directions

In Chapter 2, genetic analysis revealed that *gna-3* is epistatic to *gnb-1* with regard to control of submerged conidiation. *gnb-1* is epistatic to *gna-2* and *gna-3* for aerial hyphal height, while *gnb-1* appears to act upstream of *gna-1* and *gna-2* during aerial conidiation. None of the activated Gα alleles restored female fertility to Δ*gnb-1* mutants, and the *gna-3*^{Q208L} allele inhibited formation of female reproductive structures, consistent with a need for Gα proteins to cycle through the inactive GDP-bound form for these processes.

Genetic epistasis analysis was used to probe genetic interactions between *cpc-2*, *gnb-1*, *gng-1* and the three Gα genes. The results showed that *gna-3* is epistatic to *cpc-2* during conidiation in submerged culture whereas *gna-1* shows partial epistasis during this phenotype. *gna-3* operates downstream of *cpc-2* during aerial hyphae height development. During sexual development, none of the activated Gα alleles restore fertility to the sterile Δ*cpc-2* mutant, but activation of the gna-3 allele helps the Δ*cpc-2* strain to make perithecia and therefore make a significant progress in the sexual cycle. Apical extension on media supplemented with 3-aminotriazole revealed a previously unknown role for *gna-1* and *gna-3* in general amino acid control. Yeast two hybrid mating assays revealed that CPC-2 interacts with GNA-1 and GNA-3.

Future studies could involve finding novel interactors for GNB-1, using cDNA libraries or mass spectrometry approaches . Competitive binding assays between the GEF RIC8, and GNB-1 can indicate binding specificities during the G protein signaling process. The protein-protein interaction platform being currently developed (Shouqiang Ouyang, Katherine Borkovich, unpublished data) will be crucial to test interactions between CPC-2 and components of the G protein pathway.

Since RACK1 is multifunctional in its roles, and its homologs in fungi show a variety of defective phenotypes, it is possible that Δ*cpc-2* has more phenotypes in terms of growth and development or signaling mechanisms. Biochemical assays showing that CPC-2 functions as a GDI could straightaway show that it acts as another Gβ subunit. To identify additional interactors, mass spectrometry and peptide identification and could be performed using the S-tagged CPC-2 strain. Alternatively, other interactors can be identified using cDNA libraries and yeast two hybrid assays. It would not be surprising if other WD repeat proteins/peptides were detected through such screens. It has been shown through mass spectrometry that RIC8 interacts with CPC-2 (Jacqueline Servin and Katherine Borkovich, unpublished data). A Δ*ric8* Δ*cpc-2* double mutant strain resembles the Δ*ric8* mutant, indicating that the cytosolic GEF masks the defects of the Δ*cpc-2* strain (Jacqueline Servin, unpublished data). Additional phenotypic analysis of this double mutant could show into how a cytosolic GEF and a putative Gβ protein regulate aspects of fungal growth.

Analyzing the different MAP kinase levels in the Δ*cpc-2* is another direction that can be employed to explore other functions, and whether any epistatic relationships are observed with the Gα mutants. It has been known that RACK1 interacts with Protein Phosphatase 2A (PP2A) and PKCβII [reviewed in (1)]. This will give more clues regarding the downstream effectors of G protein signaling pathway.

To explore the possibility of *cpc-2* interacting with the ribosomal machinery, western analysis on ribosomal fractions using the S-tagged CPC-2 strain would be most indicative. Additionally, Gα western analysis can also be performed simultaneously to see if any Gα proteins are present. A comparision between amino acid starvations conditions (using 3-AT) and normal conditions would also elucidate if there are any differences with ribosomal associations between starved and non-starved conditions.

To directly examine the role of Gα genes in amino acid regulation, it would be necessary to analyze the mRNA or protein level of a certain amino acid (arginine or histidine) in starved and non-starved conditions, using Gα gene deletion mutants (particularly, Δ*gna-1* and Δ*gna-3*). This can be done using northern analysis or quantitative PCR (qPCR) for transcript levels, or western analysis for protein levels. This would give direct hints if the regulation of the amino acid protein by the Gα genes is transcriptional, post-transcriptional or post translational. This might explain the sensitivity of Gα mutants on 3-AT. It has been observed that ARG-2 interacts with GNA-1 in a mass spectrometry approach (Alexander Michkov and Katherine Borkovich, unpublished data). Follow-up studies would elucidate this result as well.

References-

1. **Adams, D. R., D. Ron, and P. A. Kiely**. 2011. RACK1, A multifaceted scaffolding protein: Structure and function. Cell Commun Signal **9**.
2. **Aramayo, R., and R. L. Metzenberg**. 1996. Gene replacements at the *his-3* locus of *Neurospora crassa*. Fungal Genet. Newsl. **43**:9-13.
3. **Baasiri, R. A., X. Lu, P. S. Rowley, G. E. Turner, and K. A. Borkovich**. 1997. Overlapping functions for two G protein alpha subunits in Neurospora crassa. Genetics **147**:137-145.
4. **Barthelmess, I. B.** 1984. A Lethal Allele at the Putative Regulatory Locus, Cpc-1, of Cross-Pathway Control in Neurospora-Crassa. Molecular & General Genetics **194**:318-321.
5. **Barthelmess, I. B., and J. Kolanus**. 1990. The range of amino acids whose limitation activates general amino-acid control in Neurospora crassa. Genet Res **55**:7-12.
6. **Beadle, G. W., and E. L. Tatum**. 1941. Genetic Control of Biochemical Reactions in *Neurospora*. Proceedings of the National Academy of Sciences of the United States of America **27**:499-506.
7. **Bell-Pedersen, D., J. C. Dunlap, and J. J. Loros**. 1992. The Neurospora circadian clock-controlled gene, ccg-2, is allelic to eas and encodes a fungal hydrophobin required for formation of the conidial rodlet layer. Genes Dev **6**:2382-2394.
8. **Bistis, G. N.** 1981. Chemotropic Interactions between Trichogynes and Conidia of Opposite Mating-Type in Neurospora-Crassa. Mycologia **73**:959-975.
9. **Borkovich, K. A., L. A. Alex, O. Yarden, M. Freitag, G. E. Turner, N. D. Read, S. Seiler, D. Bell-Pedersen, J. Paietta, N. Plesofsky, M. Plamann, M. Goodrich-Tanrikulu, U. Schulte, G. Mannhaupt, F. E. Nargang, A. Radford, C. Selitrennikoff, J. E. Galagan, J. C. Dunlap, J. J. Loros, D. Catcheside, H. Inoue, R. Aramayo, M. Polymenis, E. U. Selker, M. S. Sachs, G. A. Marzluf, I. Paulsen, R. Davis, D. J. Ebbole, A. Zelter, E. R. Kalkman, R. O'Rourke, F. Bowring, J. Yeadon, C. Ishii, K. Suzuki, W. Sakai, and R. Pratt**. 2004. Lessons from the genome sequence of *Neurospora crassa*: tracing the path from genomic blueprint to multicellular organism. Microbiol. Mol. Biol. Rev. **68**:1-108.
10. **Bramley, P. M., and A. Mackenzie**. 1988. Regulation of carotenoid biosynthesis. Curr Top Cell Regul **29**:291-343.
11. **Chang, B. Y., R. A. Harte, and C. A. Cartwright**. 2002. RACK1: a novel substrate for the Src protein-tyrosine kinase. Oncogene **21**:7619-7629.
12. **Chen, S., E. J. Dell, F. Lin, J. Sai, and H. E. Hamm**. 2004. RACK1 regulates specific functions of Gbetagamma. The Journal of Biological Chemistry **279**:17861-17868.
13. **Chen, S., B. D. Spiegelberg, F. Lin, E. J. Dell, and H. E. Hamm**. 2004. Interaction of Gbetagamma with RACK1 and other WD40 repeat proteins. J Mol Cell Cardiol **37**:399-406.

14. **Christianson, T. W., R. S. Sikorski, M. Dante, J. H. Shero, and P. Hieter**. 1992. Multifunctional yeast high-copy-number shuttle vectors. Gene **110**:119-122.
15. **Colot, H. V., G. Park, G. E. Turner, C. Ringelberg, C. M. Crew, L. Litvinkova, R. L. Weiss, K. A. Borkovich, and J. C. Dunlap**. 2006. A high-throughput gene knockout procedure for *Neurospora* reveals functions for multiple transcription factors. Proc. Natl. Acad. Sci. USA **103**:10352-10357.
16. **Davis, R. H., and F. J. deSerres**. 1970. Genetic and microbiological research techniques for *Neurospora crassa*. Methods Enzymol. **71A**:79-143.
17. **Dell, E. J., J. Connor, S. Chen, E. G. Stebbins, N. P. Skiba, D. Mochly-Rosen, and H. E. Hamm**. 2002. The betagamma subunit of heterotrimeric G proteins interacts with RACK1 and two other WD repeat proteins. J Biol Chem **277**:49888-49895.
18. **Eaton, C. J., I. E. Cabrera, J. A. Servin, S. J. Wright, M. P. Cox, and K. A. Borkovich**. 2012. The guanine nucleotide exchange factor RIC8 regulates conidial germination through Galpha proteins in Neurospora crassa. PLoS One **7**:e48026.
19. **Ebbole, D. J., J. L. Paluh, M. Plamann, M. S. Sachs, and C. Yanofsky**. 1991. Cpc-1, the General Regulatory Gene for Genes of Amino-Acid Biosynthesis in Neurospora-Crassa, Is Differentially Expressed during the Asexual Life-Cycle. Molecular and Cellular Biology **11**:928-934.
20. **Ebbole, D. J., and M. S. Sachs**. 1990. A rapid and simple method for isolation of *Neurospora crassa* homokaryons using microconidia. Fungal Genet. Newsl. **37**:17-18.
21. **Garcia-Higuera, I., C. Gaitatzes, T. F. Smith, and E. J. Neer**. 1998. Folding a WD repeat propeller. Role of highly conserved aspartic acid residues in the G protein beta subunit and Sec13. J Biol Chem **273**:9041-9049.
22. **Gerbasi, V. R., C. M. Weaver, S. Hill, D. B. Friedman, and A. J. Link**. 2004. Yeast Asc1p and mammalian RACK1 are functionally orthologous core 40S ribosomal proteins that repress gene expression. Mol Cell Biol **24**:8276-8287.
23. **Guo, J., S. Wang, J. Wang, W.-D. Huang, J. Liang, and J.-G. Chen**. 2009. Dissection of the relationship between RACK1 and heterotrimeric G-proteins in Arabidopsis. Plant Cell Physiol **50**:1681-1694.
24. **Hoffmann, B., C. Wanke, S. K. Lapaglia, and G. H. Braus**. 2000. c-Jun and RACK1 homologues regulate a control point for sexual development in Aspergillus nidulans. Mol Microbiol **37**:28-41.
25. **Ivey, F. D., P. N. Hodge, G. E. Turner, and K. A. Borkovich**. 1996. The G alpha i homologue gna-1 controls multiple differentiation pathways in Neurospora crassa. Mol Biol Cell **7**:1283-1297.
26. **Ivey, F. D., A. M. Kays, and K. A. Borkovich**. 2002. Shared and independent roles for a Galpha(i) protein and adenylyl cyclase in regulating development and stress responses in Neurospora crassa. Eukaryot Cell **1**:634-642.

27. **Ivey, F. D., Q. Yang, and K. A. Borkovich**. 1999. Positive regulation of adenylyl cyclase activity by a galphai homolog in Neurospora crassa. Fungal Genet Biol **26**:48-61.
28. **Kays, A. M., and K. A. Borkovich**. 2004. Severe impairment of growth and differentiation in a *Neurospora crassa* mutant lacking all heterotrimeric G alpha proteins. Genetics **166**:1229-1240.
29. **Kays, A. M., P. S. Rowley, R. A. Baasiri, and K. A. Borkovich**. 2000. Regulation of conidiation and adenylyl cyclase levels by the G-alpha protein GNA-3 in *Neurospora crassa*. Mol. Cell. Biol. **20**:7693-7705.
30. **Kim, H., and K. A. Borkovich**. 2004. A pheromone receptor gene, *pre-1*, is essential for mating type-specific directional growth and fusion of trichogynes and female fertility in *Neurospora crassa*. Mol Microbiol **52**:1781-1798.
31. **Kim, H., S. J. Wright, G. Park, S. Ouyang, S. Krystofova, and K. A. Borkovich**. 2012. Roles for receptors, pheromones, G proteins, and mating type genes during sexual reproduction in Neurospora crassa. Genetics **190**:1389-1404.
32. **Kritsky, M. S., T. A. Sokolovsky, T. A. Belozerskaya, and E. K. Chernysheva**. 1982. Relationship between cyclic AMP level and accumulation of carotenoid pigments in Neurospora crassa. Arch Microbiol **133**:206-208.
33. **Kruger, D., J. Koch, and I. B. Barthelmess**. 1990. Cpc-2, a New Locus Involved in General Control of Amino-Acid Synthetic Enzymes in Neurospora-Crassa. Current Genetics **18**:211-215.
34. **Krystofova, S., and K. A. Borkovich**. 2005. The heterotrimeric G-protein subunits GNG-1 and GNB-1 form a Gbetagamma dimer required for normal female fertility, asexual development, and Galpha protein levels in *Neurospora crassa*. Eukaryot Cell **4**:365-378.
35. **Krystofova, S., and K. A. Borkovich**. 2006. The predicted G-protein-coupled receptor GPR-1 is required for female sexual development in the multicellular fungus Neurospora crassa. Eukaryotic Cell **5**:1503-1516.
36. **Kuroha, K., M. Akamatsu, L. Dimitrova, T. Ito, Y. Kato, K. Shirahige, and T. Inada**. 2010. Receptor for activated C kinase 1 stimulates nascent polypeptide-dependent translation arrest. EMBO Rep **11**:956-961.
37. **Larkin, M. A., G. Blackshields, N. P. Brown, R. Chenna, P. A. McGettigan, H. McWilliam, F. Valentin, I. M. Wallace, A. Wilm, R. Lopez, J. D. Thompson, T. J. Gibson, and D. G. Higgins**. 2007. Clustal W and Clustal X version 2.0. Bioinformatics **23**:2947-2948.
38. **Li, D., P. Bobrowicz, H. H. Wilkinson, and D. J. Ebbole**. 2005. A mitogen-activated protein kinase pathway essential for mating and contributing to vegetative growth in Neurospora crassa. Genetics **170**:1091-1104.
39. **Li, L., and K. A. Borkovich**. 2006. GPR-4 Is a Predicted G-Protein-Coupled Receptor Required for Carbon Source-Dependent Asexual Growth and Development in *Neurospora crassa*. Eukaryot. Cell **5**:1287-1300.
40. **Li, L., S. J. Wright, S. Krystofova, G. Park, and K. A. Borkovich**. 2007. Heterotrimeric G protein signaling in filamentous fungi. Annu. Rev. Microbiol. **61**:423-452.

41. **Lopez-Bergami, P., H. Habelhah, A. Bhoumik, W. Zhang, L. H. Wang, and Z. Ronai**. 2005. RACK1 mediates activation of JNK by protein kinase C [corrected]. Mol Cell **19**:309-320.
42. **Loros, J. J., and J. C. Dunlap**. 1991. Neurospora crassa clock-controlled genes are regulated at the level of transcription. Mol Cell Biol **11**:558-563.
43. **McLeod, M., B. Shor, A. Caporaso, W. Wang, H. Chen, and L. Hu**. 2000. Cpc2, a fission yeast homologue of mammalian RACK1 protein, interacts with Ran1 (Pat1) kinase to regulate cell cycle progression and meiotic development. Molecular and Cellular Biology **20**:4016-4027.
44. **Muller, F., D. Kruger, E. Sattlegger, B. Hoffmann, P. Ballario, M. Kanaan, and I. B. Barthelmess**. 1995. The Cpc-2 Gene of Neurospora-Crassa Encodes a Protein Entirely Composed of Wd-Repeat Segments That Is Involved in General Amino-Acid Control and Female Fertility. Molecular & General Genetics **248**:162-173.
45. **Neves, S. R., P. T. Ram, and R. Iyengar**. 2002. G protein pathways. Science (New York, N Y) **296**:1636-1639.
46. **Ninomiya, Y., K. Suzuki, C. Ishii, and H. Inoue**. 2004. Highly efficient gene replacements in Neurospora strains deficient for nonhomologous end-joining (vol 101, pg 12248, 2004). Proceedings of the National Academy of Sciences of the United States of America **101**:16391-16391.
47. **Nunez, A., A. Franco, M. Madrid, T. Soto, J. Vicente, M. Gacto, and J. Cansado**. 2009. Role for RACK1 orthologue Cpc2 in the modulation of stress response in fission yeast. Molecular biology of the cell **20**:3996-4009.
48. **Nunez, A., A. Franco, T. Soto, J. Vicente, M. Gacto, and J. Cansado**. 2010. Fission Yeast Receptor of Activated C Kinase (RACK1) Ortholog Cpc2 Regulates Mitotic Commitment through Wee1 Kinase. J Biol Chem **285**:41366-41373.
49. **Palmer, D. A., J. K. Thompson, L. Li, A. Prat, and P. Wang**. 2006. Gib2, a novel Gbeta-like/RACK1 homolog, functions as a Gbeta subunit in cAMP signaling and is essential in Cryptococcus neoformans. J Biol Chem **281**:32596-32605.
50. **Paluh, J. L., M. J. Orbach, T. L. Legerton, and C. Yanofsky**. 1988. The Cross-Pathway Control Gene of Neurospora-Crassa, Cpc-1, Encodes a Protein Similar to Gcn4 of Yeast and the DNA-Binding Domain of the Oncogene V-Jun-Encoded Protein. Proceedings of the National Academy of Sciences of the United States of America **85**:3728-3732.
51. **Pandey, A., M. G. Roca, N. D. Read, and N. L. Glass**. 2004. Role of a mitogen-activated protein kinase pathway during conidial germination and hyphal fusion in Neurospora crassa. Eukaryot Cell **3**:348-358.
52. **Park, G., S. Pan, and K. A. Borkovich**. 2008. Mitogen-activated protein kinase cascade required for regulation of development and secondary metabolism in Neurospora crassa. Eukaryot Cell **7**:2113-2122.
53. **Perkins, D.** 1985. Advantages of using the inactive-mating-type a^{m1} strain as a helper component in heterokaryons. Neurospora Newslett. **31**:41-42.

54. **Rachfall, N., K. Schmitt, S. Bandau, N. Smolinski, A. Ehrenreich, O. Valerius, and G. H. Braus**. 2013. RACK1/Asc1p, a ribosomal node in cellular signaling. Mol Cell Proteomics **12**:87-105.
55. **Raju, N. B.** 1992. Genetic control of the sexual cycle in *Neurospora*. Mycol. Res. **96**:241-262.
56. **Ron, D., C. H. Chen, J. Caldwell, L. Jamieson, E. Orr, and D. Mochly-Rosen**. 1994. Cloning of an intracellular receptor for protein kinase C: a homolog of the beta subunit of G proteins. Proc Natl Acad Sci U S A **91**:839-843.
57. **Rosenberg, G., and M. L. Pall**. 1979. Properties of two cyclic nucleotide-deficient mutants of Neurospora crassa. J Bacteriol **137**:1140-1144.
58. **Rosenberg, G. B., and M. L. Pall**. 1983. Characterization of an ATP-Mg2+-dependent guanine nucleotide-stimulated adenylate cyclase from Neurospora crassa. Arch Biochem Biophys **221**:243-253.
59. **Runne, C., and S. Chen**. 2013. WD40-repeat proteins control the flow of Gbetagamma signaling for directional cell migration. Cell Adh Migr **7**:214-218.
60. **Sattlegger, E., A. G. Hinnebusch, and I. B. Barthelmess**. 1998. cpc-3, the Neurospora crassa homologue of yeast GCN2, encodes a polypeptide with juxtaposed eIF2 alpha kinase and histidyl-tRNA synthetase-related domains required for general amino acid control. J Biol Chem **273**:20404-20416.
61. **Sengupta, J., J. Nilsson, R. Gursky, C. M. Spahn, P. Nissen, and J. Frank**. 2004. Identification of the versatile scaffold protein RACK1 on the eukaryotic ribosome by cryo-EM. Nat Struct Mol Biol **11**:957-962.
62. **Shor, B., J. Calaycay, J. Rushbrook, and M. McLeod**. 2003. Cpc2/RACK1 is a ribosome-associated protein that promotes efficient translation in Schizosaccharomyces pombe. The Journal of Biological Chemistry **278**:49119-49128.
63. **Siegel, J. N., and A. C. Gentile**. 1966. Effect of 3-amino-1,2,4-triazole on histidine metabolism in algae. Plant Physiol **41**:670-672.
64. **Springer, M. L.** 1993. Genetic control of fungal differentiation: The three sporulation pathways of *Neurospora crassa*. BioEssays **15**:365-374.
65. **Turner, G. E., and K. A. Borkovich**. 1993. Identification of a G protein alpha subunit from Neurospora crassa that is a member of the Gi family. J Biol Chem **268**:14805-14811.
66. **Vogel, H. J.** 1964. Distribution of Lysine Pathways among Fungi - Evolutionary Implications. Am Nat **98**:435-446.
67. **Wang, L., P. Berndt, X. Xia, J. Kahnt, and R. Kahmann**. 2011. A seven-WD40 protein related to human RACK1 regulates mating and virulence in Ustilago maydis. Mol Microbiol **81**:1484-1498.
68. **Wang, S., J.-Z. Chen, Z. Zhang, S. Gu, C. Ji, R. Tang, K. Ying, Y. Xie, and Y. Mao**. 2003. Cloning, expression and genomic structure of a novel human GNB2L1 gene, which encodes a receptor of activated protein kinase C (RACK). Mol Biol Rep **30**:53-60.
69. **Westergaard, M., and H. K. Mitchell**. 1947. Neurospora-V - a Synthetic Medium Favoring Sexual Reproduction. Am J Bot **34**:573-577.

70. **Winston, F., C. Dollard, and S. L. Ricupero-Hovasse**. 1995. Construction of a set of convenient Saccharomyces cerevisiae strains that are isogenic to S288C. Yeast (Chichester, England) **11**:53-55.
71. **Won, S., A. V. Michkov, S. Krystofova, A. V. Garud, and K. A. Borkovich**. 2012. Genetic and physical interactions between Galpha subunits and components of the Gbetagamma dimer of heterotrimeric G proteins in Neurospora crassa. Eukaryot Cell **11**:1239-1248.
72. **Wright, S. J., R. Inchausti, C. J. Eaton, S. Krystofova, and K. A. Borkovich**. 2011. RIC8 is a guanine-nucleotide exchange factor for Galpha subunits that regulates growth and development in Neurospora crassa. Genetics **189**:165-176.
73. **Yang, Q., and K. A. Borkovich**. 1999. Mutational activation of a G-alpha i causes uncontrolled proliferation of aerial hyphae and increased sensitivity to heat and oxidative stress in *Neurospora crassa*. Genetics **151**:107-117.
74. **Yang, Q., S. I. Poole, and K. A. Borkovich**. 2002. A G-protein beta subunit required for sexual and vegetative development and maintenance of normal G alpha protein levels in *Neurospora crassa*. Eukaryot Cell **1**:378-390.
75. **Zeller, C. E., S. C. Parnell, and H. G. Dohlman**. 2007. The RACK1 ortholog Asc1 functions as a G-protein beta subunit coupled to glucose responsiveness in yeast. J Biol Chem **282**:25168-25176.